



Two-Stage Automated Coffee Bean Sorter: A Precise System for Green Coffee Beans
Using Machine Vision and Density-Based Analysis

A Thesis
Presented to the Faculty of the
Department of Electronics and Computer Engineering
Gokongwei College of Engineering
De La Salle University

In Partial Fulfillment of the
Requirements for the Degree of
Bachelor of Science in Computer Engineering

by
DELA CRUZ John Carlo Theo S.
PAREL Pierre Justine P.
TABIOLO Jiro Renzo D.
VALENCERINA Ercid Bon B.

April, 2025



De La Salle University

ORAL DEFENSE RECOMMENDATION SHEET

This thesis, entitled **Two-Stage Automated Coffee Bean Sorter: A Precise System for Green Coffee Beans Using Machine Vision and Density-Based Analysis**, prepared and submitted by thesis group, AISL-1-2425-C3, composed of:

DELA CRUZ, John Carlo Theo S.
PAREL, Pierre Justine P.
TABIOLO, Jiro Renzo D.
VALENCERINA, Ercid Bon B.

in partial fulfillment of the requirements for the degree of **Bachelor of Science in Computer Engineering (BS-CPE)** has been examined and is recommended for acceptance and approval for **ORAL DEFENSE**.

Dr. Melvin K. Cabatuan
Adviser

April 5, 2025



ABSTRACT

The study proposes to develop a two-stage automated coffee bean sorter that identifies the good beans, less-dense beans and at the same time segregating the defective coffee bean using machine vision and density-based analysis. In the first stage, the defective beans will be detected through the use of machine vision, parameters such as size and defects are taken into account. The second stage is used to categorize each bean by its density, which is calculated by its mass and volume. Thus, beans with relatively low density and not within the size threshold, are sorted out. The system aims to incorporate machine vision and density analysis to reduce human labor and provide an alternative to manual sorting methods for the farmers and coffee bean producers.

Index Terms—computer vision, deep learning, density-based analysis, Arabica, green coffee beans, sorting.



50

TABLE OF CONTENTS

51

Oral Defense Recommendation Sheet	ii
-----------------------------------	----

52

Abstract	iii
----------	-----

53

Table of Contents	iv
-------------------	----

54

List of Figures	ix
-----------------	----

55

List of Tables	xi
----------------	----

56

Abbreviations and Acronyms	xii
----------------------------	-----

57

Notations	xiii
-----------	------

58

Glossary	xiv
----------	-----

59

Chapter 1 INTRODUCTION	1
------------------------	---

60

1.1 Background of the Study	2
---------------------------------------	---

61

1.2 Prior Studies	3
-----------------------------	---

62

1.3 Problem Statement	7
---------------------------------	---

63

1.4 Objectives and Deliverables	8
---	---

64

1.4.1 General Objective (GO)	8
--	---

65

1.4.2 Specific Objectives (SOs)	8
---	---

66

1.4.3 Expected Deliverables	9
---------------------------------------	---

67

1.5 Significance of the Study	11
---	----

68

1.5.1 Technical Benefit	11
-----------------------------------	----

69

1.5.2 Impact to the Coffee Industry	11
---	----

70

1.6 Assumptions, Scope, and Delimitations	12
---	----

71

1.6.1 Assumptions	12
-----------------------------	----

72

1.6.2 Scope	12
-----------------------	----

73

1.6.3 Delimitations	13
-------------------------------	----

74

1.6.4 Overview of the Methodology	13
---	----

75

1.6.5 Estimated Work Schedule & Budget	15
--	----

76

Chapter 2 LITERATURE REVIEW	17
-----------------------------	----

77

2.1 Existing Work	18
-----------------------------	----



78	2.2 Lacking in the Approaches	26
79	2.3 Summary	28
80	Chapter 3 THEORETICAL CONSIDERATIONS	29
81	3.1 Theoretical Framework	30
82	3.2 Conceptual Framework	30
83	3.3 Quality Assurance Theory	32
84	3.4 Artificial Intelligence Theory	33
85	3.5 Computer Vision Theory	34
86	3.6 Performance Evaluation	35
87	3.7 Existing Technologies and Approaches	36
88	3.8 Density Measurement	36
89	3.9 Summary	37
90	Chapter 4 DESIGN CONSIDERATIONS	38
91	4.1 Mechanical Design	39
92	4.1.1 Screw Feeder	39
93	4.1.2 Rotating Conveyor Table	40
94	4.1.3 Inspection Tray (1st Stage)	41
95	4.1.4 Density Sorter (2nd Stage)	42
96	4.2 Embedded Systems	42
97	4.2.1 Microcontroller	42
98	4.2.2 Sensors	44
99	4.2.3 Motor control	46
100	4.2.4 Operating Voltage	48
101	4.3 Computer Vision System	49
102	4.3.1 Image Processing	49
103	4.3.2 Object Detection and Classification Models	50
104	4.3.3 Object Classification Models	50
105	4.4 Serial Communication	51
106	4.5 Graphical User Interface (GUI)	52
107	4.6 Density Analysis	53
108	4.7 Technical Standards	53
109	4.7.1 Hardware	53
110	4.7.2 Software	54
111	4.7.3 Green Coffee Bean Sorting	55
112	Chapter 5 METHODOLOGY	56
113	5.1 Description of the System	59
114	5.2 Research Design	62



115	5.3 Dataset Collection	63
116	5.3.1 Dataset Collection and Model Training	64
117	5.3.2 Utilization of Open-Source Database	65
118	5.3.3 First Iteration of Dataset Collection	66
119	5.3.4 Second Iteration of Dataset Collection	68
120	5.4 Density Threshold Calibration Using Water Displacement Method	69
121	5.5 Dataset Preparation and Model Training	70
122	5.5.1 Dataset Splitting	70
123	5.5.2 Image Annotation	70
124	5.5.3 Dataset Augmentation Techniques	71
125	5.5.4 Model Evaluation	71
126	5.5.5 Model Benchmarking and Selection	73
127	5.6 Hardware Development	73
128	5.6.1 Screw Feeder	74
129	5.6.2 Rotating Conveyor Table	75
130	5.6.3 Inspection Tray	78
131	5.6.4 Density Sorter	79
132	5.7 Hardware and Software Integration	80
133	5.7.1 Serial Communication	80
134	5.7.2 Recommended Standard 232 (RS-232)	81
135	5.8 Prototype Setup	83
136	5.8.1 Actual Setup	83
137	5.8.2 Lighting Setup for Inspection Tray	85
138	5.8.3 System Operation	89
139	5.9 Prototype Testing	91
140	5.9.1 Sorting Speed	91
141	5.9.2 Defect Sorting Accuracy	92
142	5.9.3 Density Sorting Accuracy	94
143	Chapter 6 RESULTS AND DISCUSSIONS	95
144	6.1 Description of the New Custom Dataset	99
145	6.2 Performance of Classification Models on Custom Dataset	100
146	6.2.1 EfficientNetV2S	101
147	6.2.2 YOLOv8	103
148	6.2.3 YOLOv11-cla	105
149	6.2.4 YOLOv12-cla	107
150	6.3 Actual Performance of Trained Models in the System	108
151	6.4 Sorting Speed	111



152	Chapter 7 CONCLUSIONS, RECOMMENDATIONS, AND FUTURE DI-	
153	RECTIVES	113
154	7.1 Concluding Remarks	114
155	7.2 Contributions	114
156	7.3 Recommendations	115
157	7.4 Future Prospects	115
158	References	116
159	Appendix A STUDENT RESEARCH ETHICS CLEARANCE	119
160	Appendix B ANSWERS TO QUESTIONS TO THIS THESIS	121
161	Appendix C REVISIONS TO THE PROPOSAL	124
162	Appendix D REVISIONS TO THE FINAL	130
163	Appendix E USAGE EXAMPLES	134
164	E1 Equations	135
165	E2 Notations	137
166	E2.1 Math alphabets	137
167	E2.2 Vector symbols	137
168	E2.3 Matrix symbols	137
169	E2.4 Tensor symbols	138
170	E2.5 Bold math version	139
171	E2.5.1 Vector symbols	139
172	E2.5.2 Matrix symbols	139
173	E2.5.3 Tensor symbols	139
174	E3 Abbreviation	143
175	E4 Glossary	145
176	E5 Figure	147
177	E6 Table	153
178	E7 Algorithm or Pseudocode Listing	157
179	E8 Program/Code Listing	159
180	E9 Referencing	161
181	E9.1 A subsection	162
182	E9.1.1 A sub-subsection	163
183	E10 Citing	164
184	E10.1 Books	164
185	E10.2 Booklets	166



De La Salle University

186	E10.3 Proceedings	166
187	E10.4 In books	166
188	E10.5 In proceedings	167
189	E10.6 Journals	167
190	E10.7 Theses/dissertations	169
191	E10.8 Technical Reports and Others	169
192	E10.9 Miscellaneous	170
193	E11 Index	171
194	E12 Adding Relevant PDF Pages	172
195	Appendix F VITA	176
196	Appendix G ARTICLE PAPER(S)	178



197

LIST OF FIGURES

198	1.1	Gantt Chart for John Carlo Dela Cruz	15
199	1.2	Gantt Chart for Pierre Parel	16
200	1.3	Gantt Chart for Jiro Tabiolo	16
201	1.4	Gantt Chart for Ercid Bon Valencerina	16
202	3.1	Theoretical Framework	30
203	3.2	Conceptual Framework	31
204	4.1	Screw Feeder Diagram	39
205	4.2	Rotating Conveyor Table 3D Design, 32-inch Rotary Table Accumulator (RTA)	40
206	4.3	Inspector Tray 3D Design	41
207	4.4	Arduino Nano Microcontroller	42
208	4.5	Infrared Sensor	44
209	4.6	TOF10120	45
210	4.7	12V NEMA 17 Stepper Motor	46
211	4.8	6V DC Motor	47
212	4.9	TB6612FNG Motor Driver	47
213	4.10	12V Power Supply	48
214	4.11	MT3608 Step-Up Module	49
215	4.12	C920 Camera	49
216	4.13	Graphical User Interface	52
217	5.1	System Block Diagram	59
218	5.2	Schematic Diagram of the System	60
219	5.3	Design Overview of the System	61
220	5.4	Design and Development Research (DDR) Methodology	62
221	5.5	Data Collection Process	63
222	5.6	Manual Sorting Process	64
223	5.7	First Iteration of Data Collection Setup	66
224	5.8	Sample Images from the First Iteration of Dataset Collection	67
225	5.9	Sample Images from the Second Iteration of Dataset Collection	68
226	5.10	Screw Feeder 3D Design	74
227	5.11	Rotating Conveyor Table 3D Design	75
228	5.12	Rotating Conveyor Table with Aluminum Guides	76
229	5.13	Rotating Conveyor Table with IR Sensor	77
230	5.14	Inspection Tray 3D Design	78



231	5.15 Precision Scale	79
232	5.16 Serial Communication Flow for Stage 1 Classification	80
233	5.17 Precision Scale Integration with RS232 for Stage 2 Classification	81
234	5.18 Actual System Setup	83
235	5.19 First Iteration of Lighting Setup	86
236	5.20 Second Iteration of Lighting Setup	87
237	5.21 Final Iteration of Lighting Setup	88
238	5.22 Top and Bottom View of the Cameras	89
239	6.1 Normalized Confusion Matrix for EfficientNetV2S on Test Dataset	101
240	6.2 Normalized Confusion Matrix for YOLOv8 on Test Dataset	103
241	6.3 Normalized Confusion Matrix for YOLOv11 on Test Dataset	105
242	6.4 Normalized Confusion Matrix for YOLOv12 on Test Dataset	107
243	E.1 A quadrilateral image example.	147
244	E.2 Figures on top of each other. See List. E.6 for the corresponding \LaTeX code.	149
245	E.3 Four figures in each corner. See List. E.7 for the corresponding \LaTeX code.	151



246

LIST OF TABLES

247	1.1	Summary of the Literature Review	4
248	1.2	Comparison Table on Existing Studies	6
249	1.3	Expected Deliverables per Objective	10
250	1.4	Budget Plan	15
251	2.1	Review of Related Literature	18
252	2.2	Comparing Proposed Study and Existing Studies	26
253	5.1	Summary of methods for reaching the objectives	57
254	5.2	Sorting Speed Testing Table	91
255	5.3	Good Bean Classification Accuracy Testing Table	92
256	5.4	Specific Defect Classification Accuracy Testing Table	93
257	5.5	Dataset Distribution for Overall Testing	94
258	6.1	Summary of results for achieving the objectives	96
259	6.2	Class Distribution Summary	99
260	6.3	Dataset Split Summary	99
261	6.4	Specific Performance of the Models for Each Defect	108
262	6.5	Model Performance Comparison	111
263	6.6	Sorting Speed Test Conditions	112
264	C.1	Summary of Revisions to the Proposal	125
265	D.1	Summary of Revisions to the Thesis	131
266	E.1	Feasible triples for highly variable grid	153
267	E.2	Calculation of $y = x^n$	157



268

ABBREVIATIONS

269	AC	Alternating Current	143
270	CSS	Cascading Style Sheet	143
271	HTML	Hyper-text Markup Language	143
272	XML	eXtensible Markup Language	143



273

NOTATION

274	$ \mathcal{S} $	the number of elements in the set \mathcal{S}	145
275	\emptyset	the set with no elements	145
276	$h(t)$	impulse response	135
277	\mathcal{S}	a collection of distinct objects	145
278	\mathcal{U}	the set containing everything	145
279	$x(t)$	input signal represented in the time domain	135
280	$y(t)$	output signal represented in the time domain	135

281 Throughout this thesis, mathematical notations conform to ISO 80000-2 standard, e.g.,
282 variable names are printed in italics, the only exception being acronyms like, e.g., SNR,
283 which are printed in regular font. Constants are also set in regular font like j . Standard
284 functions and operators are also set in regular font, e.g., in $\sin(\cdot)$, $\max\{\cdot\}$. Commonly
285 used notations are t , f , $j = \sqrt{-1}$, n and $\exp(\cdot)$, which refer to the time variable, frequency
286 variable, imaginary unit, n th variable, and exponential function, respectively.



287

GLOSSARY

288

Functional Analysis

the branch of mathematics concerned with the study of spaces of functions

289

matrix

a concise and useful way of uniquely representing and working with linear transformations; a rectangular table of elements



290

LISTINGS

291	E.1 Sample \LaTeX code for equations and notations usage	136
292	E.2 Sample \LaTeX code for notations usage	140
293	E.3 Sample \LaTeX code for abbreviations usage	144
294	E.4 Sample \LaTeX code for glossary and notations usage	146
295	E.5 Sample \LaTeX code for a single figure	148
296	E.6 Sample \LaTeX code for three figures on top of each other	150
297	E.7 Sample \LaTeX code for the four figures	152
298	E.8 Sample \LaTeX code for making typical table environment	155
299	E.9 Sample \LaTeX code for algorithm or pseudocode listing usage	158
300	E.10 Computing Fibonacci numbers	159
301	E.11 Sample \LaTeX code for program listing	160
302	E.12 Sample \LaTeX code for referencing sections	161
303	E.13 Sample \LaTeX code for referencing subsections	162
304	E.14 Sample \LaTeX code for referencing sub-subsections	163
305	E.15 Sample \LaTeX code for Index usage	171
306	E.16 Sample \LaTeX code for including PDF pages	172



De La Salle University

307

Chapter 1

308

INTRODUCTION



1.1 Background of the Study

Coffee is one of the most globally consumed beverages. It is a vital product in the global market, with production reaching 168.2 million bags in 2022-2023. The coffee industry is expected to grow even more in the coming years, with output projected to rise by 5.8% in 2023-2024 [International Coffee Association, 2023]. In the Philippines, coffee holds a strong cultural significance, with the local industry continuously expanding. The country is the 14th largest coffee producer in the world. Locally, the industry is expected to grow at a compound annual growth rate (CAGR) of 3.5% from 2021 to 2025, driven by small-scale farm households [Santos and Baltazar, 2022]. With a growing popularity among coffee enthusiasts, the demand for specialty coffee is increasing as well. Consumers are becoming more selective about the quality of their coffee beans [Tampon, 2023].

To stay competitive in the rapidly evolving coffee industry, farmers carefully select high-quality coffee beans for production. Grading green coffee beans is a crucial part of coffee production, as it is directly associated with the quality of the cup quality of coffee brews [Barbosa et al., 2019]. Coffee grading is a process in the industry that determines the quality of coffee beans, using various parameters such as size, density, color, and defects, ensuring that only high quality beans are selected for consumption [Córdoba et al., 2021]. The size of coffee beans is determined using a screen size and sorting procedure, where the coffee beans are categorized into different screen sizes, with larger beans considered higher quality [González et al., 2019]. The density of a bean can be calculated by the ratio of its mass and volume, which greatly influences the roasting process and overall quality of the coffee [Datov and Lin, 2019]. Color is also another indicator for quality, with darker beans being preferred for their richer flavor profile. On the other hand, defects are classified



among 3 categories: Category 1 includes the most severe issues such as foreign matter and black beans, Category 2 includes less severe defects like broken beans, and Category 3 includes minor defects like slight discoloration. Determining the quality of the coffee beans in relation to their defect values is based on quality standards and grading systems such as SCAA protocols guidance or the Philippine National Standard on Green Coffee Bean [Bureau of Agriculture and Fisheries Standards, 2012].

Traditionally, this stage of assessing and categorizing coffee beans relies on visual evaluation, which is time-consuming and labor-intensive, making it prone to human error. One of the biggest challenges in coffee bean production is ensuring consistency in quality. As the demand for specialty coffee continues to grow, there has also been an increase for the need of more efficient and accurate sorting methods. The application of modern technology can help reduce the labor costs and minimize human errors in these tasks. In recent years, computer vision was used alongside various machine learning models and techniques, such as convolutional neural networks (CNNs), support vector machines (SVMs), or K-nearest neighbors (KNN) models, where the models were trained on labeled data to classify images of coffee beans into different quality categories. The proposed aims to utilize this technology to develop a two-stage automated coffee bean sorting system using machine vision and density-based analysis to categorize and identify and segregate specialty-grade green coffee beans from non-specialty and defective coffee beans.

1.2 Prior Studies

Identifying and sorting specialty-grade coffee beans can be strenuous since the traditional way of classifying a specialty-grade coffee is by manually sorting the coffee bean batch and



354 classifying them according to the set of standards of the SCAA. The existing work aims
 355 to solve these problems through image processing and implementing deep learning-based
 356 models to automatically sort the coffee beans while achieving high accuracy. However,
 357 these solutions only automate detecting either one of the parameters such as defects, color,
 358 and size, while the proposed system considers density, size, color and defects all in one
 359 system. Hence, eliminating human intervention or labor. The table below shows the
 360 comparison of existing solutions to the researcher's proposal aligning with the traditional
 361 way of sorting coffee beans.

TABLE 1.1 SUMMARY OF THE LITERATURE REVIEW

Existing Literature	Description
Defect Detection	<p>The existing literature focuses on using various machine learning models such as YOLO, KNN, and CNN to detect defects in green coffee beans, through identifying visible defects like black spots, broken beans, discoloration, and more. These existing approaches heavily rely on visual characteristics and do not consider other key factors that affect green coffee bean quality like density, which can enhance classification accuracy. The proposed system integrates density and size analysis alongside the defecting various levels of defects on the coffee bean for a more holistic detection and classification.</p>



Coffee Bean Grading and Quality Assessment

The existing literature utilize algorithms such as artificial neural networks, support vector machine, and random forest to grade and classify coffee beans according to the specified grading system. These methods primarily focus on visual features of the beans, which do not account the bean's density and size, which are both essential factors for classifying specialty-grade coffee beans. Additionally, there is a lack of practical implementation of automated sorting systems, as these focus on simply classifying the beans. Through a two-stage process, the proposed system will take into consideration both the visual inspection and the density measurement, which leads to a more complete classification of coffee beans.



Automated Sorting and Classification System	Research has been conducted on developing that automate the process of sorting coffee beans according to various parameters. Some studies focus on sorting defectives against non-defective, while others focus on other visual parameters like defects and roast profiles. These systems focus only on visual characteristics, without considering the actual size of the bean and its density as parameters for better classification accuracy. The proposed system will integrate the use of visual, density, and size parameters to enable a comprehensive automated sorting solution for classifying specialty-grade coffee beans.
---	---

362

TABLE 1.2 COMPARISON TABLE ON EXISTING STUDIES

Proposed System	[Balay et al., 2024]	[Lualhati et al., 2022]
-----------------	----------------------	-------------------------



- | | | |
|---|--|---|
| <ul style="list-style-type: none"> • Defect sorting using Efficient-NetV2. • Considers classification of 10 defect types. • The system considers density parameters to sort out less-dense beans. • The system includes a graphical user interface for farmers to visualize the cumulative data of the defects present in the batch. • The system also includes AI-generated recommendations on the possible interventions for the farmers based on the data gathered from the sorting system. | <ul style="list-style-type: none"> • Defect sorting using YOLOv8 • The study considered only 6 types of defects. | <ul style="list-style-type: none"> • Defect sorting using YOLOv2 and InceptionV3. • The study considered only 2 types of defects. |
|---|--|---|

1.3 Problem Statement

The Philippine coffee industry is a growing market, however it is stuck with using traditional methods in sorting green coffee beans. Often relying on manually sorting the beans, it exposes a number of problems that are apparent in the industry. Relying on manual sorting increases production cost which results in higher prices for quality coffee beans. To make the Philippine coffee beans more competitive to the exported beans, reducing the price is crucial. Another problem that is encountered in manual sorting heavily focuses only on the physical attributes of the bean like size and appearance. There are standards that need to be met, which forces the farmers to resort to manual sorting to comply with the standards



of the SCAA. The SCAA standards require a 300g batch of green coffee beans must not contain any defects and the size consistency of the beans must not exceed 5% variance. Another reason why coffee processors still opt to do manual sorting is because there are no commercially available and reliable GCB sorting machines [Lualhati et al., 2022]. There is a need for a coffee sorter that is able to efficiently and accurately sort GCB. Coffee bean selection is carried out either manually, which is a costly and unreliable process [Santos et al., 2020]. The manual sorting process limits scalability and quality control, putting the strain on farmers as coffee shop owners' demands for high-quality coffee continue to rise [Lualhati et al., 2022].

1.4 Objectives and Deliverables

1.4.1 General Objective (GO)

GO: To develop an automated (Arabica) green coffee bean sorter that identifies good, less-dense and defective beans from an unsorted batch of coffee beans. The system will utilize machine vision and density-based analysis for defect detection and classification of the coffee beans, ensuring efficient coffee bean sorting.;

1.4.2 Specific Objectives (SOs)

- SO1: To gather and create a dataset consisting of 500 high-resolution images of good Arabica green coffee beans and 200 high-resolution images per classification of defective beans (Category 1 & Category 2).;
- SO2: To improve the synchronization between the machine vision system and the



- 392 embedded sorting mechanism, ensuring defect sorting of at least 20 beans per minute
393 for stage one, solving issues such as non-synchronization of the system.;
- 394 • SO3: To achieve an accuracy of at least 85% in classifying defective green coffee
395 beans using computer vision;
 - 396 • SO4: To achieve an accuracy of at least 85% in filtering out less-dense green coffee
397 beans;

398 **1.4.3 Expected Deliverables**

399 Table 1.3 shows the outputs, products, results, achievements, gains, realizations, and/or
400 yields of the Thesis.



TABLE 1.3 EXPECTED DELIVERABLES PER OBJECTIVE

Objectives	Expected Deliverables
GO: To develop an automated (Arabica) green coffee bean sorter that identifies good, less-dense and defective beans from an unsorted batch of coffee beans. The system will utilize machine vision and density-based analysis for defect detection and classification of the coffee beans, ensuring efficient coffee bean sorting.	A Two-Stage Automated Coffee Bean Sorter System that identifies defective, good beans, and less-dense green coffee bean using machine vision and density-based analysis.
SO1: To gather and create a dataset consisting of 500 high-resolution images of good Arabica green coffee beans and 200 high-resolution images per classification of defective beans (Category 1 & Category 2).	<ul style="list-style-type: none"> • Data Gathering • Image Collection through High Quality Camera
SO2: To improve the synchronization between the machine vision system and the embedded sorting mechanism, ensuring defect sorting of at least 20 beans per minute for stage one, solving issues such as non-synchronization of the system.	<ul style="list-style-type: none"> • Improving the synchronization of machine vision and embedded sorting mechanism of the system.
SO3: To achieve an accuracy of at least 85% in classifying defective green coffee beans using computer vision	<ul style="list-style-type: none"> • Computer Vision Program • Sorting Mechanism
SO4: To achieve an accuracy of at least 85% in filtering out less-dense green coffee beans	<ul style="list-style-type: none"> • Density-based Analysis • Sorting Mechanism



1.5 Significance of the Study

The study explores the implementation of machine Vision and density analysis of an automated coffee bean sorter that can identify and sort out the defective, less-dense and good green coffee beans. This said system would aid coffee sorters to mitigate manual labor and to ensure that the sorting process of the GCB are accurate. In order to test the effectiveness of the system, the study would gather data and compare the time efficiency and accuracy of the manual sorting by an expert sorter to be compared with the proposed system. The system proposes significance to specific parts of society as follows:

1.5.1 Technical Benefit

This study would benefit the academe as this introduces a significant advancement in coffee bean sorting technology by implementing both machine vision and density-based analysis to detect and sort good coffee beans, less-dense and separating defective ones. The proposed system would mitigate manual sorting that leads into insufficiency like human error and fatigue. The system would improve the overall efficiency by operating at a faster rate compared to manual labor. As a result, it would serve as a proof of concept for the implementation of machine vision and density-based analysis in agricultural industries specifically in the Philippine coffee industry.

1.5.2 Impact to the Coffee Industry

The study would aid coffee farmers and producers, by providing an automated system that ensures accurate sorting of Arabica green coffee beans, the system aims to have an accurate output to help maintain to yield higher quality coffee beans and allows coffee businesses



422 to scale up their operations, increase the competitiveness of exporting those beans, and
423 meet demand more efficiently. The productivity given from the system would potentially
424 strengthen the foundation of local coffee producers.

425 **1.6 Assumptions, Scope, and Delimitations**

426 **1.6.1 Assumptions**

- 427 1. There would be a defective coffee bean from the green coffee bean test batch;
- 428 2. Identifying the defective coffee beans using the machine vision and density-based
429 analysis would be much more efficient and accurate than manually sorting them;
- 430 3. During testing, test batches will contain 50% good beans and 50% defective beans,
431 60% good beans and 40% defective beans, 70% good beans and 30% defective beans,
432 80% good beans and 20% defective beans, 90% good beans and 10% defective beans,
433 100% good beans;

434 **1.6.2 Scope**

- 435 1. The study only focuses on Arabica green coffee beans;
- 436 2. The study has two stages, the first stage would segregate the defective green coffee
437 beans from the batch, then the second stage would identify the specialty-grade green
438 coffee beans depending on its density;



1.6.3 Delimitations

1. The batch of coffee beans to be used for testing and dataset collection will consist solely of Arabica beans from the same origin, farmer, and processed in the same way;
2. The system is only limited to unroasted green coffee beans;
3. The batch of coffee beans to be used should only be dehulled and not sorted visually and by density;
4. Since the system is considering several types of defects and density parameter, sorting time is compromised;
5. The system is designed to perform individual scanning of each coffee bean;

1.6.4 Overview of the Methodology

The rapid advancements in computer engineering have led to innovative solutions across various domains, including artificial intelligence and embedded systems. This thesis presents a novel approach to automated coffee bean sorting, addressing key challenges in manual classification and proposing a two-stage system that integrates machine vision and density-based analysis.

The study explores fundamental principles and technologies relevant to coffee bean classification, including machine vision, deep learning, and density-based sorting. By combining theoretical analysis with practical implementation, the proposed system aims to enhance sorting accuracy, reduce human labor, and improve efficiency and quality output in coffee production.



459 The study aims to develop a two-stage automated coffee bean sorting system using
460 machine vision and density-based analysis to categorize and identify good and dense
461 green coffee beans and segregate defective beans. First stage of the coffee bean sorting
462 by segregating the defective beans from the rest. Then the second stage will then focus
463 on sorting green coffee beans by identifying each bean's density, with classification and
464 processing achieved through density-based analysis. This approach ensures consistency
465 and improve coffee sorting to aid farmers providing a high-accuracy method for coffee
466 bean sorting.

467 The study's objective is to create a dataset consisting of 500 high-resolution images of
468 Arabica specialty-grade green coffee beans from a certain origin, to ensure sufficient data
469 for training and validation of the algorithm in the machine vision system. The system will
470 capture real-time data on the visual and density characteristics of each green coffee beans,
471 to aid coffee farmers from sorting each coffee bean efficiently. In the succeeding chapters,
472 the study will delve into existing research on automated coffee bean sorting systems, with a
473 focus on machine vision, density analysis, and their applications in the coffee industry. The
474 study would explore gaps in current manual sorting practices and demonstrate the system's
475 ability to improve overall efficiency through implementing advanced technologies.



476

1.6.5 Estimated Work Schedule & Budget

TABLE 1.4 BUDGET PLAN

Item	Quantity	Price	Total
IP Camera	2	999	1,998
Arduino Nano	2	300	600
ToF10120	1	400	400
Acrylic Platform	1	67	67
12 NEMA Stepper Motor	1	405	405
6V DC Motor	1	150	150
TB6612FNG Motor Driver	1	50	50
MT3608 Step-Up Module	1	50	50
Lighting Equipment (LED Bar, Ring, Spotlight)	3	80	240
Precision Weighing Scale	1	2,000	2,000
HX711	1	69	69
Rotating Conveyor Table 3D Printing	1	5,000	5,000
Inspection Tray 3D Printing	1	4,700	4,700
Density Sorter 3D Printing	1	2,500	2,500
Screw Feeder 3D Printing	1	3,500	3,500
Other Hardware Components/Wires	Approximate	Approximate	Approximate
Total Estimate		21,879 + approximate additional hardware components	

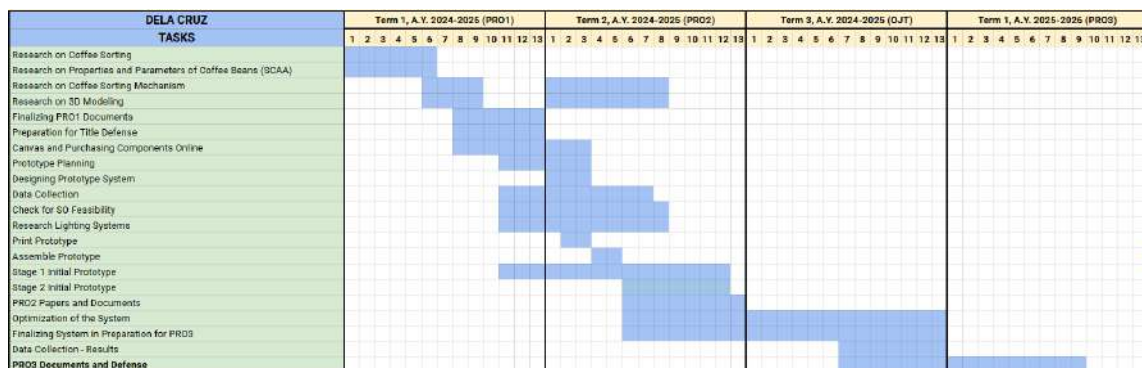


Fig. 1.1 Gantt Chart for John Carlo Dela Cruz

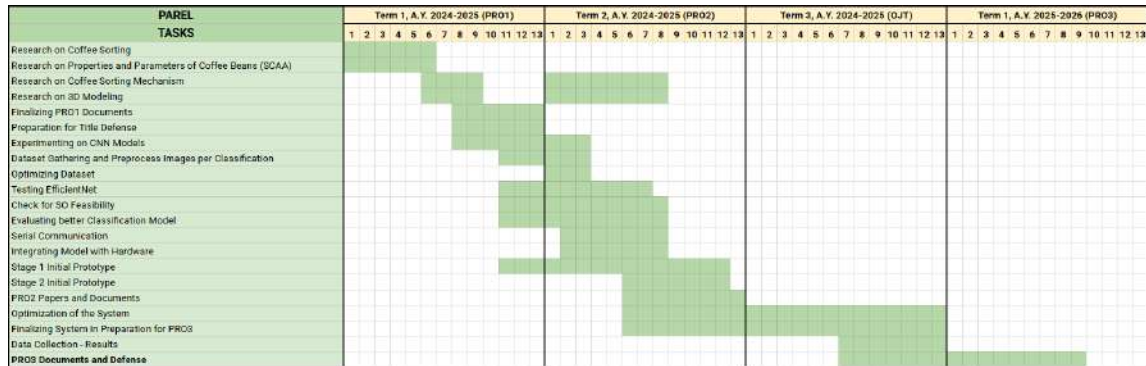


Fig. 1.2 Gantt Chart for Pierre Parel

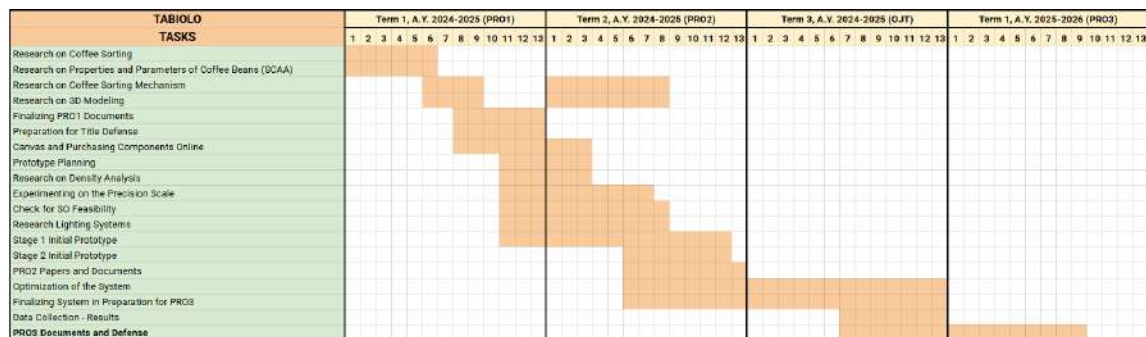


Fig. 1.3 Gantt Chart for Jiro Tabiolo

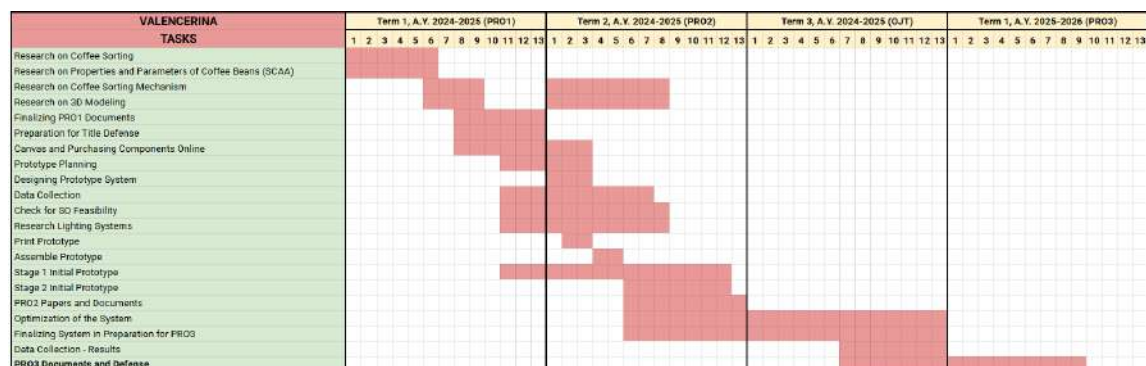


Fig. 1.4 Gantt Chart for Ercid Bon Valencerina



477

Chapter 2

478

LITERATURE REVIEW



2.1 Existing Work

TABLE 2.1 REVIEW OF RELATED LITERATURE

Literature	Description of the Literature
[Balay et al., 2024]	This study focused on the development of an automatic green coffee bean sorter. The algorithm used is the YOLOv8 to train the model, while a Raspberry Pi was used in order to test the model along with the sorting mechanism. There are a total of 6 defects that the system can detect these are full black, partial black, chipped, dried cherry, shell and dried cherries. A total of 10 trial were done to effectively test the system. Out of the 10 trials, 9 trials were found to have an average target sensitivity of 97.8%, with an average time of 2 minutes and 32 seconds for a total of 100 beans.
[Amadea et al., 2024]	In this study, a system was developed to detect defects in Arabica green coffee beans. The study used two different models such as Detection Transform (DETR) and You Only Look Once version 8 (YOLOv8). Upon comparison, YOLOv8 showed strengths in defect detection. On the other hand, DETR model showed significant strengths than the YOLOv8 model when it comes to defect detection.



[de Oliveira et al., 2016]	This study constructed a computer vision system that outputs measurements of green coffee beans, classifying them based on their color. In the system, Artificial Neural Network (ANN) was used as the transformation model. On the other hand, the Bayes classifier was used in classifying the coffee beans into four (whitish, cane green, green, and bluish-green). The model was able to achieve a small error of 1.15%, while the Bayes classifier achieved a 100% accuracy. To concluded, the developed system was able to effectively classify the coffee beans based on their color.
[Balbin et al., 2020]	In this study, the objective is to provide better technology for local coffee producers to increase export-quality beans production. Thus, the study proposed a device that can evaluate the size, quality, and roast level of a batch of beans fed into the machine. The model used in the system was the Black Propagation Neural Network (BPNN), together with other image processing techniques such as K-mean shift, Blob, and Canny Edge. These techniques were used to extract the features of the beans and analyzed using RGB analysis.



[Pragathi and Jacob, 2024]	The paper discusses the use of machine learning algorithms such as KNN and CNN to classify the specialty type coffee bean for Arabica. The coffee bean quality of an Arabica can be classified by the number of defective coffee bean presents in a sample. The defects are classified into two categories named primary and secondary.
[Lualhati et al., 2022]	With the lack of a locally made green coffee bean sorter in the Philippines, the researchers aimed to design and implement a device that will handle the sorting. The paper discusses the development of a Green Coffee Bean (GCB) quality sorter. The system used a PID based algorithm and image processing algorithm for sorting. It utilized two cameras to capture images of both sides of the GCB, this was done to check for the quality of the GCB through a prediction test. The paper conducted a total of 5 tests, each with varying conditions. The designed system on average got an accuracy score of 89.17% and sorting speed of 2 h and 45 mins per 1 Kg of GCB.



[García et al., 2019]

The paper discusses the use of computer vision for quality and defective inspection for GCBs. The paper makes use of parameters such as color, morphology, shape, and size to determine the quality of the GCB. It makes use of the algorithm k-nearest neighbors (KNN) to differentiate the quality and to identify the defective beans. The designed prototype makes use of an Arduino MEGA board to gather the data and a DSLR camera to capture the GCB. The type of bean used was an Arabica, and a total of 444 grains were used to test the prototype. The accuracy score for both the quality evaluation and defective beans resulted in an average of 94.79% and 95.78% respectively.



[Akbar et al., 2021]

The researchers proposed a system that sorts the Arabica coffee into 2 classes, defective and non-defective. After the classification into two classes, the coffee beans are then graded based on the quality consisting of: specialty grade, premium grade, exchange grade, below grade, and off grade. Utilizing computer vision for classifying the defective and non-defective beans, the researchers used the color histogram and the Local Binary Pattern (LBP) to get the color and the texture of the beans. The data gathered from both the color histogram and LBP are used to train two models, the random forest algorithm and the KNN algorithm. The results from both algorithms are both promising, with an average accuracy score of 86.56% using the random forest algorithm and 80.8% for the KNN algorithm. However, this result shows that utilizing the random forest algorithm provided better accuracy scores for the model.



[Huang et al., 2019]

The paper discusses the development of a GCB sorter in real-time by using Convolutional Neural Network (CNN). The researchers used a total of 72,000 images of good and bad beans, 36,000 per category respectively. A total of 7,000 images for the beans were picked at random to test the model, while the remaining was used to train the model. To test the model, a webcam was used to record the coffee beans, however this resulted in capturing only the topside of the bean, to solve this the beans were flipped to provide accurate results. This resulted in an average accuracy score of 93.34% with a false positive rate of 0.1007.



[Luis et al., 2022]

The paper focuses on using You Only Look Once (YOLOv5) as the algorithm for detecting the defective GCB. The researchers used a Raspberry Pi camera to capture the images of the coffee beans. To test the effectiveness of the developed system a total of 45 trials were conducted with varying classification that the model was trained on. The model tested a total of 15 trials for each classification, these classifications are black, normal and broken. Each classification provided different accuracy results, for the blackened coffee bean, a total of 106 coffee beans were tested which resulted with an 100% accuracy by correctly identifying 106 blackened coffee beans. For the normal coffee bean, a total of 117 beans were used which resulted in an accuracy score of 91.45% since only 107 out of 117, were accurately classified. Lastly, a total of 104 broken beans were used, which resulted with an accuracy score of 94.23% since only 98 beans were correctly classified. The average accuracy score of the system developed resulted in an average of 95.11%.



[Santos et al., 2020]	<p>In this study, the development of quality assessment of coffee beans through computer vision and machine learning algorithms. The main parameters that this study considers are the shape and color features of the coffee bean and they used machine learning techniques such as Support Vector Machine (SVM), Deep Neural Network (DNN) and Random Forest (RF), to identify the coffee beans' defect. The script written in Python Language was used to extract shape and color features of the coffee beans based on the datasets. Overall, the system had a very high accuracy (88%) on classifying coffee beans through the models that have been developed.</p>
[Arboleda et al., 2020]	<p>The study proposed a novel solution that deals with the low signal-to-noise ratio. The study shows a way of extracting features of an image in context with green coffee beans. The researchers concluded a new edge detection approach for green coffee beans. It was achieved by using the heuristic approach in calculating the right values for the discriminant and finding the best pixel formation.</p>



[Susanibar et al., 2024]

The proposed system aims to implement a GCB automated classification based on size and defects. The paper classified each bean into three different sizes. The system used two stages to identify the sizes of each bean. Firstly the entrance of the system was measured to ensure that the bigger beans are not able to pass through. The second stage involves the use of a cylindrical sieve with holes. This resulted with an average accuracy score of 96% for classifying the beans in size. However, the system does not provide a good accuracy score in classifying beans in terms of its defect since it only averaged 80% when classifying the defects of the beans.

[Srisang et al., 2019]

The study proposed an oscillating sieve as the main way for sorting Robusta coffee beans. Sizes are differentiated into 4 classes: extra large (XL), large (L), medium (M), small (S). The sieve resulted in an accuracy score of around 79% in classifying the sizes of the coffee beans.

480

481

2.2 Lacking in the Approaches

TABLE 2.2 COMPARING PROPOSED STUDY AND EXISTING STUDIES

Existing Studies	Proposed Study
------------------	----------------



- | | |
|---|---|
| <ul style="list-style-type: none">• Uses computer vision to classify green coffee bean grade based on its visual characteristics such as size, color, and shape.• Most related studies classify defective and non-defective beans only.• The density parameter of the green coffee beans is not considered.• Similar study [Lualhati et al., 2022] only considered three classifications of GCBs: Good, Black, and Irregular-Shaped beans.• Similar automated GCB sorter [Balay et al., 2024] only considered one side of the bean.• Existing classification of GCBs with automated sorters do not have an integrated graphical user interface (GUI) for data analytics. | <ul style="list-style-type: none">• Computer vision will be used to analyze the physical characteristics of the bean, including its volume.• Density parameters will be considered by implementing a weighing scale to the system.• The system will implement two stages of sorting:<ul style="list-style-type: none">– The first stage sorts out the defective beans.– The second stage sorts out the potential specialty-grade beans based on their density and size.• The system is designed to inspect both sides, utilizing two cameras.• The system is designed with a GUI for farmers to visualize the cumulative data of the defects present in the batch. |
|---|---|



2.3 Summary

The various related literature discusses the numerous technological advancements related to coffee bean sorting to aid coffee farmers and producers on efficient sorting and classification of beans. These studies provide insights regarding the various methods used in the field of coffee sorting that utilize machine vision, density-based analysis, and deep learning to identify and classify coffee beans based on their physical parameters. Numerous studies discussed parameters like size, defects, and color. However, existing studies tend to focus primarily on visual characteristics and lack integration density analysis for accurate classification of green coffee beans. The review literature identifies and acknowledges the gaps in current sorting practices, such as the lack of comprehensive systems that implement machine vision and density-based analysis. The study aims to address these gaps by proposing a two-stage sorting system that automates both detection of defective beans and the classification of less-dense beans. Density and size will play a significant role, as it is linked to identifying the quality of the coffee bean. However, related literature mentioned overlooks this parameter for classifying the coffee bean. Higher density beans are often associated with higher quality coffee beans, into being potential specialty-grade coffee after roasting and cupping.



De La Salle University

499

Chapter 3

500

THEORETICAL CONSIDERATIONS



501

3.1 Theoretical Framework

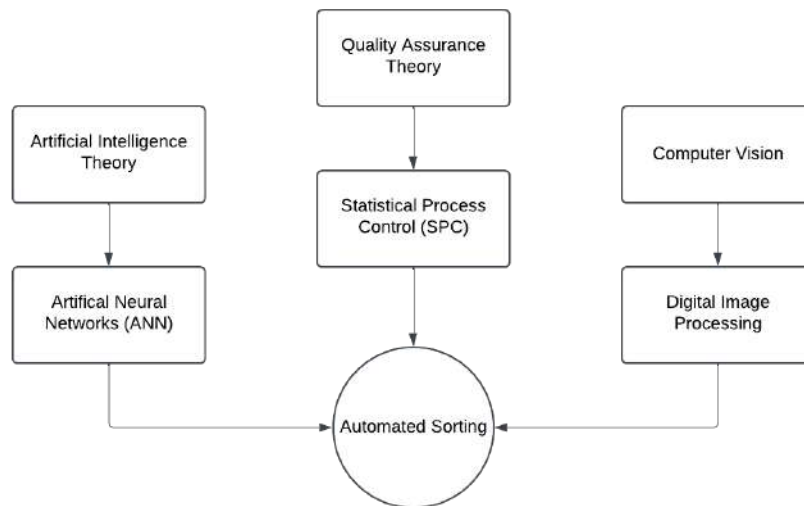


Fig. 3.1 Theoretical Framework

502 The theoretical framework discusses the multiple concepts that are involved in this
 503 study. These key concepts are crucial to ensuring the success of the thesis. There are three
 504 main concepts that are key to this study, the Artificial Intelligence Theory, the Quality
 505 Assurance Theory and lastly, Computer Vision.

506

3.2 Conceptual Framework

507 The conceptual framework shows the implementation of two systems which consists of
 508 machine vision and embedded systems. The framework describes the thought process of
 509 both systems with the end goal of integrating both systems. The machine vision handles
 510 the defect classification of the system, whereas the embedded system handles the sorting of

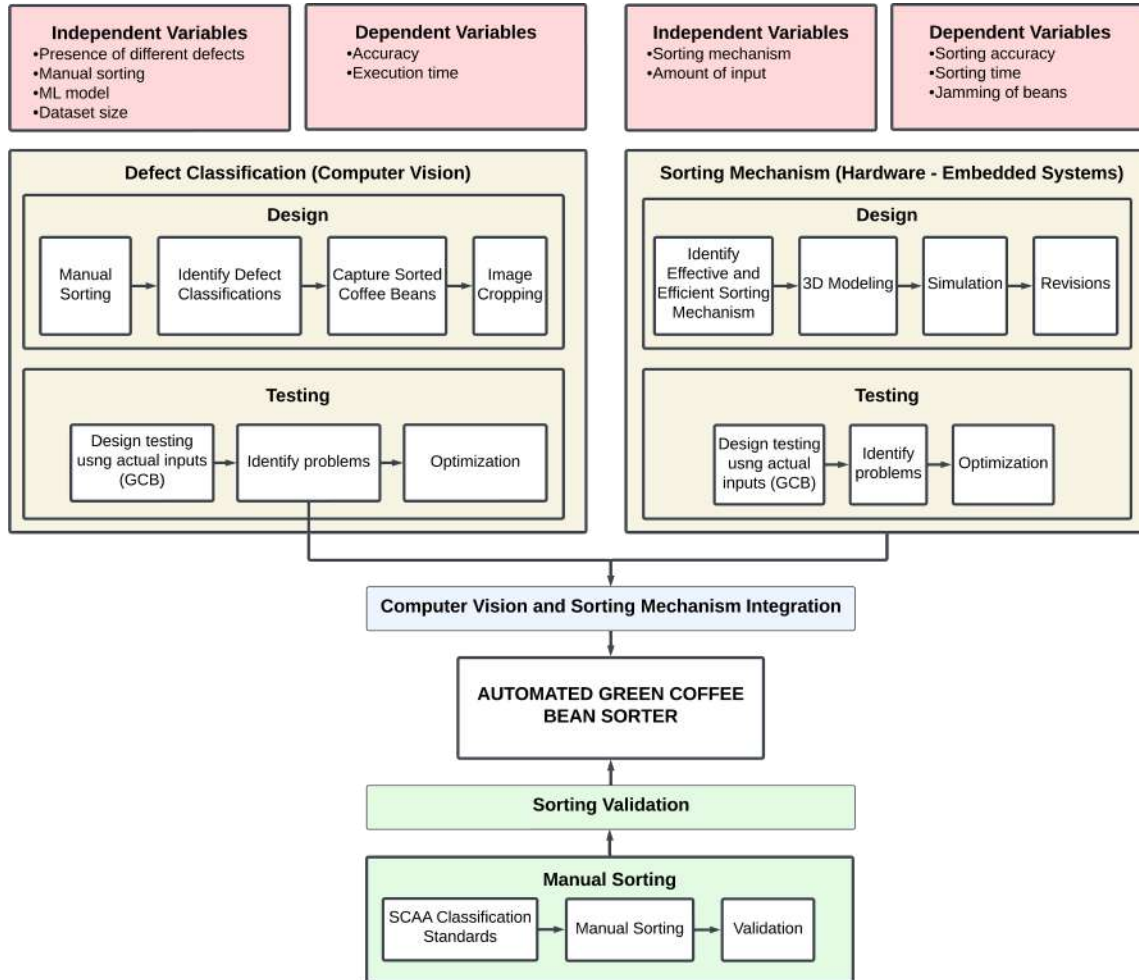


Fig. 3.2 Conceptual Framework

the beans. By integrating both systems together, creates an automated green coffee bean
 sorter. The data validation is done by sorting through the tested coffee beans by the system
 following the standards of the SCAA.



3.3 Quality Assurance Theory

Quality assurance theory refers to the set of principles and practices that focuses on establishing a systematic process to ensure that a product or service conforms to a predetermined standard. In the aspect of food and agriculture, there are a number of practices and principles that ensure the safety and quality of food products. According to [da Cruz et al., 2006], there are a number of practices in place that must be followed, one of which is Good Agricultural Practices, where these procedures are aimed to reduce hazards related to product safety at the farm level. Another one of said practices is the Good manufacturing practice, which were formerly called support programs that provide foundations to the overall food safety management programme. This includes cleaning, maintenance, personnel training, calibration equipment, quality control, and pest control. Industries that adopt such practices produce the following results, better quality products, greener initiatives and better productivity within a department. Lastly, hazard analysis and critical control points (HACCP), is a science-based system that was created to identify potential hazards and actions to control said hazards. This practice is used to ensure food safety.

In the context of coffee beans, there are a number of systems in place to ensure that quality beans are being provided to the consumer market. The governing body known as the Specialty Coffee Association (SCAA) has implemented grades to green coffee beans to provide a better way to classify said beans. These grades can be differentiated into 5 grades namely, Specialty Grade, Premium Coffee Grade, Exchange Coffee Grade, Below Standard Coffee Grade, and Off grade Coffee. They are classified according to the number of defects found in a sample batch of 300 grams and according to their size. Specialty grade coffee beans are supposed to contain less than 5 defects in a sample batch while also



not allowing any primary defects to be present; it should only have less than 5% difference between its sizes. Coffee beans in this grade should also contain a special attribute whether in its body, flavor, aroma, or acidity, and its moisture content should only be in the range of 9-13%. Premium Coffee grade beans should only contain 8 full defects in a sample batch but primary defects are allowed in the sample batch. Similarly to specialty grade coffee beans, its sizes should only contain a 5% difference to one another; it should also contain a special attribute and moisture content should also be similar to its specialty grade counterpart. Exchange coffee grade should contain defects ranging from 9-23 beans in a sample batch, with sizes that can vary up to 50% difference in weight but also only 5% in its sizes. Below standard and off grade coffee beans are classified according to the number of defects present in a sample batch; 24-86 beans for below standard while more than 86 beans for off grade. These gradings are used to ensure that quality green coffee beans are produced and ensure that consumers are provided with the best quality available.

3.4 Artificial Intelligence Theory

Artificial Intelligence in defect classification are widely used in this industry which are commonly used in manufacturing and industrial applications. Several deep learning techniques are used in order to achieve an effective defect classification. Models such as convolutional neural networks (CNNs) and You Only Look Once (YOLO) are widely used for classification. CNN utilizes an image based analysis and feature extraction approach to identify different classifications. CNN is more effective in analyzing grid-like data like images, making it suitable for defect classification [Das et al., 2019]. One of its major advantages is its ability to automatically detect important features such as shape, patterns,



and edges. Although it may have its own advantages, there are also disadvantages that need to be taken into account, mainly in scenarios that involve class imbalance and complex backgrounds (Moon, 2021) . YOLO is another model that is suitable for defect classification, its ability to provide real-time defect classification while also providing high accuracy is essential in some industries. In YOLO, there are several versions that are developed over the years, which are supposed to bring several improvements in terms of speed, accuracy, and computational efficiency. Combining different models is also effective, in the case of [Deepti and Prabadevi, 2024], they combined transformer architecture with YOLOv7 to enhance its feature extraction, this resulted in an increase of 5.4% in mean average precision and F1 score.

3.5 Computer Vision Theory

There are fundamental concepts that need to be done for image processing in detection. There are pre-processing techniques like preprocessing and segmentation. Pre-processing is a general term for preparing an image to be analyzed by the system, this includes techniques such as denoising an image, applying filters, and enhancing the image to further improve the visibility of defects [Lee and Tai, 2020] . Segmentation is dividing the images into segments to make the analysis simpler, methods such as histogram segmentation and active contour models helps in isolating the regions of interest.

For defect classification, feature extraction is important to identify the relevant features then extracting said features to to help indicate specific defects, this utilizes the edges, textures, and shapes to help in defect classification [Wu et al., 2024]. BY utilizing OpenCV and deep learning models is advisable for automatic feature extraction. Models like CNN,



can automatically extract features from images, which greatly reduces the need for manual extraction, this helps in a more robust and scalable solution [Bali and Tyagi, 2020]. The versatility of OpenCV library which allows support for multiple image pre-processing tasks, when combined with deep learning models can be applied to different fields.

3.6 Performance Evaluation

Accuracy, precision, recall, and F1 score are common measures to assess how well classification models predict. Accuracy measures how good a model is by computing the ratio of correct predictions to all predictions. While appropriate for balanced datasets, accuracy can be deceptive when dealing with imbalanced classes, since a model can be very accurate by predicting the majority class. Precision measures how well positive predictions are obtained by calculating the number of correct predicted positive instances. This is particularly important when false positives are costly, such as in the case of spam. Recall, or sensitivity, measures how well a model identifies true positive instances, which is very important in cases where failing to detect a positive instance is costly, such as in medical diagnosis. Since precision and recall trade off each other, the F1 score reconciles the two by computing their harmonic mean. This measure is particularly appropriate when a trade-off between precision and recall is desired, so that neither false positives nor false negatives dominate the assessment. In general, these measures provide a general impression of how good a model is and help decide how well-suited the model is for different applications.



3.7 Existing Technologies and Approaches

The paper done by [Lualhati et al., 2022], is a green coffee bean sorter that utilizes MATLAB as its image processing. The system created uses a PID based algorithm and image processing algorithm for sorting. The system utilized two cameras to capture both sides of the bean. The system of Lualhati et al. comprises only 3 green coffee bean classifications, which are good, black and deformed coffee beans. The developed system uses multiple stepper motors for the defect sorting, while 2 cameras were used to handle the green coffee bean detection.

The paper of [Balay et al., 2024], is an automatic sorting for green coffee beans utilizing computer vision and machine learning for defect classification. The system developed uses the YOLOv8 model alongside a Raspberry Pi based image processing to identify and classify the green coffee beans. The defects that the group classified are full black, partial black, chipped, dried cherry, shell, and insect damage. The system developed uses a conveyor belt and sorting motor for an automated defect separation. They used one camera module, the raspberry pi camera module 3 NoIR for the defect detection of the system.

3.8 Density Measurement

In measuring the density of the coffee bean there are a number ways this can be done, one way is by measuring the bulk density of the batch. This is done by measuring the mass of a batch then dividing it to a fixed volume. The more appropriate method for measuring the density of the coffee bean is called “free settle” density or free-flow density. This is defined as the ratio of the mass of the coffee beans to the volume they occupy after being allowed to flow freely into a container. It is expressed in grams per liter or kilograms per cubic meter.



$$d = \frac{m_2 - m_1}{V} \tag{3.1}$$

622 where m_2 is the mass of the green coffee bean, m_1 is the mass of the empty con-
623 tainer, and V is the capacity (in liters) of the container [International Organization for
624 Standardization, 1995].

625 **3.9 Summary**

626 This chapter gives the theoretical and conceptual backgrounds of an automated green coffee
627 bean sorter using Artificial Intelligence (AI), Quality Assurance, and Computer Vision. The
628 theoretical background focuses on key concepts like deep learning models (CNNs, YOLO)
629 used for defect classification, quality assurance principles (GAP, GMP, HACCP) ensuring
630 food safety, and computer vision algorithms (preprocessing, segmentation, and feature
631 extraction) used for image analysis. The conceptual background explains the integration of
632 machine vision for defect detection with embedded systems for sorting, thus conforming to
633 the SCAA coffee grading standards. Performance metrics like accuracy, precision, recall,
634 and F1 score are used for evaluating the performance of the model. Current technologies, for
635 instance, those of [Lualhati et al., 2022] and [Balay et al., 2024], provide insights relevant
636 to image processing and machine learning-based sorting techniques, thus contributing to
637 automated coffee bean classification development.



638

Chapter 4

639

DESIGN CONSIDERATIONS



4.1 Mechanical Design

4.1.1 Screw Feeder

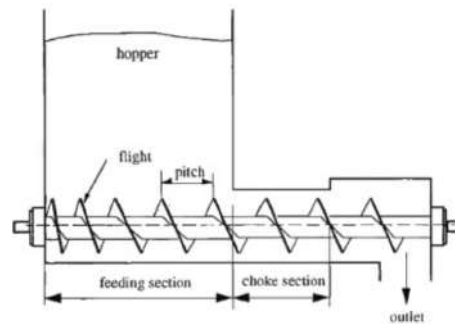


Fig. 4.1 Screw Feeder Diagram

Figure 4.1 shows the diagram of a screw feeder. Screw feeders are usually used in industrial fields like agriculture, chemicals, plastics, cements, poultry and food processing. According to [Minglani et al., 2020], screw feeders are specifically used to transport or move granular materials at a controlled rate like corn and wheat. It consists of a rotating screw and small feeding section or the hopper. Despite having big batches of a certain material, screw feeders can control the rate of which these materials are dispensed. With this concept, the group decided to utilize a screw feeder as the input mechanism for the system. This mechanism allows a controlled rate of coffee bean dispensing, which is a significant factor to avoid overcrowding in the rotating conveyor table causing the beans to jam. In addition, batches of coffee beans can be put at once instead of just adding a certain amount of beans at a time.



Fig. 4.2 Rotating Conveyor Table 3D Design, 32-inch Rotary Table Accumulator (RTA)

4.1.2 Rotating Conveyor Table

After the inputted beans comes out from the screw feeder, the coffee beans would then be placed in the rotating conveyor table. According to the study of [Dabek et al., 2022]. The conveyor table is used as a transportation systems for all forms of bulk materials to a certain machine or destination. The system utilizes the rotating conveyor table to have a controlled movement of coffee beans towards the first stage of the system. The improvised linearization system, consisting of metal guide rails and dividers ensures that beans align in a single path, reducing random movement, and improving the flow of the input beans. An infrared sensor would detect each bean as it passes, to control the movement of the bean preventing clogging and ensuring efficient operation.

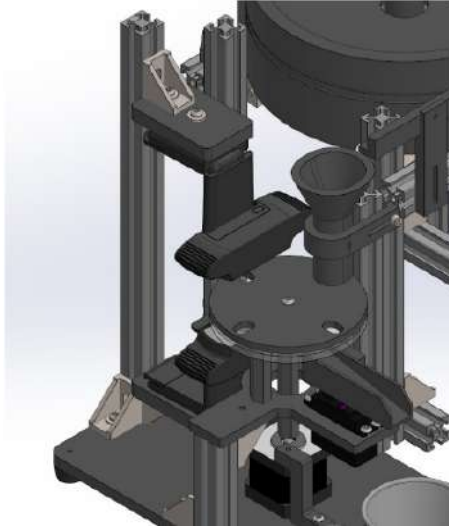


Fig. 4.3 Inspector Tray 3D Design

663 4.1.3 Inspection Tray (1st Stage)

664 The inspection tray serves as the platform for the machine vision based analysis of coffee
665 beans. It is designed with 8 holes, allowing uniform placements and optimal camera
666 positioning for the system. The system utilizes a two-layer structure: a stationary acrylic
667 platform and a rotating 3D-printed platform with holes. The rotating mechanism sequen-
668 tially positions each bean between two webcams, which captures and analyzes its physical
669 characteristics from top and bottom perspective. This design captures both sides of the
670 bean, ensuring a better classification of the bean. After inspection, the bean moves onto a
671 slide, where it is either directed to the second stage for density analysis (Good) or sorted
672 out as a defect.



4.1.4 Density Sorter (2nd Stage)

In measuring the density of the coffee bean there are a number ways this can be done, one way is by measuring the bulk density of the batch. This is done by measuring the mass of a batch then dividing it to a fixed volume. The more appropriate method for measuring the density of the coffee bean is called “free settle” density or free-flow density. This is defined as the ratio of the mass of the coffee beans to the volume they occupy after being allowed to flow freely into a container. It is expressed in grams per liter or kilograms per cubic meter.

4.2 Embedded Systems

4.2.1 Microcontroller

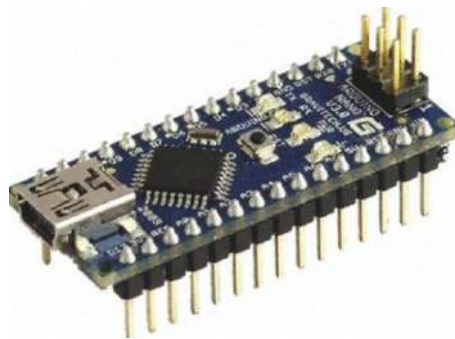


Fig. 4.4 Arduino Nano Microcontroller

Since the system is composed of two stages of sorting: defect sorting through computer vision and density-based analysis—the group decided to utilize two Arduino Nano microcontrollers to modularize the control process. The first Arduino Nano microcontroller is tasked to handle the computer vision-based defect sorting through serial communication with OpenCv operating in Python. In addition, it handles the operation of defect sorting



687 consisting of a stepper motor for the rotation of the inspection tray and a servo motor for the
688 slider, which directs the beans to the designated bin (defect or good bin). On the other hand,
689 the second Arduino Nano microcontroller manages the density-based analysis and sorting,
690 which consists of another stepper motor to direct the beans to its respective bin (dense
691 and less-dense bin), the precision scale which is interfaced through RS232, and the top
692 feeder where the input beans are poured. The use of separate Arduino microcontrollers is
693 advantageous when it comes to the computer vision-based sorting of beans. This is because
694 serial communication is much faster when code complexity is significantly reduced. With
695 this, a designated microcontroller handles the computer vision part and two-way serial
696 communication between the microcontroller and the computer vision algorithm running in
697 Python. Most importantly, the use of two microcontrollers allowed the system to not rely
698 solely on a sequential approach. This means that the two stages of sorting are not relying
699 on the timing of each other, allowing the inspection tray and the top feeder to operate
700 independently. Thus, resulting in a much faster and efficient sorting process.



701

4.2.2 Sensors



Fig. 4.5 Infrared Sensor

702 To ensure that the beans are falling in a one-by-one manner onto the inspection tray, the
703 group placed an IR sensor at the edge of the top feeder. This IR sensor triggers the DC
704 motor that runs the feeder to stop, and runs small steps until the bean is dropped. The
705 addition of the IR sensor at the edge of the feeder allows the motor to run continuously
706 until another bean is detected. With this, the waiting time for the next bean at the inspection
707 tray is significantly lessened.



Fig. 4.6 TOF10120

708 TOF10120 or Time of Flight sensor is utilized in the system due to its high precision,
709 non-contact measurement capability. This sensor is used to estimate the volume of each
710 bean, which is essential for computing the density. In the second stage of sorting, where
711 beans are classified based on density, the sensor plays a crucial role in determining the
712 approximate volume of each bean by measuring its height or dimensions as it passes
713 through the system.



714

4.2.3 Motor control



Fig. 4.7 12V NEMA 17 Stepper Motor

715

716

717

718

719

720

721

722

723

Two NEMA 17 12V stepper motors, paired with L298N motor drivers were used to control the movement of the inspection tray in the first stage and the density-based sorting mechanisms in the second stage. In these mechanisms, the group decided to use stepper motors to ensure precise and accurate movements. Precise and accurate movements are needed for the inspection tray to make sure every movement of the hole is perfectly aligned to the camera. Thus, allowing a more uniform and consistent angle for each bean to be inspected through the computer vision. In addition, NEMA 17 stepper motors were the best choice for these mechanisms due to its high torque, which is essential because it will be moving weighted objects.



Fig. 4.8 6V DC Motor

724 For the rotating conveyor table (top feeder), where the beans are initially poured, a
725 6V DC motor is used. The group decided to use this motor due to its high RPM, which
726 is needed for a fast rotation of the rotating conveyor table. The speed of the feeder is
727 regulated to prevent clogging and ensure that the beans are evenly spaced before they
728 enter the inspection tray. The motor speed is fine-tuned through pulse-width modulation
729 (PWM) to synchronize with the stepper motor-driven inspection tray, ensuring a steady
730 input without overwhelming the system.

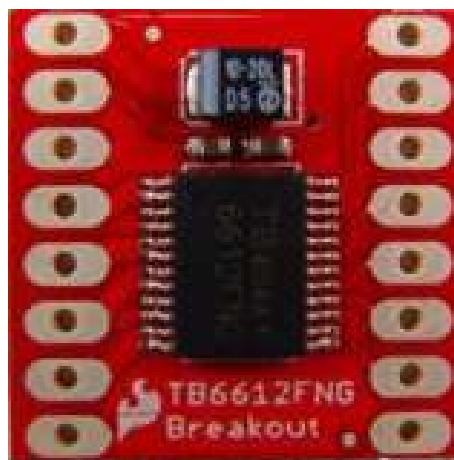


Fig. 4.9 TB6612FNG Motor Driver



To drive the 6V DC motor, the group utilized TB6612FNG, a motor driver module. This module also allowed PWM control for the motor, which is essential for reducing the speed of the motor when needed.

4.2.4 Operating Voltage



Fig. 4.10 12V Power Supply

The main power supply comes from a 12V external power supply, which provides enough voltage for all the components and keeps the voltage from dropping and interfering with system performance. The Arduino microcontroller is powered via its VIN pin, so it can function without the need for a USB connection and maintains a stable 5V logic output for sensor and actuator control. The NEMA 17 stepper motors that operate the inspection tray and density sorter are directly powered from the 12V supply and fed into L298N motor drivers to adjust voltage and monitor current flow. Operating these motors at 12V provides best torque output, which is vital in ensuring consistent movement during the sorting process.



Fig. 4.11 MT3608 Step-Up Module

744 For the top feeder mechanism, a step-up module is needed to supply the sufficient
745 voltage needed for the motor—6V. From the 5V output of the Arduino, the step-up module
746 will be utilized to convert it into 6V.

747 4.3 Computer Vision System

748 4.3.1 Image Processing



Fig. 4.12 C920 Camera



The system requires clear images of the coffee beans for accurate processing by the detection and classification models. Two C920 cameras will be used to capture images from opposite sides of each bean—one positioned on top and the other at the bottom. The captured images will then be processed within the laptop using the detection and classification models to identify and categorize the beans.

4.3.2 Object Detection and Classification Models

The object detection model identifies and isolates the coffee beans from the background. For this task, different models were explored:

1. RF-DETR

A transformer-based object detection model that eliminates the need for anchor boxes, improving small object detection.

2. YOLOv11

A CNN-based YOLO variant that incorporates the C3k2 block, SPPF, and C2PSA components to enhance feature extraction and detection accuracy.

3. YOLOv12

The latest YOLO version and attention-centric model that integrates transformer-based components to enhance performance while maintaining real-time efficiency.

4.3.3 Object Classification Models

Following detection, each identified coffee bean was cropped and classified based on its defect type. The classification models used included:



1. **EfficientNetV2**

A convolutional neural network (CNN) designed for high efficiency and accuracy, balancing computational cost and performance.

2. **YOLOv8**

A lightweight yet highly accurate model that supports both object detection and classification, making it suitable for real-time applications.

3. **YOLOv11**

A classification-specific adaptation of YOLOv11, leveraging enhanced feature extraction techniques for defect recognition.

4. **YOLOv12**

A classification variant of YOLOv12, incorporating advanced attention mechanisms to improve accuracy.

4.4 Serial Communication

Serial communication is used for sensors and motors for arduino due to the simplicity, reliability and efficient transfer of data between different devices. The precision scale uses a RS232 and a MAX TTL converter to send the data from the precision to the arduino to get the weight values of each green coffee bean. To sort out the good from defective beans the system utilizes a servo motor. The data from python is received by the arduino through serial communication. The python side is responsible for the decision and defect classification while the arduino is responsible for controlling the servo motor.

4.5 Graphical User Interface (GUI)



Fig. 4.13 Graphical User Interface

The proposed system would be integrating a graphical user interface developed using PyGui and ChatGPT API. The GUI would serve as the control center platform for the system. This would provide real-time feedback and insights for users. As shown in Figure 8, a concept of how the GUI would interact with the system would be a start button, once the button is executed the system would then be expecting inputs and start sorting. There would be real-time feedback during the sorting process, then some visual markers to indicate their classification, and an elapsed time so the user would be aware of the time of the sorting process. Once the system is done, the user can click the end button and the summary report would generate in an orderly manner, providing tables of classification that was detected through the process. In the bottom part of the GUI, ChatGPT API would be integrated and would offer recommendations based on the detected quality and classification of the coffee beans.



802 4.6 Density Analysis

803 The density analysis works by using a precision scale to measure the mass of the bean. To
804 get the data from the precision scale, serial communication is used from the scale to an
805 arduino nano. This is done by using a RS232 with a Max TTL converter for the arduino to
806 read the data from the precision scale. To sort out the good from defective beans the system
807 utilizes a servo motor for the density sorting mechanism. The servo motor is used to sort
808 the dense from the less dense beans. The sorting mechanism developed consists of gears
809 and cross-shaped modules to properly capture the beans and properly sort them out.

810 4.7 Technical Standards

811 4.7.1 Hardware

812 In the design and development of the system, the group incorporated and followed a series
813 of technical standards. One of which is ISO 12100:2010 – Safety of Machinery, where
814 general principles for risk assessment and reduction are discussed. Thus, the system is
815 designed, while keeping in mind the hazards associated with moving parts, making sure
816 that all moving parts in the system do not need to be touched for operations. An emergency
817 stop is also integrated into the system to stop all the moving parts in case of undesirable
818 incidents [International Organization for Standardization, 2010].

819 On top of this, ISO 14121-1 – Risk Assessment for Machinery was also followed to
820 further assess the potential risks throughout the system. The standard includes identify-
821 ing and quantifying hazards such as electrical short circuits, faulty wirings, and motor
822 overheating [International Organization for Standardization, 2007]. With this, the system



823 included protective enclosures for the electrical wirings, proper grounding of the circuits,
 824 and controlled motor actuation. More specifically, for motors, it was made sure that the
 825 design has sufficient voltage and ampere to power the different kinds of motors used with
 826 the use of L298N, and MT3608 modules. These are the main components for adjusting
 827 motor speeds dynamically during the sorting process.

828 Lastly, ISO 30071-1 was standard used to provide sufficient lighting during data
 829 collection, and real time bean inspection during sorting process. This standard helps ensure
 830 consistent and non-glare lighting conditions, which are essential for the machine vision
 831 cameras to accurately capture bean features [International Organization for Standardization,
 832 2019]. Uniform illumination improves the reliability of image classification by reducing
 833 shadow artifacts and reflections, thereby enhancing overall detection performance.

834 4.7.2 Software

835 For the software side of the system, the first applicable standard is ISO/IEC 25024 – Sys-
 836 tems and Software Engineering – Measurement of Data Quality, which offers a systematic
 837 method for measuring the quality of datasets utilized in information systems [International
 838 Organization for Standardization, 2015]. This standard was used during the dataset gather-
 839 ing and training for the different coffee bean defects like black, sour, insect damage, fungus
 840 damage, broken, floaters, and dried cherry. Practically, this included pre-processing the
 841 image data to eliminate noise, balance class distribution, and verify ground truth labels.

842 Lastly, ISO/IEC 23053 – Framework for Artificial Intelligence (AI) offers a reference
 843 architecture to build and integrate machine learning building blocks [International Organi-
 844 zation for Standardization, 2022]. This standard was highly applicable in determining the
 845 design of the machine vision module, where a pre-trained deep learning model is utilized



for the classification of bean defects. This standard provides guidelines on best practice for the overall machine learning cycle, ranging from data acquisition, feature extraction, and model training through to model evaluation, deployment, and monitoring.

4.7.3 Green Coffee Bean Sorting

For sorting green coffee beans, Specialty Coffee Association of America (SCAA) Standards for Green Coffee Bean Sorting was incorporated to maintain conformity. The standards set the definition for the classification of primary and secondary defects (i.e., black, sour, insect-damaged, broken, and floater beans) and sets the maximum allowable defect counts for specialty-grade coffee. The SCAA standards were applied to mark the training set of the machine vision model and also to set up the thresholds of defect classification, so visually defective beans can be correctly classified and rejected. Also, the sorting mechanism based on density points towards SCAA bean weight and volume guidelines using a precision scale and ToF sensor to sort beans based on within-acceptability density limits.

On the other hand, the system also adheres to PNS/BAFS 341:2022, the Philippine National Standard for Agricultural Machinery – Coffee Green Bean Grader – Specifications and Methods of Test [Bureau of Agriculture and Fisheries Standards, 2022]. It sets local criteria for testing coffee grading equipment on performance, safety, construction aspects, and methods of test. For the purposes of this research, PNS/BAFS 341:2022 is used as a reference for the design of the sorting mechanism, specifically in terms of the materials used in construction, handling of beans, and the efficiency with which the mechanical and electronic subsystems segregate. It also guides the testing procedure employed to verify sorting precision, capacity, and rates of misclassification under test conditions.



De La Salle University

868

Chapter 5

869

METHODOLOGY



TABLE 5.1 SUMMARY OF METHODS FOR REACHING THE OBJECTIVES

Objectives	Methods	Locations
GO: To develop an automated (Arabica) green coffee bean sorter that identifies good, less-dense and defective beans from an unsorted batch of coffee beans. The system will utilize machine vision and density-based analysis for defect detection and classification of the coffee beans, ensuring efficient coffee bean sorting.	<ul style="list-style-type: none"> • DDR Methodology • Description of the System 	Sec. 5.1 on p. 59 Sec. 5.2 on p. 62
SO1: To gather and create a dataset consisting of 500 high-resolution images of good Arabica green coffee beans and 200 high-resolution images per classification of defective beans (Category 1 & Category 2).	<ul style="list-style-type: none"> • Dataset Collection • Manual Sorting 	Sec. 5.3 on p. 63

Continued on next page



Continued from previous page

Objectives	Methods	Locations
SO2: To improve the synchronization between the machine vision system and the embedded sorting mechanism, ensuring defect sorting of at least 20 beans per minute for stage one, solving issues such as non-synchronization of the system.	<ul style="list-style-type: none"> • Data Collection • Dataset preprocessing • Model Training • Serial Communication 	Sec. 5.3 on p. 63 Sec. 5.5 on p. 70
Sec. 5.7.1 on p. 80 SO3: To achieve an accuracy of at least 85% in classifying defective green coffee beans using computer vision	<ul style="list-style-type: none"> • Dataset preprocessing • Model Training 	Sec. 5.5 on p. 70
SO4: To achieve an accuracy of at least 85% in filtering out less-dense green coffee beans	<ul style="list-style-type: none"> • Density Threshold Calibration Using Water Displacement Method • Density Sorter 	Sec. 5.4 on p. 69 Sec. 5.6.4 on p. 79



870

5.1 Description of the System

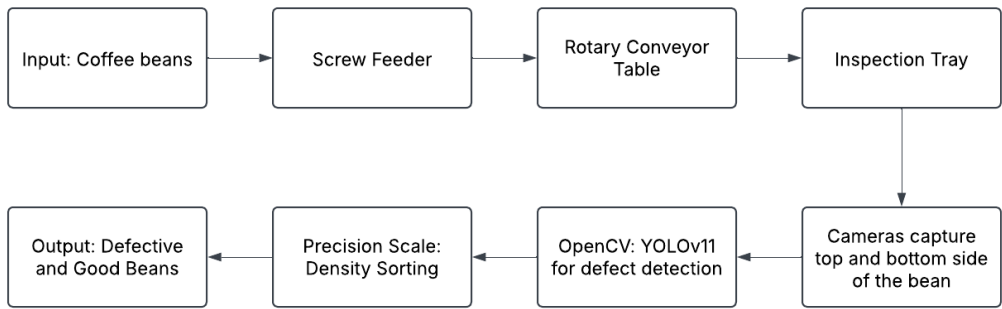


Fig. 5.1 System Block Diagram

871

The proposed system is a two-staged automated green coffee bean sorting machine, integrating both machine vision and density analysis. Firstly, the coffee beans are introduced into the system through a funnel, which directs them to a conveyor belt mechanism. In the first stage, the green coffee beans will be sorted depending on their visual characteristics. In this stage, the physical qualities of the bean is analyzed such as size, color, and defect. If the bean is defective, the system will automatically sort it out. Then, all the non-defective beans will go through the second stage of the system. In the second stage, there will be an IR sensor and a weighing scale. The IR sensor will help the system to calculate for the estimated volume of the bean. The volume and mass of the bean in hand, the density of the bean can be calculated. Depending on the density threshold and size threshold set by the user, the bean will be classified whether it is good or not.

881

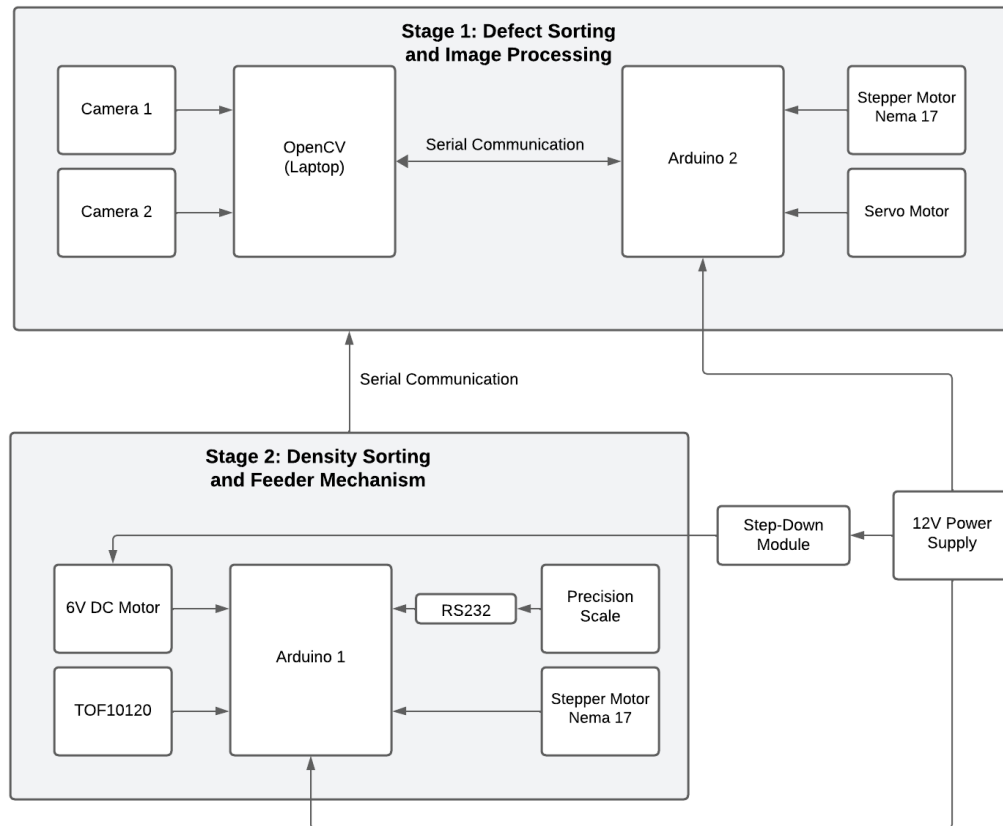


Fig. 5.2 Schematic Diagram of the System

Figure 5.2 shows the schematic diagram of the proposed system. Arduino Uno micro-controller makes all the mechanical components such as the servo motor, stepper motors, and the conveyor belt. The servo motor controls the rotating mechanism for bean sorting. On the other hand, the stepper motors operate a slide mechanism to direct the beans. Two cameras, integrated with OpenCV via Python, handle machine vision algorithms, and image processing for defect detection of the beans. A ToF10120 sensor provides precise distance measurement. A precision weighing scale measures the density of each bean for classification. The Arduino communicates with the OpenCV system through serial



communication, ensuring smooth coordination.

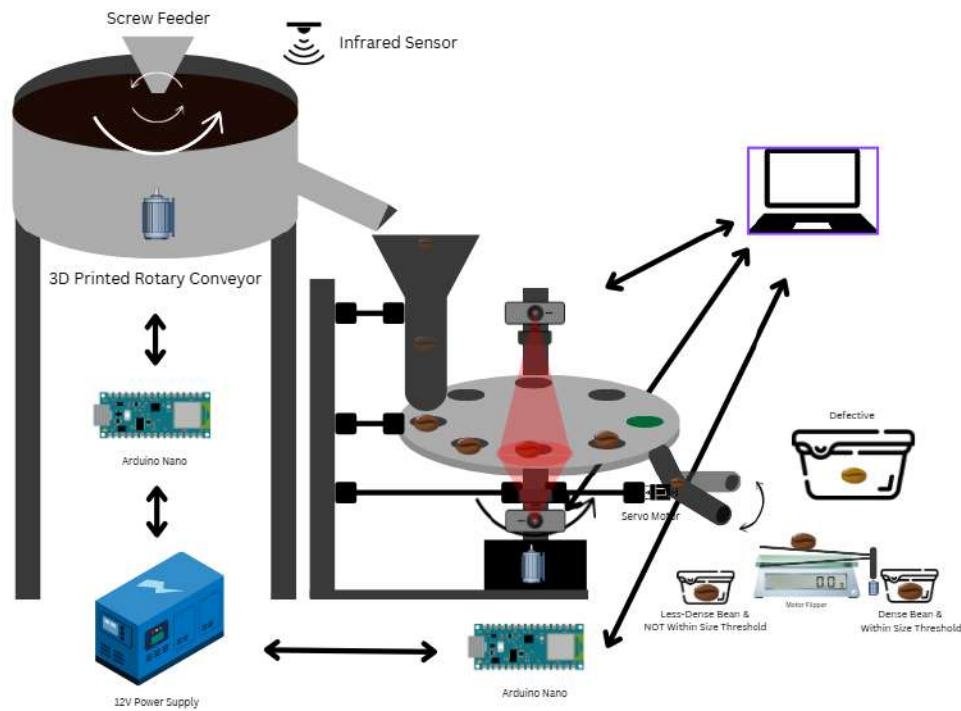


Fig. 5.3 Design Overview of the System

Figure 5.3 shows the design overview of the system. Beans are first arranged through a hopper and a conveyor belt. On top of the conveyor belt, a 3D-printed guide is attached for the beans to maintain a linear formation. Then, the beans are expected to fall into another funnel attached to a tube. The tube is directly attached to a rotating mechanism that allows the beans to be inspected and sorted one-by-one. In this stage, defective beans are sorted out. Then, the non-defective beans are transferred onto the precision scale to analyze the density. The less-dense beans are sorted out of the batch.

898

5.2 Research Design

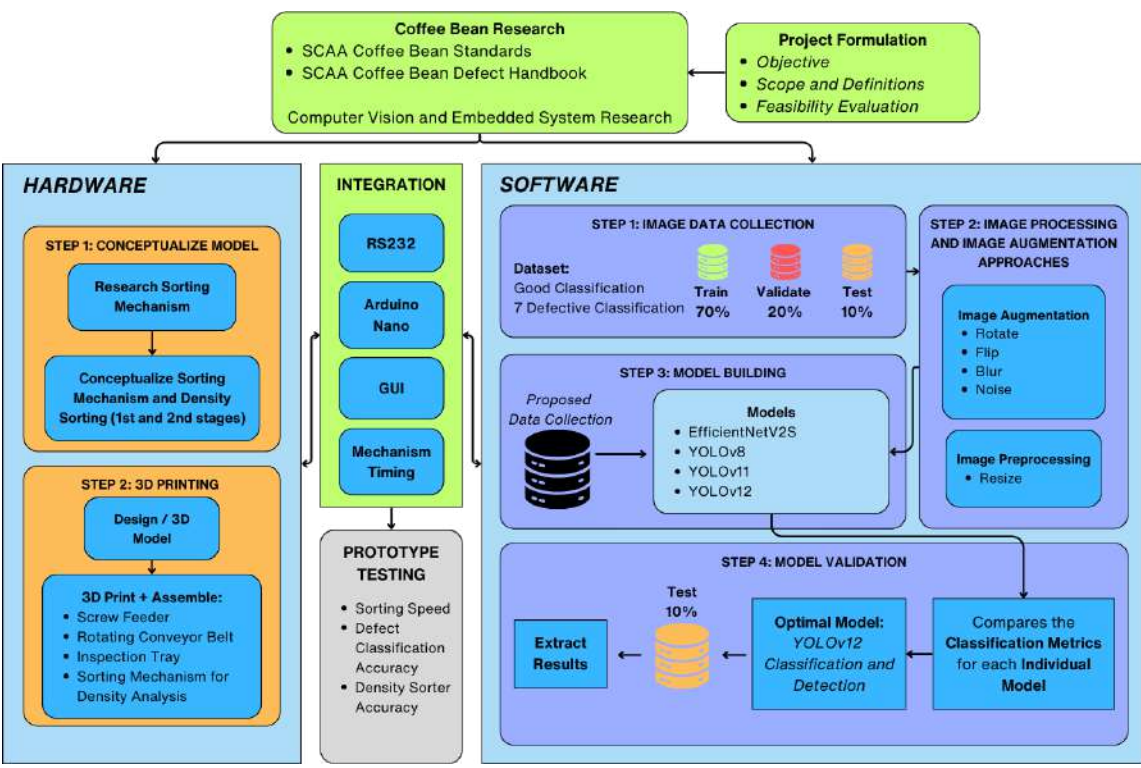


Fig. 5.4 Design and Development Research (DDR) Methodology

899

The researchers opted for a Design and Development Research model for the research.

900

As shown in Figure 5.4, there are multiple levels that were needed in order to develop a

901

working prototype for the system.



902

5.3 Dataset Collection

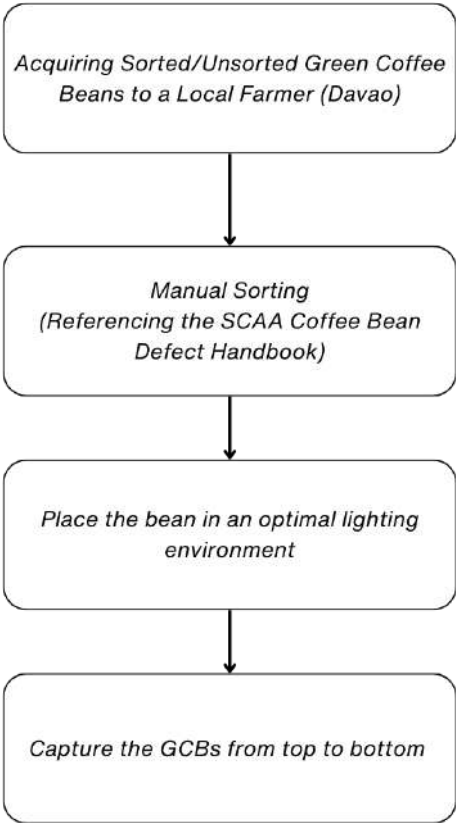


Fig. 5.5 Data Collection Process

903
904
905
906
907
908
909

For dataset collection, Arabica green beans from a farm will be used. Each bean will be captured by a high-resolution camera under sufficient and consistent lighting. Proper lighting is crucial, as it directly affects the visibility of the bean’s physical features, minimizing shadows, grain, and other noise that could result from inconsistent illumination. The top and bottom side pictures of the beans are to be collected. In addition, defective beans of the same type and origin will be gathered to identify the different classification of defects (primary and secondary). This study focuses on defects such as Broken, Dried Cherry,



Floater, Full Black, Full Sour, Fungus Damage, and Insect Damage. The dataset will include at least 500 images of good beans and a minimum of 200 images for each defect category. To expand the dataset and enhance model training, augmentation techniques such as scaling, rotation, and mirroring will be applied.

5.3.1 Dataset Collection and Model Training

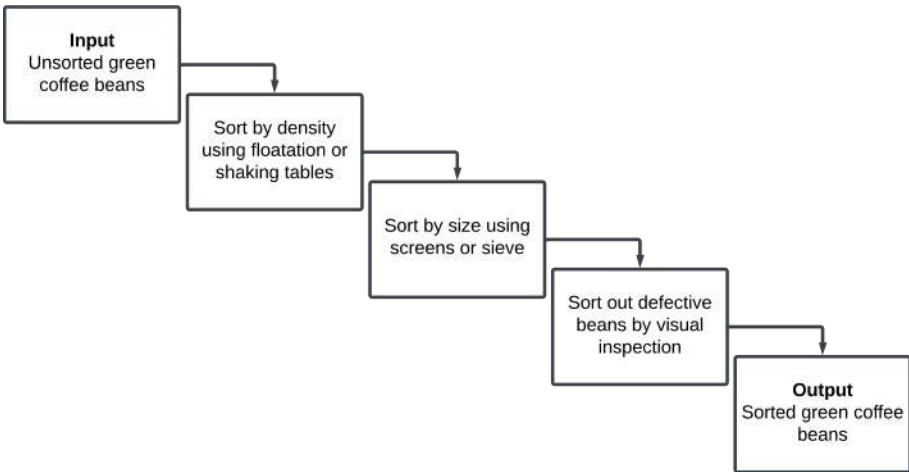


Fig. 5.6 Manual Sorting Process

The diagram in Figure 5.6 depicts the representation of the process of manual sorting of unsorted green coffee beans through a series of steps. First, the beans are sorted by density using methods such as floatation or shaking tables. This helps in separating the denser beans, usually pertaining to a more developed and higher quality bean. Then, the beans are sorted by size using screens and sieves with specific dimensions depending on the variety of the beans. After this, a thorough visual inspection is performed by the sorters to identify and remove the defective beans from the batch. To ensure consistency and accuracy, the group follows the Specialty Coffee Association of America (SCAA) Standards Defect



Handbook, which provide documentation and guidelines for identifying and classifying defective beans. Finally, the process results in the output of sorted green coffee beans, ready for further processing or sale. To ensure the dataset reflects real-world conditions, the group acquired Arabica green coffee beans from Davao. These beans were manually sorted to properly classify defective characteristics before capturing images for dataset creation. This step was crucial for improving the efficiency of batch image capture and ensuring accurate model training, making the system more applicable to Philippine coffee producers.

5.3.2 Utilization of Open-Source Database

To establish a foundation for the system’s model, the group initially referenced an open-source dataset from Kaggle. This dataset provides an original 500x500px images of Arabica green coffee beans categorize as defective or good. This dataset also provided insights into how individual beans were captured, including factors such as lighting, camera positioning, focus, and resolution. By analyzing the dataset, the group gained a better understanding of how to achieve a high-quality data collection, ensuring that the collected dataset would contribute to high model accuracy when it is fed into the system.



938

5.3.3 First Iteration of Dataset Collection



Fig. 5.7 First Iteration of Data Collection Setup

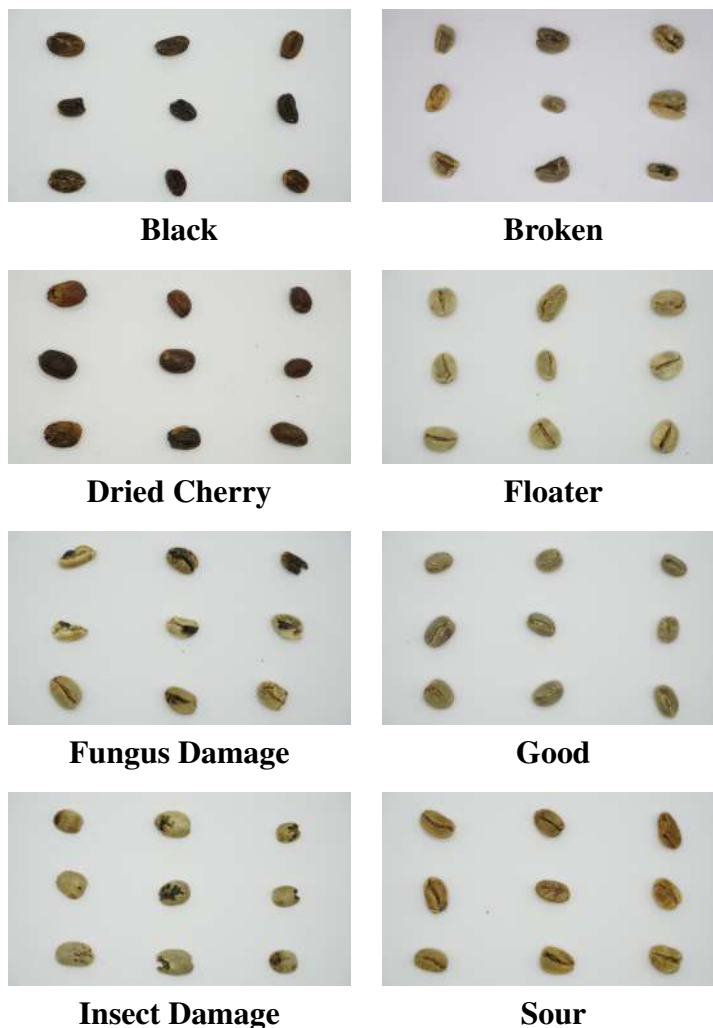


Fig. 5.8 Sample Images from the First Iteration of Dataset Collection

939 The first iteration of data collection utilized a Sony A6300 camera with its Kit Lens, set
 940 at 1/200 Shutter Speed, 1000 ISO, and a Distance of 50mm. The beans were captured in
 941 batches of nine, carefully arranged within the camera's field of view following the rule of
 942 thirds. The rule of thirds is a photographic composition principle where an image is divided
 943 into a 3x3 grid, creating nine equal grid lines to create balance to the photo. By aligning



the coffee beans with the rule of thirds, the group ensured a structured and even distribution of the beans within the frame. This setup also made it easier to automate the cropping process, as the predefined positions of the beans allowed a Python script to accurately extract individual images.

5.3.4 Second Iteration of Dataset Collection



Fig. 5.9 Sample Images from the Second Iteration of Dataset Collection



The second iteration focused on real-world implementation, using the system’s built-in webcam to capture images directly from the inspection tray. This setup represents the ideal condition, as it replicates the actual environment where the model will operate. The images captured in this iteration directly reflect what the system will process in a practical application, allowing for better generalization and real-time adaptability.

5.4 Density Threshold Calibration Using Water Displacement Method

Setting the threshold for bean density is crucial for the stage 2 sorting of the system, which involves measuring the density of each bean. In order to set a threshold for density-based classification, a calibration batch of Good quality coffee beans was chosen. The beans were confirmed to be free of defects and representative of typical specialty-grade coffee by the farmer. The threshold density was calculated by determining the average density of this batch through direct measurements of mass and volume.

The total volume of the batch of beans was measured by the water displacement technique, a commonly used method to measure the volume of solids that are irregularly shaped. The beans were fully immersed in a water-filled graduated cylinder, and the rise in water level was measured. The volume of water displaced is equivalent to the combined volume of the batch of beans, measured in cubic centimeters (cm³).

The overall weight of the beans was determined by a high-precision digital scale (at least to 0.001 g resolution). Both the mass and volume are known, and the batch density may be calculated through the use of the standard formula for density:



$$\text{Batch Density} = \frac{\text{Total Mass of Beans (g)}}{\text{Total Volume Displaced (cm}^3\text{)}}$$

This computed average density served as the threshold value in the system. During automated classification, individual bean density is calculated using estimated volume (from image analysis) and actual weight (from the precision scale via RS232 communication). Beans with a density lower than the threshold are classified as less dense, while those meeting or exceeding the threshold are considered dense, indicating higher quality.

5.5 Dataset Preparation and Model Training

5.5.1 Dataset Splitting

The dataset is divided into train, validation, and test sets in a 70-20-10 ratio. The training dataset will be used for model learning, which allows it to identify patterns in the image. The validation set is used to assess the model’s performance and fine-tune the parameters of the model during training. This is an iterative process wherein the model learns from the training data and is then evaluated on and fine-tuned on the validation dataset. Finally, the test set is used for evaluating the model’s final performance, assessing its ability to generalize to new data.

5.5.2 Image Annotation

Roboflow Annotate was used to label images of coffee beans. The platform was used for two separate datasets: one for the detection model, the other for the classification model. In the detection dataset, bounding boxes were drawn around individual coffee beans and



labeled accordingly. For the classification dataset, the trained detection model was used to crop individual coffee beans from the raw dataset, which were categorized into the eight different classifications. Roboflow was chosen for its ability to store datasets in the cloud and its support for different annotation formats, such as COCO and YOLO, ensuring compatibility with different deep learning models during experimentation.

5.5.3 Dataset Augmentation Techniques

Data augmentation techniques were applied using Roboflow's tools to improve the model generalization. Different augmentations such as rotation, flipping, blur, brightness and contrast adjustment, and noise were used to simulate variations, which helps prevent overfitting and improve the model's ability to identify defects in different lighting conditions and orientations.

5.5.4 Model Evaluation

Each trained model will be tested on the system, with a predetermined set of beans. The results from this test are analyzed by using a confusion matrix, providing a detailed breakdown of the model's performance for each category. The confusion matrix provides a way to interpret classification results by defining the following parameters:

- **True Positives (TP)** - The number of correctly classified instances for a specific defect type.
- **False Positives (FP)** - The number of times a different category was incorrectly classified as this defect type.



1008 • **True Negatives (TN)** - All correctly classified instances excluding the defect category
1009 in question.

1010 • **False Negatives (FN)** - The number of times this defect type was classified as
1011 something else.

1012 Through these parameters, key performance metrics such as accuracy, precision, recall,
1013 and F1-score were computed to evaluate the system’s performance in different classifica-
1014 tions as shown below. This test will assist in determining what types of defects the system
1015 correctly classifies and which types might need improvements in image preprocessing,
1016 dataset expansion, or optimization of the machine learning model. The outcome will be
1017 applied to optimize the sorting algorithm for minimal misclassifications to ensure greater
1018 reliability in real-world defect detection.

1019 1. **Accuracy** measures overall correctness of the classification model

$$Accuracy = \frac{TP + TN}{TP + TN + FP + FN} \quad (5.1)$$

1020 2. **Precision** measures how many of the predicted positive classifications were actually
1021 correct

$$Precision = \frac{TP}{TP + FP} \quad (5.2)$$

1022 3. **Recall** evaluates how well the model identifies actual positive cases

$$Recall = \frac{TP}{TP + FN} \quad (5.3)$$

1023 4. **F1-score** represents the harmonic mean of precision and recall

$$F1-Score = 2 \times \frac{Precision \times Recall}{Precision + Recall} \quad (5.4)$$



5.5.5 Model Benchmarking and Selection

Several models were trained and tested within the actual system to determine the most effective one. These models trained and evaluated include EfficientNetV2, YOLOv8, YOLOv11, and YOLOv12. Each model was assessed using the defined performance metrics and compared accordingly. The model with the highest overall performance will be selected for deployment in the system.

5.6 Hardware Development

The hardware elements of the system, two-stage automated coffee bean sorter, are developed to provide effective and precise sorting using a mix of mechanical and electronic components. Each element is designed and tested to maximize the sorting process while providing system reliability.



1035

5.6.1 Screw Feeder

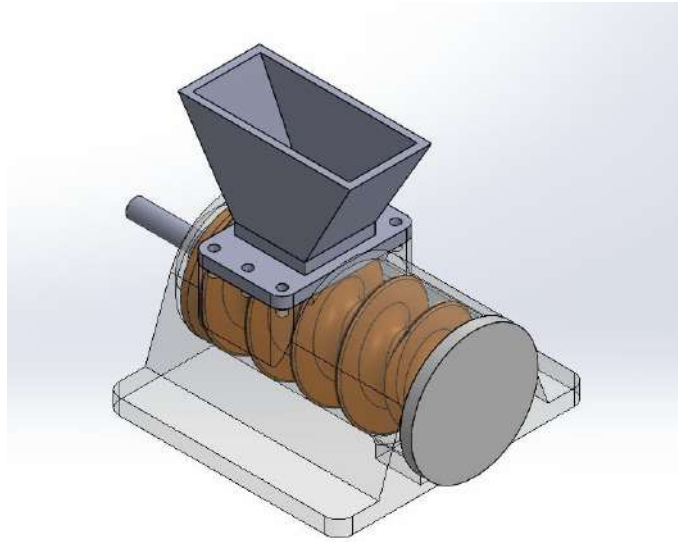


Fig. 5.10 Screw Feeder 3D Design

1036

1037

1038

1039

1040

1041

1042

1043

Screw feeder is the most essential of the devices as it governs the beans of coffee moving into the system. It operates mostly to deliver the beans consistently in terms of volume and ensures they do not bundle up and fall into the system in heavy masses, causing beans build up on the rotating conveyor table. The feeder is driven by a 12V DC motor, and the rotation speed is regulated using PWM. Through a constant and controlled flow, the screw feeder avoids clogging and provides a consistent input into the inspection tray, enhancing overall system performance. Figure 5.10 shows the actual 3D model design of the screw feeder used in the system.



1044

5.6.2 Rotating Conveyor Table

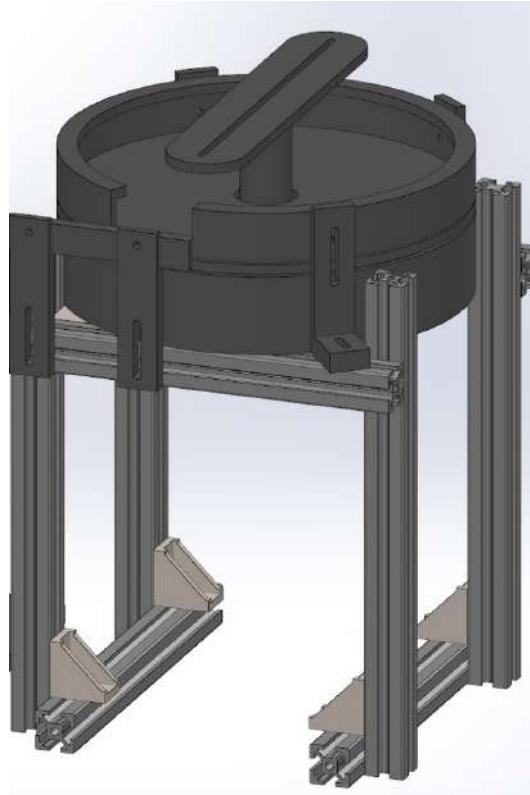


Fig. 5.11 Rotating Conveyor Table 3D Design

1045

The conveyor table, as shown in Figure 5.11, rotates to move the coffee beans from the feeding mechanism to the inspection tray. The table contains aluminum guides to linearly arrange the beans prior to dropping on the inspection tray. The conveyor is powered by a 12V DC motor, which offers consistent movement and regulated speed to avoid misalignment. By incorporating a turning mechanism, the conveyor guarantees beans are well oriented prior to inspection tray entry, minimizing classification errors due to faulty positioning.

1046

1047

1048

1049

1050

1051



Fig. 5.12 Rotating Conveyor Table with Aluminum Guides

As shown in Figure 5.12, the installed aluminum guides on the rotating conveyor table ensures coffee beans to be linearly arranged. This linear arrangement of beans significantly helped the system to ensure that coffee beans are dropped onto the slide, which connects the conveyor table to the inspection try, in a one-by-one manner. In addition, the aluminum guides are also installed to keep the beans from accumulating in one area, which can cause the jamming of beans. The researchers tested the different motor speeds to observe the optimal settings that will not cause bean jamming and meet the minimum sorting speed of the system.

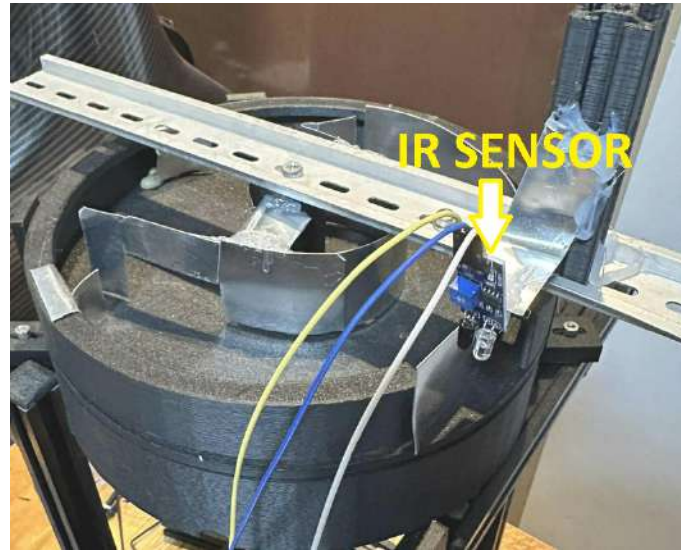


Fig. 5.13 Rotating Conveyor Table with IR Sensor

Initially, the rotating conveyor table is set at a fixed and slow speed to ensure that coffee beans are dropped into the inspection tray one-by-one. However, at this rate, the time travel time of the first bean dropped from the center of the table is very long. Thus, the group decided to add an IR sensor at the edge of the rotating table as seen in Figure 5.13. The sensor's responsibility is to detect if there is a bean at the edge. If there is no bean detected, the rotating table is set to a higher speed to expedite the process. On the other hand, if a bean is detected by the sensor, the rotation of the table is adjusted in such a way that it is able to drop the beans one-by-one onto the inspection tray. With this sensor integrated into the system, a higher speed can be set for the rotating table, minimizing the time travel of the beans from the center to the inspection tray, resulting to a faster sorting time for the first stage.



1071

5.6.3 Inspection Tray

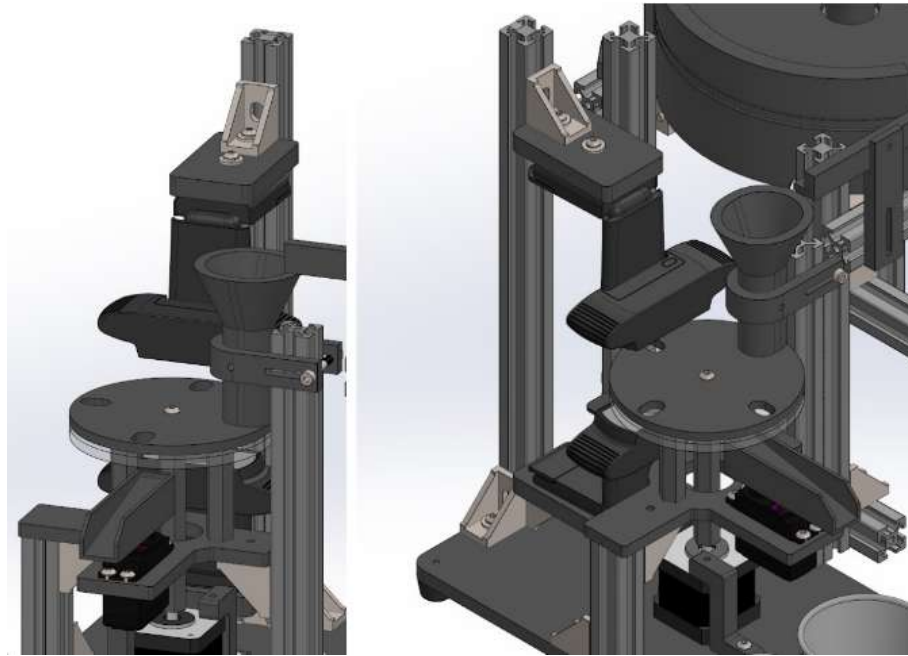


Fig. 5.14 Inspection Tray 3D Design

1072

1073

1074

1075

1076

1077

1078

1079

1080

1081

The inspection tray is the main component for the first-stage sorting mechanism. The inspection tray is used to support beans in a stable and constrained position for a short time, enabling the camera to take high-resolution images without motion blur. The NEMA 17 stepper motor drives the movement of the inspection tray, enabling accurate alignment with the vision system's image processing pipeline. The tray surface is created to reduce reflections and enhance contrast so that the camera can precisely detect defects like cracks, discoloration, or insect infestation. In addition, the surface is made of clear acrylic to allow a clear image for the camera positioned at the bottom of the tray. Lastly, a rotatable slider controlled by a 5V servo motor serves as the main segregator of the good beans from the defective beans.



1082 **5.6.4 Density Sorter**

1083 The density sorter is the second-stage sorting system, tasked with sorting coffee beans
1084 according to their measured density. This is achieved by initially measuring each bean's
1085 mass using a precision weighing scale and volume using the ToF10120 infrared sensor.
1086 After calculating the density, the system triggers a sorting system powered by a NEMA 17
1087 stepper motor, which sorts beans into various collection bins according to their classification.
1088 This sorting operation is such that high-density, specialty-grade beans are kept separate
1089 from low-density, commercial-grade or defective beans. The density sorter's accuracy is
1090 verified by comparing the results of its classification to manual weighing measurements
1091 (ground truth data).



Fig. 5.15 Precision Scale

1092 The U.S. Solid Electronic Precision Balance (0.01g, 1200g capacity, RS232 port,
1093 AC/DC power) was selected for the density sorting mechanism because it is highly accurate,
1094 transmits data in real-time, and is well-calibrated. Its 0.01g precision guarantees accurate
1095 mass readings, which are critical to precise density calculations in sorting coffee beans.
1096 The RS232 port facilitates smooth integration with the microcontroller for automatic data



1097 processing and sorting decisions, minimizing manual errors. Its dual power source (AC
1098 and battery) also guarantees uninterrupted operation in different environments, making it a
1099 dependable and efficient part of the coffee bean sorting system.

1100 **5.7 Hardware and Software Integration**

1101 **5.7.1 Serial Communication**

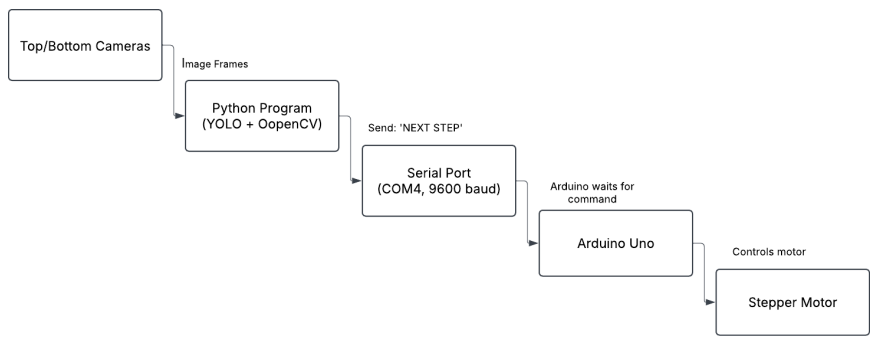


Fig. 5.16 Serial Communication Flow for Stage 1 Classification

1102 The system is generally composed of hardware and software components. Hardware
1103 components are mainly responsible for collecting data from the coffee beans such as the
1104 camera and IR sensor, and the sorting mechanisms such as servo motors and stepper motors.
1105 On the other hand, the software components are the brain of the system which is mainly
1106 responsible for data processing such as image detection, defect classification of the beans,
1107 volume and density computation, and control of the mechanisms. Since the system has
1108 two major components, software and hardware, they should be integrated together for
1109 the system to be as effective. Thus, serial communication was utilized to integrate the
1110 hardware and software components of the system. Serial communication is a significant



1111 component in the system as it serves as the communication medium of the hardware and
1112 software. It enables real-time coordination between the software (YOLO-based image
1113 detection, classification, and density computation) and the hardware (running in Arduino
1114 microcontrollers). The said communication is established with the use of a USB serial
1115 interface using the pyserial library in Python. In addition, this is configured at a baud rate
1116 of 9600.

1117 **5.7.2 Recommended Standard 232 (RS-232)**

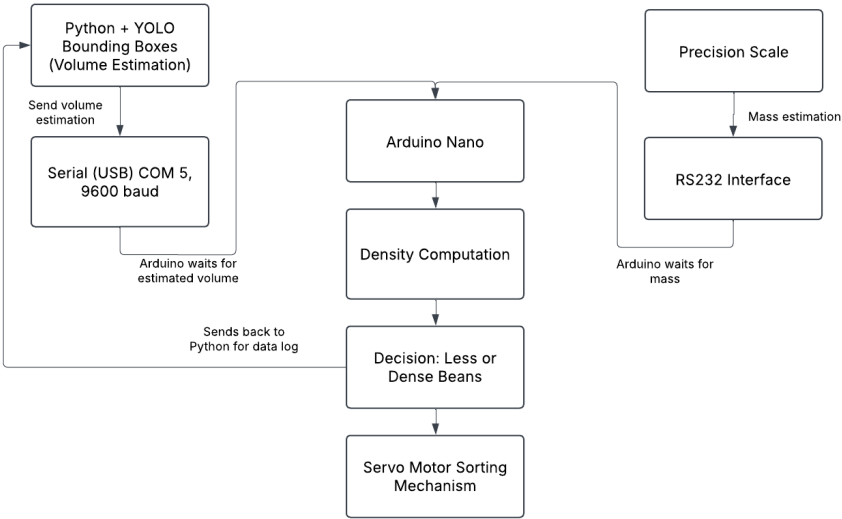


Fig. 5.17 Precision Scale Integration with RS232 for Stage 2 Classification

1118 The stage 2 classification is mainly composed of the sorting mechanism itself, and the
1119 precision scale to measure the mass of each bean. The bounding boxes from the stage 1
1120 classification are used to estimate each bean's volume. Additionally, the beans depth is
1121 also estimated through the IR sensor placed in the rotating conveyor table. With these
1122 measurements, the volume of each bean, the volume can be calculated using the Tri-axial



1123 Ellipsoid's volume formula. The system, specifically at the inspection tray mechanism
1124 where the YOLO detection and classification is implemented, has a function `move_stepper()`
1125 responsible for sending the command from the Python code to the Arduino microcontroller.
1126 When the Arduino receive this command, it executes motor movement that allows the
1127 stepper motor to move at a certain angle that allows the camera to capture the bean.
1128 This function is crucial for the system as this is how each bean in the inspection tray is
1129 fed to the image processing side of the system. This movement rotates the mechanism
1130 holding the coffee beans, positioning the next bean beneath the top and bottom cameras
1131 for inspection. After the motor completes the movement, the Arduino will send back a
1132 message to the program running Python, signalling that the bean is ready for image capture
1133 and further processing. In addition, the Python script is continuously or constantly waiting
1134 for the Arduino's message through the `arduino.readline()` function, ensuring seamless
1135 communication and faster processing.



5.8 Prototype Setup

5.8.1 Actual Setup

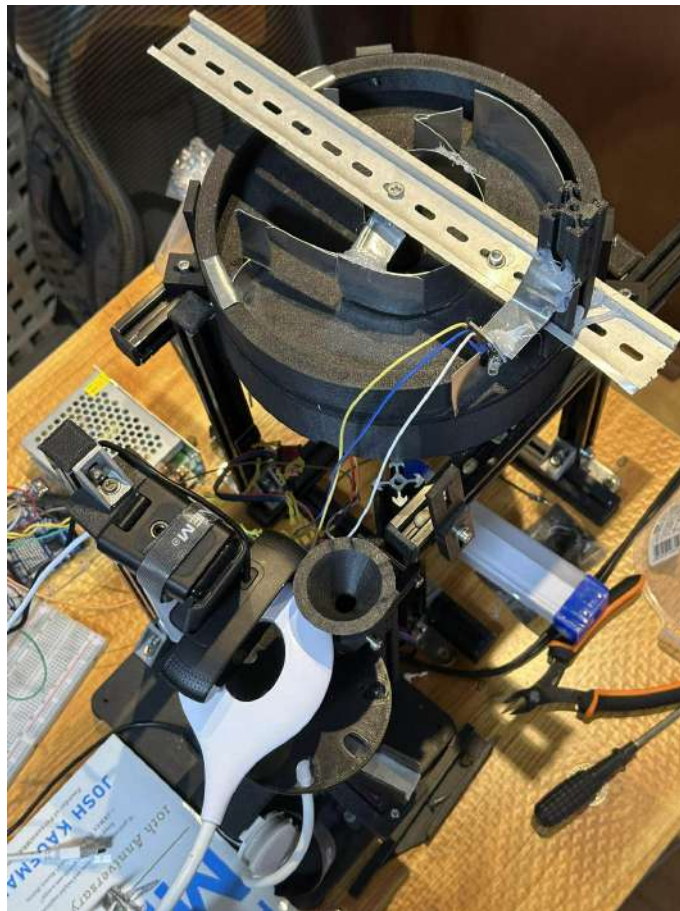


Fig. 5.18 Actual System Setup

Physical integration of the automatic coffee bean sorter system comprises various integrated parts with the purpose of enabling effective, accurate, and methodical sorting in terms of visual defects as well as density categorization. The system involves integration of mechanical, electronic, and computer vision technologies for optimizing sorting. To



begin the process, coffee beans are added to a revolving conveyor table, which is the main mechanism of transport used for feeding the beans into the inspection system. The conveyor features aluminum guides positioned strategically along it to ensure linear alignment of the beans as they travel. Linear alignment is required to avoid overlap and misclassification, since individual processing by the machine vision system is necessary for each bean. Once the beans travel further along the conveyor, they are conveyed onto the inspection tray. There, they are viewed in multiple perspectives by two high-definition cameras. A two-camera imaging process ensures improved defect detection by providing a full, thorough evaluation of the surface, shape, and texture of the bean. The images are then processed with a deep learning-based classification algorithm that classifies each bean as either defective or good according to predefined defect types like black beans, dried cherries, fungus damage, insect damage, sour beans, floaters, and broken beans.

After classification, the system triggers the defect sorting mechanism, which physically takes out defective beans from the processing line. The mechanism includes a servo motor-powered sorting slide, which diverts defective beans into a distinct collection bin. Good beans that are classified are taken to the second level of sorting, which is density-based classification. At the density-based sorting level, good beans are weighed individually with a high-precision electronic balance. The U.S. Solid Electronic Precision Balance (0.01g, RS232) is embedded within the system to accurately weigh the mass of each bean. A Time-of-Flight (ToF) sensor also estimates the volume of each bean, permitting the calculation of the density of beans. According to the calculation of density, beans are automatically sorted into corresponding collection bins using a second sorting mechanism regulated by a NEMA 17 stepper motor.



5.8.2 Lighting Setup for Inspection Tray

Lighting has a key importance in the image-based detection and classification system, specifically for the inspection tray. For the model to be more accurate and precise in classifying good and defective beans, correct lighting is important such that details like surface texture, color difference, and defects are properly rendered by the imaging system. Asymmetrical, unsteady, or low-quality lighting can create shadows, reflections, or over-exposure, all of which lower the quality of input images and thus decrease the accuracy of object detection and classification models like YOLO. To improve the consistency and definition of images taken during inspection, the lighting arrangement above the inspection tray was refined incrementally throughout development. The refinements were intended to maximize the illumination conditions for both the top and bottom camera modules.



Fig. 5.19 First Iteration of Lighting Setup

Figure 5.19 shows the initial lighting setup that the researchers implemented on the system. The initial lighting arrangement was based on a single top-mounted LED lighting. Although the arrangement was more than bright enough for the top camera, it introduced random shadows and highlights onto the bottom camera. As a result, only one side of the bean is accurately inspected. These random elements impacted the model's performance in detecting bean contours and separating surface flaws, particularly for dark beans or reflective-surface beans.

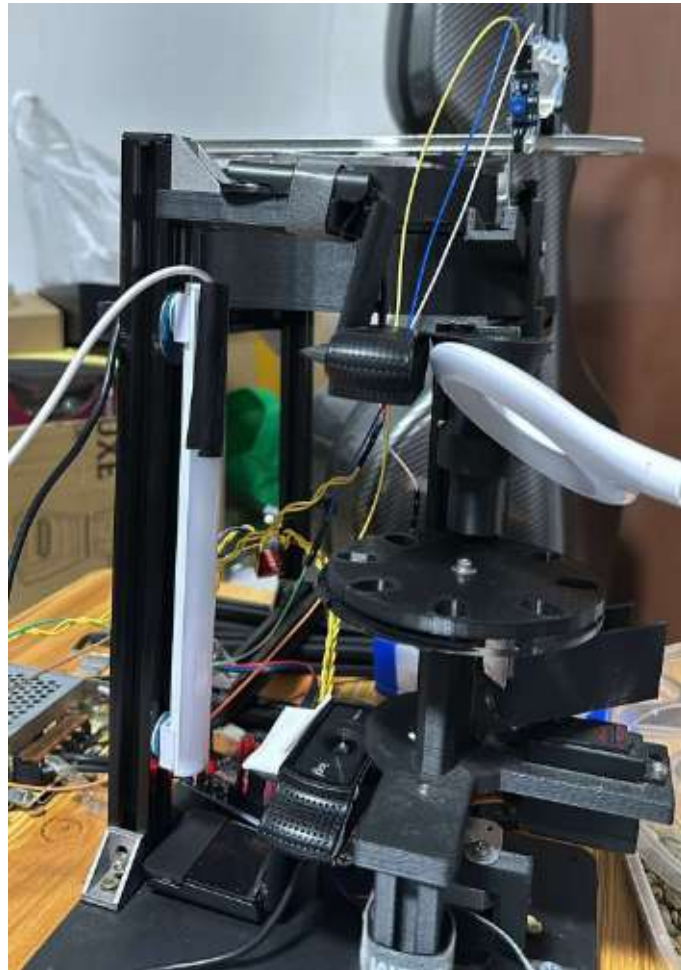


Fig. 5.20 Second Iteration of Lighting Setup

For the second iteration of the lighting setup, the researchers decided to add another LED strip lighting at the side of the inspection tray, while keeping the LED lighting mounted at the top. This provided good lighting for both top and bottom cameras. However, the view of the bottom camera is still a bit dark.

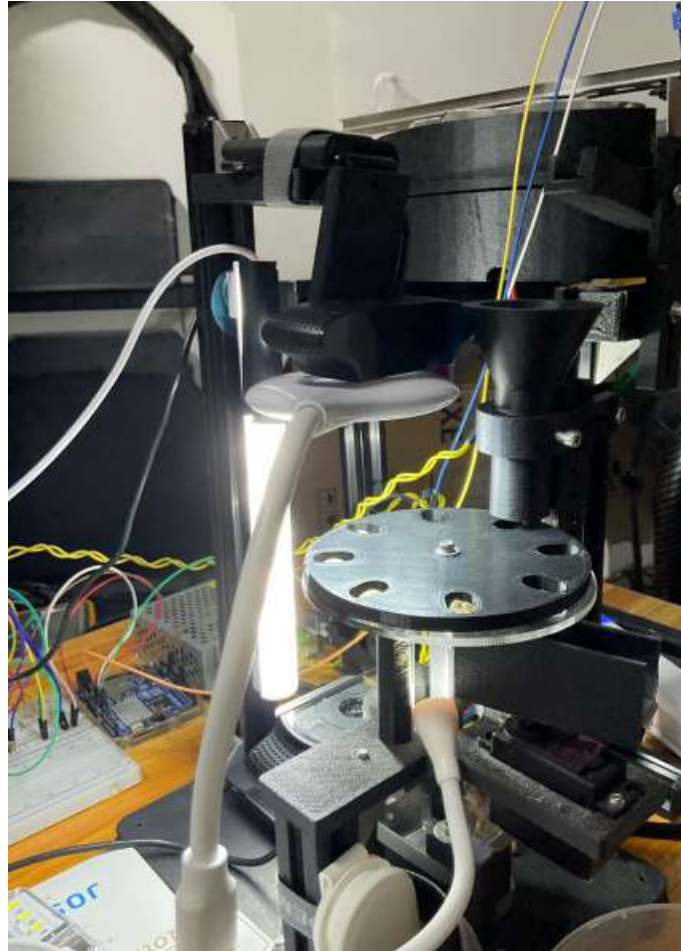


Fig. 5.21 Final Iteration of Lighting Setup

To ensure that both camera views have sufficient lighting and avoid shadows, the researchers decided to use a total of three LED lights. One is a small ring light placed exactly above the inspection tray. Another LED light is a strip light placed at the side of the inspection tray to improve lighting at the side of each bean. Lastly, another small LED light is placed under the inspection tray to ensure that the bottom camera has enough lighting.



Fig. 5.22 Top and Bottom View of the Cameras

5.8.3 System Operation

The system operation follows a sequential process to ensure the effective sorting of green coffee beans (GCBs) based on its classification and density. The automated system consists of two primary stages: 1st Stage which is the machine vision-based classification and 2nd stage which is the density-based sorting.

The process begins in the inputting of unsorted GCBs (Contains good and defective beans) into the screw feeder, which regulates the controlled and consistent delivery of the beans into the rotary conveyor table. The conveyor table is designed with aluminum guides to ensure a linearized formation of the beans to mitigate jamming. This also ensures a controlled movement of beans, ensuring that they drop onto the inspection tray one at a time. As the bean goes towards the edge of the conveyor table, the IR sensors detect the beans and stop the rotation to ensure the one-by-one inspection of the beans, this also prevents clogging, and jamming once the beans are dropped into the inspection tray.

The first phase involves machine-vision classification. Once the GCBs reach the inspection tray, each bean is analyzed one-by-one using a machine vision system consisting



1207 of top and bottom cameras. The system captures high-resolution images of the bean and
1208 processes the data to determine which classification it belongs. If the bean is identified as
1209 defective, a signal is sent to the servo motor, which redirects the bean into the defective bin
1210 for disposal, if the bean is classified as good, it then proceeds to the second phase of the
1211 system

1212 The second stage involves density-based sorting, where each GCB's weight is measured
1213 using a precision scale, while its volume is determined by the ToF10120 infrared sensor.
1214 The system then calculates the density and classifies the bean accordingly.

1215 The sorting mechanism activates, directing beans into designated collection bins based
1216 on their density. High-density beans, often associated with specialty-grade quality, are
1217 separated from low-density, commercial-grade, or defective beans.



5.9 Prototype Testing

5.9.1 Sorting Speed

TABLE 5.2 SORTING SPEED TESTING TABLE

Test Condition	Conveyor Table Speed (RPM)	Inspection Tray Speed (RPM)	Sorting Speed (Beans per Minute)
100% Good Beans			
80% Good, 20% Defective Beans			
70% Good, 30% Defective Beans			
50% Good, 50% Defective Beans			
100% Defective Beans			

The sorting speed of the system will be determined by conducting at least five trials. Each trial will be exactly conducted for one minute. The number of beans sorted out within the time frame are considered as the sorting speed in beans per minute. Then, the average sorting speed from the five trials is computed. In each trial session, controlled variables such as motor speed of the inspection tray and rotating conveyor table are varied to observe the optimal setting for the system, ensuring that there are no beans jamming in the tray and fast enough to meet the minimum sorting speed. Table 6.6 shows the different conditions for each trial to ensure that the sorting speed across different type of beans are considered.



1228

5.9.2 Defect Sorting Accuracy

TABLE 5.3 GOOD BEAN CLASSIFICATION ACCURACY TESTING TABLE

Test Condition	Correctly Classi- fied Beans	Misclassified Beans	Total Number of Beans
100% Good Beans			100
80% Good, 20% Defective Beans			100
70% Good, 30% Defective Beans			100
50% Good, 50% Defective Beans			100
100% Defective Beans			100

1229

1230

1231

1232

1233

1234

The defect sorting accuracy by feeding 100 beans on each trial. For testing its accuracy for detecting good beans and defective beans, five trials are conducted containing 100 beans of good beans for the first trial, 80 good and 20 defects for the second trial, 50 good and 50 defects for the third trial, 20 good and 80 defects for the fourth trial, and 100 defects for the last trial. With these, the number of correctly classified and misclassified beans are logged into the system to compute for accuracy using the formula:

$$\text{Accuracy}(\%) = \left(\frac{\text{Correctly Classified Beans}}{\text{Total Beans Tested}} \right) \times 100 \quad (5.5)$$



TABLE 5.4 SPECIFIC DEFECT CLASSIFICATION ACCURACY TESTING TABLE

Test Condition	Correctly Classified Beans	Misclassified Beans	Total Number of Beans
100% Good Beans			100
80% Good, 20% Defective Beans			100
70% Good, 30% Defective Beans			100
50% Good, 50% Defective Beans			100
100% Defective Beans			100

For further accuracy testing of the computer vision model in actual implementation, the researchers also included testing trials for each defect type. Table 5.4 shows how each trial is conducted. For example, the defect type chosen for the test is the Sour defect type. The first trial contains 100 sour beans. For the second trial, 80 sour beans and 20 randomly selected beans, excluding the chosen defect type which is sour. Thus, the random beans are always the other classes except the chosen defect type to be tested. In this test, correctly classified beans and misclassified beans are also considered to compute for the accuracy of the system. By testing the system under different defect distributions, the robustness of the machine vision model can be assessed.



TABLE 5.5 DATASET DISTRIBUTION FOR OVERALL TESTING

Bean Classification	Bean Count
Black	20
Broken	20
Dried Cherry	20
Floater	20
Fungus Damage	20
Good	20
Insect Damage	20
Sour	20
Total Beans	160

Lastly, to assess the overall accuracy and reliability of the first stage, machine vision-based defect classification, a trial consisting of a predefined dataset of 160 coffee beans was conducted. Each category consists of 20 beans as shown in Table 5.5, including good beans and the other defect types such as black, dried cherry, fungus, insect damage, sour, floater, and broken beans.

5.9.3 Density Sorting Accuracy

To assess the accuracy of the mechanism, it will rely on measuring the accuracy and the reliability of the density sorting mechanism in sorting out the dense beans to the less dense beans. To successfully determine the accuracy of the system, the basis will be the scale, where the system should be able to sort the dense beans to the less dense bean in relation to the detected weight in the scale. A successful system should be able to sort with an accuracy of 85



De La Salle University

1256

Chapter 6

1257

RESULTS AND DISCUSSIONS



TABLE 6.1 SUMMARY OF RESULTS FOR ACHIEVING THE OBJECTIVES

Objectives	Results	Locations
GO: To develop an automated (Arabica) green coffee bean sorter that identifies good, less-dense and defective beans from an unsorted batch of coffee beans. The system will utilize machine vision and density-based analysis for defect detection and classification of the coffee beans, ensuring efficient coffee bean sorting.	<ul style="list-style-type: none"> Achieved to gather and create a unique dataset consisting of 500 good and 200 defective beans Achieved improvisation of the synchronization between the machine vision and embedded system. 	Sec. 6.1 on p. 99
SO1: To gather and create a dataset consisting of 500 high-resolution images of good Arabica green coffee beans and 200 high-resolution images per classification of defective beans (Category 1 & Category 2).	<ul style="list-style-type: none"> Acquired 257 images of Black coffee beans Gathered 301 images of Broken coffee beans Gathered 305 images of Dried Cherry coffee beans Acquired 288 images of Floater coffee beans Acquired 301 images of Fungus Damage coffee beans Gathered 1565 images of Good coffee beans Acquired 345 images of Insect Damage coffee beans Gathered 320 images of Sour coffee beans 	Sec. 6.1 on p. 99

Continued on next page



Continued from previous page

Objectives	Results	Locations
SO2: To improve the synchronization between the machine vision system and the embedded sorting mechanism, ensuring defect sorting of at least 20 beans per minute for stage one, solving issues such as non-synchronization of the system.	<ul style="list-style-type: none"> Achieved 22 beans per minute for stage one of the system 	Sec. 6.4 on p. 111

Continued on next page



Continued from previous page

Objectives	Results	Locations
SO3: To achieve an accuracy of at least 85% in classifying defective green coffee beans using computer vision	<ul style="list-style-type: none"> Achieved 90.07% testing accuracy in classifying Black coffee beans. Achieved 90.07% testing accuracy in identifying Broken coffee beans. Attained 90.65% testing accuracy in recognizing Dried Cherry coffee beans. Recorded 87.78% testing accuracy in detecting Floater coffee beans. Achieved 90.65% testing accuracy in classifying Fungus Damage coffee beans. Reached 90.07% testing accuracy in identifying Good coffee beans. Attained 90.07% testing accuracy in detecting Insect Damage coffee beans. Achieved 90.65% testing accuracy in classifying Sour coffee beans. Achieved 90.00% overall testing accuracy of the system. 	Sec. 6.3 on p. 108
SO4: To achieve an accuracy of at least 85% in filtering out less-dense green coffee beans	<ul style="list-style-type: none"> To achieve 90% in filtering out less-dense coffee beans 	



6.1 Description of the New Custom Dataset

TABLE 6.2 CLASS DISTRIBUTION SUMMARY

Class Name	Image Count
Black	205
Broken	203
Dried Cherry	206
Floater	202
Fungus Damage	207
Good	604
Insect Damage	201
Sour	202
Total	2030

Table 6.2 presents the dataset's class distribution after adjustments. The image counts for each category were increased such that the minimum is above 200, with "Good" exceeding 543; for instance, Black has 205 images and Good has 604 images. The table confirms a total of 2,030 images distributed across the eight classes, ensuring a balanced dataset that maintains diversity while meeting the minimum requirements.

TABLE 6.3 DATASET SPLIT SUMMARY

Split	Percentage	Image Count	Augmentation
Train	70%	1421	Original training images are augmented three times
Validation	20%	406	Non-augmented
Test	10%	203	Non-augmented

Table 6.3 outlines the dataset split into training, validation, and test sets. The training set comprises 70% (1,421 images), while the validation and test sets account for 20% (406



1266 images) and 10% (203 images) respectively, with the training images later augmented 3×
1267 per image.

1268 **6.2 Performance of Classification Models on Cus-**
1269 **tom Dataset**

1270 Four different classification models, such as EfficientNet, YOLOv8, YOLOv11 and
1271 YOLOv12, were benchmarked to determine the most optimal model to be used for the sys-
1272 tem. Each model was trained using a custom dataset manually gathered by the researchers.
1273 In addition, augmentations such as rotation, flip, blur and noise, were applied.



1274

6.2.1 EfficientNetV2S

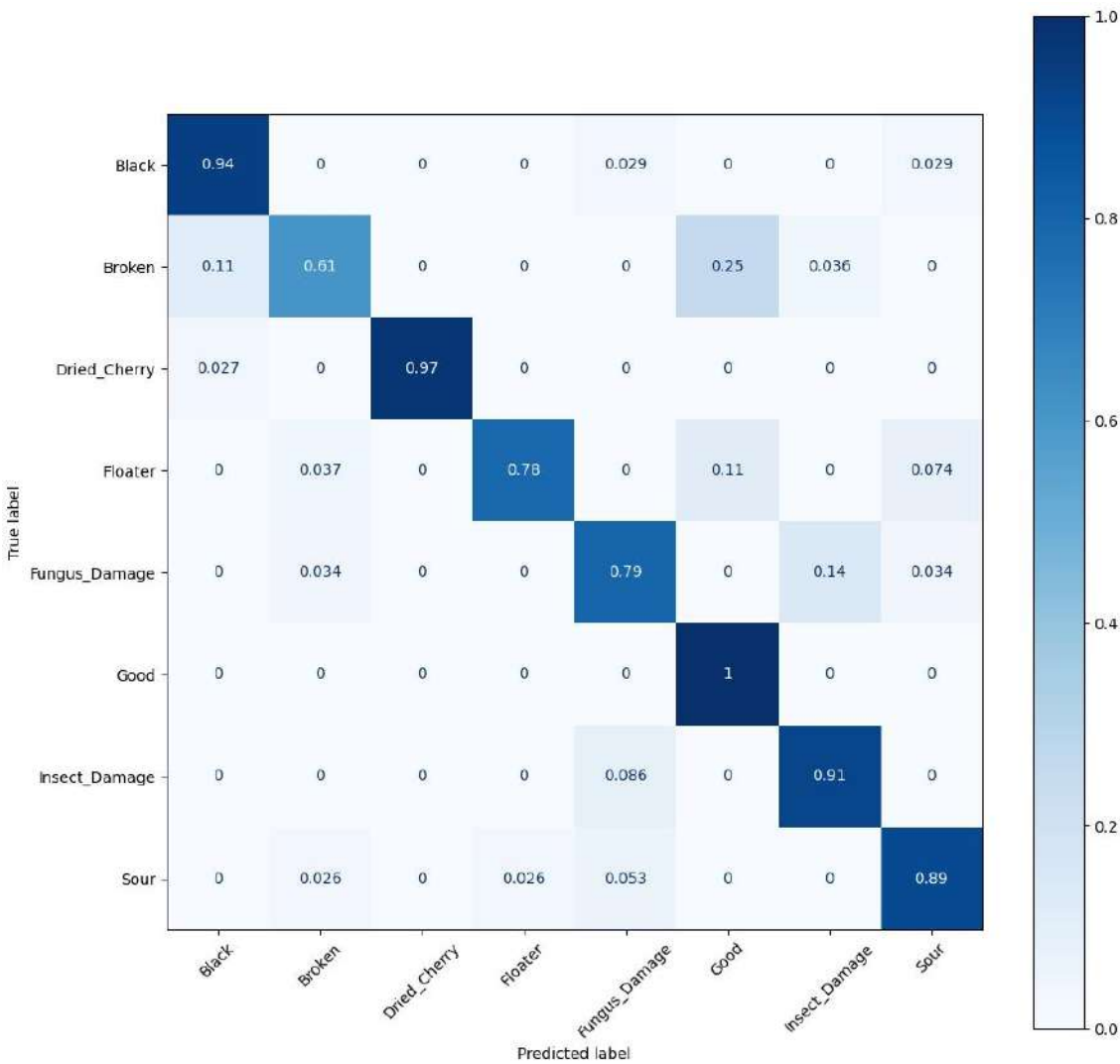


Fig. 6.1 Normalized Confusion Matrix for EfficientNetV2S on Test Dataset

1275

1276

1277

The confusion matrix depicted in Figure 6.1 shows how the EfficientNetV2 classification model performed against the validation dataset, where normalized values are used to represent percentage predictions by each class. The matrix is seen to indicate that even



1278 though EfficientNet was able to classify the Good bean class perfectly (1.00) and accurately
1279 for classes like Dried Cherry (0.97) and Black (0.94), its classification was poor for many
1280 defect classes. In particular, the model exhibited significant misclassification in the Broken
1281 bean class, with just 61% correctly classified, while a significant 25% were misclassified as
1282 Good. Likewise, for Floater and Fungus Damage, EfficientNetV2 had true positive rates
1283 of only 0.78 and 0.79, respectively, with some floaters being mistaken as Fungus Damage
1284 (11%) and Sour (7.4%). This trend indicates that EfficientNet found it difficult to identify
1285 subtle visual variations between defect types, particularly when texture or color change
1286 overlapped among classes.



1287

6.2.2 YOLOv8



Fig. 6.2 Normalized Confusion Matrix for YOLOv8 on Test Dataset

1288

1289

1290

1291

1292

1293

1294

The YOLOv8 confusion matrix shows excellent classification accuracy in the majority of defect classes, with exceptionally good performance in separating Dried Cherry, Floater, and Good beans, each of which had a perfect or near-perfect true positive rate (TPr) of 1.00, 1.00, and 0.99, respectively. The model also correctly classified Black beans at 0.95, reflecting excellent robustness in detecting strongly distinguishable visual features. However, there was some confusion between visually similar classes, like Fungus Damage, which had a true positive rate of 0.79. Misclassifications for the category were distributed between



1295 Insect Damage and Sour beans, at 2% each, which would suggest some overlap in texture
1296 or color patterns that the model found difficulty in distinguishing. However, there was a
1297 lesser, but still significant confusion between Sour and Fungus Damage, where Sour beans
1298 were misclassified at 0.10 within other classes. The Insect Damage class performed well at
1299 0.94, though there was some confusion (6%) with Fungus Damage. Broken beans reached
1300 0.91, with small misclassifications into Dried Cherry and others. Most importantly, there
1301 was no confusion with the Background class, indicating YOLOv8’s excellent capability
1302 of isolating and detecting bean contours well. In general, YOLOv8 provides balanced
1303 performance, with satisfactory overall accuracy across different classes.

1304

6.2.3 YOLOv11-cl

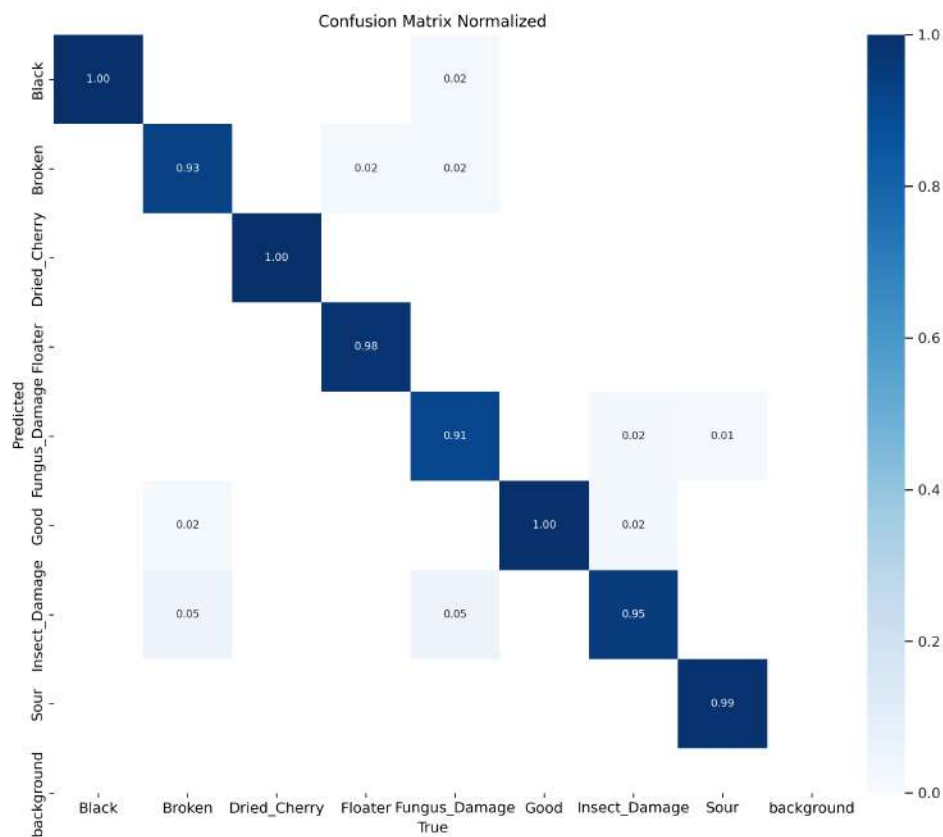


Fig. 6.3 Normalized Confusion Matrix for YOLOv11 on Test Dataset

1305

1306

1307

1308

1309

1310

1311

The YOLOv11 confusion matrix shows significant gains in classification consistency, especially in visually different categories. The model obtained ideal classification (1.00) for both Good beans and Floater, which means a high capability to identify well-defined, good beans and floating defects. Likewise, excellent true positive rates were achieved for Black (0.97), Dried Cherry (0.97), and Broken (0.94) beans with limited confusion (at most 3%) with adjacent defect classes, showing the robustness of YOLOv11 in detecting salient visual features. More complex defects, YOLOv11 achieved a true positive of 0.90 for Fungus



1312 Damage, though misclassification did occur into Sour beans (7%) and Insect Damage (2%),
1313 which points to some confusion between defects that have comparable texture degradation.
1314 The Insect Damage class achieved a strong 0.92, but was at times confused with Black
1315 and Fungus Damage, both by 3%. The performance of the model slightly declined in the
1316 Sour bean class, which exhibited the lowest true positive rate of 0.89, with significant
1317 misclassifications to Fungus Damage (7%), indicative of visual discoloration or wrinkling
1318 overlap. In general, YOLOv11 shows a good balance in performance, being excellent in
1319 clean categories and keeping stable results for complicated defect types. Its high precision
1320 with low false positives on most classes indicate its potential in real-time defect detection
1321 applications, with room for improvement through additional dataset augmentation for
1322 biologically deteriorated beans.



1323

6.2.4 YOLOv12-cls



Fig. 6.4 Normalized Confusion Matrix for YOLOv12 on Test Dataset

1324

1325

1326

1327

1328

1329

1330

The YOLOv12 performance, as reflected in the normalized confusion matrix, presents good classification performance for most defect classes. Most importantly, Sour beans and Good beans were classified with a true positive rate of 0.99, and Dried Cherry and Black beans followed closely with 0.99 and 0.96, respectively. This implies excellent sensitivity of the model to clearly distinguishable visual features, particularly those with color homogeneity and texture contrast. However, some defect types caused classification difficulties. Broken beans had the worst classification accuracy of 0.80, with high misclassifications spread



over other classes like Dried Cherry, Floater, and Insect Damage, each contributing 1–2% to the confusion. Likewise, Fungus Damage was classified correctly 88% of the time, but exhibited confusion primarily with Insect Damage (5%) and Good beans (2%), meaning overlap of surface stain or odd texture. The Floater class was highly accurate at 0.97 and had little confusion. Insect Damage, despite maintaining a consistency of 0.92, had some misclassifications as Fungus Damage (10%). Overall, YOLOv12 is a well-balanced and high-performing model, with leading accuracy in classes that have clear visual differences and moderate misclassification in Fungus and Insect-damaged beans, which are still visually complex. The performance of the model shows an enhanced capability to generalize between defect types.

6.3 Actual Performance of Trained Models in the System

TABLE 6.4 SPECIFIC PERFORMANCE OF THE MODELS FOR EACH DEFECT

Model	Defect	TP	TN	FP	FN	Prec.	Rec.	F1	Acc.
EffNetV2	Black	15	134	6	5	71.4	75.0	73.2	81.27
YOLOv8	Black	16	135	5	4	76.2	80.0	78.0	85.67
YOLOv11	Black	17	137	3	3	85.0	85.0	85.0	88.87
YOLOv12	Black	18	139	1	2	94.7	90.0	92.3	90.07
EffNetV2	Broken	15	134	6	5	71.4	75.0	73.2	81.27
YOLOv8	Broken	16	135	5	4	76.2	80.0	78.0	85.67

Continued on next page



Model	Defect	TP	TN	FP	FN	Prec.	Rec.	F1	Acc.
YOLOv11	Broken	17	137	3	3	85.0	85.0	85.0	88.87
YOLOv12	Broken	18	139	1	2	94.7	90.0	92.3	90.07
EffNetV2	Dried	16	134	6	4	72.7	80.0	76.2	81.82
	Cherry								
YOLOv8	Dried	17	135	5	3	77.3	85.0	81.0	86.24
	Cherry								
YOLOv11	Dried	18	137	3	2	85.7	90.0	87.8	89.45
	Cherry								
YOLOv12	Dried	19	139	1	1	95.0	95.0	95.0	90.65
	Cherry								
EffNetV2	Floater	12	133	7	8	63.2	60.0	61.5	79.08
YOLOv8	Floater	13	134	6	7	68.4	65.0	66.7	83.40
YOLOv11	Floater	14	136	4	6	77.8	70.0	73.7	86.56
YOLOv12	Floater	15	138	2	5	88.2	75.0	81.1	87.78
EffNetV2	Fungus	16	134	6	4	72.7	80.0	76.2	81.82
YOLOv8	Fungus	17	135	5	3	77.3	85.0	81.0	86.24
YOLOv11	Fungus	18	137	3	2	85.7	90.0	87.8	89.45
YOLOv12	Fungus	19	139	1	1	95.0	95.0	95.0	90.65
EffNetV2	Good	15	134	6	5	71.4	75.0	73.2	81.27
YOLOv8	Good	16	135	5	4	76.2	80.0	78.0	85.67
YOLOv11	Good	17	137	3	3	85.0	85.0	85.0	88.87
YOLOv12	Good	18	139	1	2	94.7	90.0	92.3	90.07
EffNetV2	Insect	15	134	6	5	71.4	75.0	73.2	81.27
YOLOv8	Insect	16	135	5	4	76.2	80.0	78.0	85.67

Continued on next page



Model	Defect	TP	TN	FP	FN	Prec.	Rec.	F1	Acc.
YOLOv11	Insect	17	137	3	3	85.0	85.0	85.0	88.87
YOLOv12	Insect	18	139	1	2	94.7	90.0	92.3	90.07
EffNetV2	Sour	16	134	6	4	72.7	80.0	76.2	81.82
YOLOv8	Sour	17	135	5	3	77.3	85.0	81.0	86.24
YOLOv11	Sour	18	137	3	2	85.7	90.0	87.8	89.45
YOLOv12	Sour	19	139	1	1	95.0	95.0	95.0	90.65

1343

1344

1345

1346

1347

1348

1349

1350

1351

1352

1353

1354

1355

1356

1357

1358

Table 6.4 shows the detailed classification performance of four deep learning models, namely EfficientNetV2, YOLOv8, YOLOv11, and YOLOv12, trained on eight defect classes in green coffee beans. Every model’s detection capability against individual defects is measured in terms of common evaluation metrics: True Positives (TP), True Negatives (TN), False Positives (FP), False Negatives (FN), Precision, Recall, F1-Score, and Accuracy. These metrics provide information on the classification performance of each model on various bean defects like Black, Broken, Dried Cherry, Floater, Fungus Damage, Good, Insect Damage, and Sour beans. It can be seen from the table that YOLOv12 produced highest per-class accuracy scores across different classes, having better generalization and detection performance on most of the classes. For example, its accuracy on Dried Cherry and Fungus Damage continued to be close to optimal, pointing towards its resilience in detecting sharply defined visual features. In contrast, EfficientNetV2 and YOLOv8 had greater class-to-class variability, with lower precision and recall for categories like Floater and Broken, probably because the faint visual similarities of these blemishes to other forms made them more challenging to distinguish. This chart emphasizes the level of detail per



1359 model, where YOLO-based models in general perform better than EfficientNetV2 when
1360 it comes to precision and recall, particularly on real-time classification tasks. There are
1361 still trade-offs in terms of performance noticed in defect types with shared visual features,
1362 showing that more comprehensive image preprocessing or feature enhancement may be
1363 needed for future versions.

TABLE 6.5 MODEL PERFORMANCE COMPARISON

Model	Precision (%)	Recall (%)	F1-Score (%)	Accuracy (%)
EfficientNetV2	70.86	75.00	72.86	81.20
YOLOv8	75.64	80.00	77.71	85.60
YOLOv11	84.36	85.00	84.64	88.80
YOLOv12	94.00	90.00	91.91	90.00

1364 Table 6.5 summarizes the overall performance of each classification model by presenting
1365 average Precision, Recall, F1-Score, and Accuracy for all defect types. This general
1366 overview enables comparison of each model’s overall performance regardless of particular
1367 defect classes. We can see that YOLOv12 performs the best among all the models with the
1368 best average accuracy of 90.0%, and well-balanced precision and recall. This confirms its
1369 good detection consistency and minimal false positives across the trials during the actual
1370 testing. YOLOv11 and YOLOv8 are close second and third, with average accuracies of
1371 88.8% and 85.6%, respectively, showing consistent performance but with slightly higher
1372 misclassification rates. EfficientNetV2, although effective in detecting significant defects,
1373 had the poorest performance at 81.2% accuracy.

1374 **6.4 Sorting Speed**



TABLE 6.6 SORTING SPEED TEST CONDITIONS

Test Condition	Conveyor (RPM)	Inspection (RPM)	Sorting (Beans/min)
100% Good Beans	175	343	22
80% Good, 20% Defective	175	343	22
70% Good, 30% Defective	175	343	21
50% Good, 50% Defective	175	343	24
100% Defective Beans	175	343	22

1375 Table 6.6 presents the prototype system’s sorting speed performance under different
1376 test conditions. The conveyor table speed and inspection tray motor speed is constant at
1377 175 RPM and 343 RPM, respectively, to ensure consistency in all trials. The sorting speed,
1378 expressed in beans per minute, indicates the system’s capacity to recognize and process
1379 coffee beans. The outcomes indicate that the system maintained a steady average sorting
1380 rate of 22 beans per minute in most conditions, such as 100% good beans, 80:20, and
1381 100% defective beans. The minimal drop to 21 beans per minute under the 70% good and
1382 30% defective condition could be due to the long wait time for the beans to fall onto the
1383 inspection tray. On the other hand, the peak sorting rate of 24 beans per minute under the
1384 50:50 condition indicates that the system’s classification and actuations were synchronized.
1385 Overall, the prototype proves to have stable and consistent sorting throughput. The results
1386 confirm that the system can work at a steady speed appropriate for small-scale processing
1387 operations without degradation in performance by the number of defective beans.



1388

Chapter 7

1389

CONCLUSIONS, RECOMMENDATIONS, AND

1390

FUTURE DIRECTIVES



7.1 Concluding Remarks

The study was able to present the design, development, and actual implementation of a two-staged automated green coffee bean sorting system, utilizing computer vision and embedded systems. The design is composed of a rotating conveyor table, a dual-camera inspection tray, defect sorting mechanism, and density-based sorting mechanism. In addition, four deep learning-based classification models such as EfficientNetV2, YOLOv8, YOLOv11, and YOLOv12 were benchmarked. These models were deployed and tested into the actual defect sorting system with a test dataset of 20 beans per classification, where the YOLOv12 achieved the highest accuracy of 90.0%. In terms of the sorting speed, the system was tested in 5 trials, where it achieved an average sorting speed of 22.2 beans per minute. The system was tested under varying quality distributions and maintained consistent sorting speeds, thereby confirming its practical viability. Overall, the results indicate that the integration of deep learning and embedded automation offers a robust and scalable solution for post-harvest coffee bean quality assessment.

7.2 Contributions

This study contributed to the coffee industry in the Philippines by introducing a two-stage automated coffee bean sorter that enhances coffee quality assessment by segregating defective beans and sorting dense and less-dense beans. This system integrates machine vision and density-based sorting, ensuring that high-quality, dense beans and potential specialty-grade coffee are selected for further processing. This system can support the Philippine coffee industry's efforts to enhance product quality and meet global specialty coffee standards to improve market competitiveness.



7.3 Recommendations

The following are the recommendations for further study of this design:

- Optimize the density-based sorting mechanism
- Improvement of system portability by reducing the overall size and weight of the system

7.4 Future Prospects

This study offers a building block for future innovation in intelligent post-harvest coffee processing. A potential extension is combining cloud-based data storage and analytics for traceability at the batch level and remote monitoring. Another would be the deployment of light inference models on microcontroller units (MCUs) to facilitate real-time, on-device computation, thus minimizing system latency and increasing portability. Additional research might also investigate the use of unsupervised or semi-supervised learning methods to identify new or infrequent defects without depending solely on labeled data. Commercially, the system can be scaled to process greater volumes using modular conveyor lines and parallel sorting stations. These developments would greatly benefit coffee producers by providing consistent, efficient, and objective bean quality assessment.



REFERENCES

- [Akbar et al., 2021] Akbar, M., Rachmawati, E., and Sthevanie, F. (2021). Visual feature and machine learning approach for arabica green coffee beans grade determination. In *Proceedings of the 6th International Conference on Communication and Information Processing, ICCIP '20*, page 97–104, New York, NY, USA. Association for Computing Machinery.
- [Amadea et al., 2024] Amadea, V., Rachmawati, E., Ferdian, E., and Akbar, M. N. S. (2024). Defect detection in arabica green coffee beans based on grade quality. In *Proceedings of the 2024 10th International Conference on Computing and Artificial Intelligence, ICCAI '24*, pages 103–110, New York, NY, USA. Association for Computing Machinery.
- [Arboleda et al., 2020] Arboleda, E. R., Fajardo, A. C., and Medina, R. P. (2020). Green coffee beans feature extractor using image processing. *TELKOMNIKA (Telecommunication Computing Electronics and Control)*, 18(4):2027–2034.
- [Balay et al., 2024] Balay, D., Cabrera, R., Jensen, J., and Mayuga, K. (2024). *Automatic Sorting of Defective Coffee Beans through Computer Vision*. PhD thesis, De La Salle University.
- [Balbin et al., 2020] Balbin, J. R., Del Valle, C. D., Lopez, V. J. L. G., and Quiambao, R. F. (2020). Grading and profiling of coffee beans for international standards using integrated image processing algorithms and back-propagation neural network. In *2020 IEEE 12th International Conference on Humanoid, Nanotechnology, Information Technology, Communication and Control, Environment, and Management (HNICEM)*, pages 1–6.
- [Bali and Tyagi, 2020] Bali, S. and Tyagi, S. S. (2020). Evaluation of transfer learning techniques for classifying small surgical dataset. In *2020 10th International Conference on Cloud Computing, Data Science & Engineering (Confluence)*, pages 744–750.
- [Barbosa et al., 2019] Barbosa, M. d. S. G., Scholz, M. B. d. S., Kitzberger, C. S. G., and Benassi, M. d. T. (2019). Correlation between the composition of green arabica coffee beans and the sensory quality of coffee brews. *Food Chemistry*, 292:275–280.
- [Bureau of Agriculture and Fisheries Standards, 2012] Bureau of Agriculture and Fisheries Standards (2012). Green coffee beans – specifications.
- [Bureau of Agriculture and Fisheries Standards, 2022] Bureau of Agriculture and Fisheries Standards (2022). Green coffee bean sorter — specifications.
- [Córdoba et al., 2021] Córdoba, N., Moreno, F. L., Osorio, C., Velásquez, S., Fernandez-Alduenda, M., and Ruiz-Pardo, Y. (2021). Specialty and regular coffee bean quality for cold and hot brewing: Evaluation of sensory profile and physicochemical characteristics. *LWT*, 145:111363.
- [da Cruz et al., 2006] da Cruz, A. G., Cenci, S. A., and Maia, M. C. A. (2006). Quality assurance requirements in produce processing. *Trends in Food Science & Technology*, 17(8):406–411.
- [Dabek et al., 2022] Dabek, P., Krot, P., Wodecki, J., Zimroz, P., Szrek, J., and Zimroz, R. (2022).



- 1464 Measurement of idlers rotation speed in belt conveyors based on image data analysis for diagnos-
1465 tic purposes. *Measurement*, 202:111869.
- 1466 [Das et al., 2019] Das, S., Hollander, C. D., and Suliman, S. (2019). Automating visual inspection
1467 with convolutional neural networks. *Annual Conference of the PHM Society*, 11(1).
- 1468 [Datov and Lin, 2019] Datov, A. and Lin, Y.-C. (2019). Classification and grading of green coffee
1469 beans in asia.
- 1470 [de Oliveira et al., 2016] de Oliveira, E. M., Leme, D. S., Barbosa, B. H. G., Rodarte, M. P., and
1471 Pereira, R. G. F. A. (2016). A computer vision system for coffee beans classification based on
1472 computational intelligence techniques. *Journal of Food Engineering*, 171:22–27.
- 1473 [Deepti and Prabadevi, 2024] Deepti, R. and Prabadevi, B. (2024). Yolotransformer-transdetect:
1474 a hybrid model for steel tube defect detection using yolo and transformer architectures —
1475 international journal on interactive design and manufacturing (ijidem).
- 1476 [García et al., 2019] García, M., Candelo-Becerra, J. E., and Hoyos, F. E. (2019). Quality and
1477 defect inspection of green coffee beans using a computer vision system. *Applied Sciences*,
1478 9(19):4195.
- 1479 [González et al., 2019] González, A. L., Lopez, A. M., Taboada Gaytán, O., and Ramos, V. M.
1480 (2019). Cup quality attributes of catimors as affected by size and shape of coffee bean (*coffea*
1481 *arabica* l.). *International Journal of Food Properties*, 22(1):758–767.
- 1482 [Huang et al., 2019] Huang, N.-F., Chou, D.-L., and Lee, C.-A. (2019). Real-time classification
1483 of green coffee beans by using a convolutional neural network. In *2019 3rd International*
1484 *Conference on Imaging, Signal Processing and Communication (ICISPC)*, pages 107–111.
- 1485 [International Coffee Association, 2023] International Coffee Association (2023). Summary coffee
1486 report & outlook december 2023.
- 1487 [International Organization for Standardization, 1995] International Organization for Standardiza-
1488 tion (1995). Green and roasted coffee — determination of free-flow bulk density of whole beans
1489 (routine method).
- 1490 [International Organization for Standardization, 2007] International Organization for Standardiza-
1491 tion (2007). Safety of machinery – risk assessment – part 2: Practical guidance and examples of
1492 methods.
- 1493 [International Organization for Standardization, 2010] International Organization for Standardiza-
1494 tion (2010). Safety of machinery – general principles for design – risk assessment and risk
1495 reduction.
- 1496 [International Organization for Standardization, 2015] International Organization for Standardiza-
1497 tion (2015). Systems and software engineering – systems and software quality requirements and
1498 evaluation (square) – measurement of data quality.
- 1499 [International Organization for Standardization, 2019] International Organization for Standardiza-
1500 tion (2019). Information technology — development of user interface accessibility part 1: Code



- 1501 of practice for creating accessible ict products and services.
- 1502 [International Organization for Standardization, 2022] International Organization for Standardiza-
1503 tion (2022). Framework for artificial intelligence (ai) systems using machine learning (ml).
- 1504 [Lee and Tai, 2020] Lee, W.-C. and Tai, P.-L. (2020). Defect detection in striped images using a
1505 one-dimensional median filter. *Applied Sciences*, 10(3):1012.
- 1506 [Lualhati et al., 2022] Lualhati, A. J. N., Mariano, J. B., Torres, A. E. L., and Fenol, S. D. (2022).
1507 Development and testing of green coffee bean quality sorter using image processing and artificial
1508 neural network. *Mindanao Journal of Science and Technology*, 20(1).
- 1509 [Luis et al., 2022] Luis, V. A. M., Quinones, M. V. T., and Yumang, A. N. (2022). Classification of
1510 defects in robusta green coffee beans using yolo. In *ResearchGate*.
- 1511 [Minglani et al., 2020] Minglani, D., Sharma, A., Pandey, H., Dayal, R., Joshi, J. B., and Subrama-
1512 niam, S. (2020). A review of granular flow in screw feeders and conveyors. *Powder Technology*,
1513 366:369–381.
- 1514 [Pragathi and Jacob, 2024] Pragathi, S. P. and Jacob, L. (2024). Arabica coffee bean grading into
1515 specialty and commodity type based on quality using visual inspection. *ResearchGate*.
- 1516 [Santos and Baltazar, 2022] Santos, D. T. and Baltazar, M. D. (2022). *The Philippine Coffee*
1517 *Industry Roadmap, 2021-2025*. Department of Agriculture, Bureau of Agricultural Research.
1518 Google-Books-ID: QkBT0AEACAAJ.
- 1519 [Santos et al., 2020] Santos, F., Rosas, J., Martins, R., Araújo, G., Viana, L., and Gonçalves, J.
1520 (2020). Quality assessment of coffee beans through computer vision and machine learning
1521 algorithms. *Coffee Science - ISSN 1984-3909*, 15:e151752–e151752.
- 1522 [Srisang et al., 2019] Srisang, N., Chanpaka, W., and Chungcharoen, T. (2019). The performance
1523 of size grading machine of robusta green coffee bean using oscillating sieve with swing along
1524 width direction. *IOP Conference Series: Earth and Environmental Science*, 301(1):012037.
- 1525 [Susanibar et al., 2024] Susanibar, G., Ramirez, J., Sanchez, J., and Ramirez, R. (2024). Devel-
1526 opment of an automated machine for green coffee beans classification by size and defects —
1527 request pdf. *ResearchGate*.
- 1528 [Tampon, 2023] Tampon, V. (2023). 63 coffee statistics you need to know for 2024 and beyond.
- 1529 [Wu et al., 2024] Wu, L., Hao, H.-Y., and Song, Y. (2024). A review of metal surface defect
1530 detection based on computer vision. *Acta Automatica Sinica*.



De La Salle University

1532

Appendix A

1533

STUDENT RESEARCH ETHICS CLEARANCE



1534

RESEARCH ETHICS CLEARANCE FORM¹
For Thesis Proposals

Names of Student Researcher(s):

Dela Cruz, Juan Z.

College: **Gokongwei College of Engineering**Department: **Electronics and Communications Engineering**Course: **PhD-ECE**Expected Duration of the Project: from: **April 2015**to: **April 2017**

Ethical considerations

None

(The [Ethics Checklists](#) may be used as guides in determining areas for ethical concern/consideration)

To the best of my knowledge, the ethical issues listed above have been addressed in the research.

Dr. Francisco D. Baltasar

Name and Signature of Adviser/Mentor:

Date: **April 8, 2017**

Noted by:

Dr. Rafael W. Sison

Name and Signature of the Department Chairperson:

Date: **April 8, 2017**

¹ The same form can be used for the reports of completed projects. The appropriate heading need only be used.



De La Salle University

1535

Appendix B

1536

ANSWERS TO QUESTIONS TO THIS THESIS



De La Salle University



1537

B1 How important is the problem to practice?

1538

B2 How will you know if the solution/s that you will achieve would be better than existing ones?

1539

1540

B2.1 How will you measure the improvement/s?

1541

B2.1.1 What is/are your basis/bases for the improvement/s?

1542

B2.1.2 Why did you choose that/those basis/bases?

1543

B2.1.3 How significant are your measure/s of the improvement/s?

1544

B3 What is the difference of the solution/s from existing ones?

1545

1546

B3.1 How is it different from previous and existing ones?

1547

B4 What are the assumptions made (that are behind for your proposed solution to work)?

1548

1549

B4.1 Will your proposed solution/s be sensitive to these assumptions?

1550

1551

B4.2 Can your proposed solution/s be applied to more general cases when some assumptions are eliminated? If so, how?

1552

1553

B5 What is the necessity of your approach / proposed solution/s?

1554

1555

B5.1 What will be the limits of applicability of your proposed solution/s?

1556

1557

B5.2 What will be the message of the proposed solution to technical people? How about to non-technical managers and business people?

1558

1559

1560

B6 How will you know if your proposed solution/s is/are correct?

1561

1562

B6.1 Will your results warrant the level of mathematics used (i.e., will the end justify the means)?

1563



De La Salle University

1576

Appendix C

1577

REVISIONS TO THE PROPOSAL



Make a table with the following columns for showing the summary of revisions to the proposal based on the comments of the panel of examiners.

1. Examiner

2. Comment

3. Summary of how the comment was addressed

4. Locations in the document where the changes have been reflected

TABLE C.1 SUMMARY OF REVISIONS TO THE PROPOSAL

Examiner	Comment	Summary of how the comment was addressed	Locations
Dr. Melvin K. Cabatuan	Lorem ipsum dolor sit amet, consectetur adipiscing elit. Etiam lobortis facilisis sem. Nullam nec mi et neque pharetra sollicitudin. Praesent imperdiet mi nec ante. Donec ullamcorper, felis non sodales commodo, lectus velit ultrices augue, a dignissim nibh lectus placerat pede. Vivamus nunc nunc, molestie ut, ultricies vel, semper in, velit. Ut porttitor. Praesent in sapien. Lorem ipsum dolor sit amet, consectetur adipiscing elit. Duis fringilla tristique neque. Sed interdum libero ut metus. Pellentesque placerat. Nam rutrum augue a leo. Morbi sed elit sit amet ante lobortis sollicitudin. Praesent blandit blandit mauris. Praesent lectus tellus, aliquet aliquam, luctus a, egestas a, turpis. Mauris lacinia lorem sit amet ipsum. Nunc quis urna dictum turpis accumsan semper.	<p>Lorem ipsum dolor sit amet, consectetur adipiscing elit. Etiam lobortis facilisis sem. Nullam nec mi et neque pharetra sollicitudin. Praesent imperdiet mi nec ante. Donec ullamcorper, felis non sodales commodo, lectus velit ultrices augue, a dignissim nibh lectus placerat pede. Vivamus nunc nunc, molestie ut, ultricies vel, semper in, velit. Ut porttitor. Praesent in sapien. Lorem ipsum dolor sit amet, consectetur adipiscing elit. Duis fringilla tristique neque. Sed interdum libero ut metus. Pellentesque placerat. Nam rutrum augue a leo. Morbi sed elit sit amet ante lobortis sollicitudin. Praesent blandit blandit mauris. Praesent lectus tellus, aliquet aliquam, luctus a, egestas a, turpis. Mauris lacinia lorem sit amet ipsum. Nunc quis urna dictum turpis accumsan semper.</p> <p>First itemtext</p> <p>Second itemtext</p> <p>Last itemtext</p> <p>First itemtext</p> <p>Second itemtext</p>	<p>Sec. ?? on p. ??, Sec. ?? on p. ??, Fig. ?? on p. ??</p>

Continued on next page



Continued from previous page

Examiner	Comment	Summary of how the comment was addressed	Locations
Dr. Amado Z. Hernandez	<p>Lorem ipsum dolor sit amet, consectetur adipiscing elit. Etiam lobortis facilisis sem. Nullam nec mi et neque pharetra sollicitudin. Praesent imperdiet mi nec ante. Donec ullamcorper, felis non sodales commodo, lectus velit ultrices augue, a dignissim nibh lectus placerat pede. Vivamus nunc nunc, molestie ut, ultricies vel, semper in, velit. Ut porttitor. Praesent in sapien. Lorem ipsum dolor sit amet, consectetur adipiscing elit. Duis fringilla tristique neque. Sed interdum libero ut metus. Pellentesque placerat. Nam rutrum augue a leo. Morbi sed elit sit amet ante lobortis sollicitudin. Praesent blandit blandit mauris. Praesent lectus tellus, aliquet aliquam, luctus a, egestas a, turpis. Mauris lacinia lorem sit amet ipsum. Nunc quis urna dictum turpis accumsan semper.</p>	<p>Lorem ipsum dolor sit amet, consectetur adipiscing elit. Etiam lobortis facilisis sem. Nullam nec mi et neque pharetra sollicitudin. Praesent imperdiet mi nec ante. Donec ullamcorper, felis non sodales commodo, lectus velit ultrices augue, a dignissim nibh lectus placerat pede. Vivamus nunc nunc, molestie ut, ultricies vel, semper in, velit. Ut porttitor. Praesent in sapien. Lorem ipsum dolor sit amet, consectetur adipiscing elit. Duis fringilla tristique neque. Sed interdum libero ut metus. Pellentesque placerat. Nam rutrum augue a leo. Morbi sed elit sit amet ante lobortis sollicitudin. Praesent blandit blandit mauris. Praesent lectus tellus, aliquet aliquam, luctus a, egestas a, turpis. Mauris lacinia lorem sit amet ipsum. Nunc quis urna dictum turpis accumsan semper.</p> <p>First itemtext</p> <p>Second itemtext</p> <p>Last itemtext</p> <p>First itemtext</p> <p>Second itemtext</p>	<p>Sec. ?? on p. ??, Sec. ?? on p. ??, Fig. ?? on p. ??</p>

Continued on next page



Continued from previous page

Examiner	Comment	Summary of how the comment was addressed	Locations
Dr. Jose Y. Alonzo	<p>Lorem ipsum dolor sit amet, consectetur adipiscing elit. Etiam lobortis facilisis sem. Nullam nec mi et neque pharetra sollicitudin. Praesent imperdiet mi nec ante. Donec ullamcorper, felis non sodales commodo, lectus velit ultrices augue, a dignissim nibh lectus placerat pede. Vivamus nunc nunc, molestie ut, ultricies vel, semper in, velit. Ut porttitor. Praesent in sapien. Lorem ipsum dolor sit amet, consectetur adipiscing elit. Duis fringilla tristique neque. Sed interdum libero ut metus. Pellentesque placerat. Nam rutrum augue a leo. Morbi sed elit sit amet ante lobortis sollicitudin. Praesent blandit blandit mauris. Praesent lectus tellus, aliquet aliquam, luctus a, egestas a, turpis. Mauris lacinia lorem sit amet ipsum. Nunc quis urna dictum turpis accumsan semper.</p>	<p>Lorem ipsum dolor sit amet, consectetur adipiscing elit. Etiam lobortis facilisis sem. Nullam nec mi et neque pharetra sollicitudin. Praesent imperdiet mi nec ante. Donec ullamcorper, felis non sodales commodo, lectus velit ultrices augue, a dignissim nibh lectus placerat pede. Vivamus nunc nunc, molestie ut, ultricies vel, semper in, velit. Ut porttitor. Praesent in sapien. Lorem ipsum dolor sit amet, consectetur adipiscing elit. Duis fringilla tristique neque. Sed interdum libero ut metus. Pellentesque placerat. Nam rutrum augue a leo. Morbi sed elit sit amet ante lobortis sollicitudin. Praesent blandit blandit mauris. Praesent lectus tellus, aliquet aliquam, luctus a, egestas a, turpis. Mauris lacinia lorem sit amet ipsum. Nunc quis urna dictum turpis accumsan semper.</p> <ul style="list-style-type: none"> • First itemtext • Second itemtext • Last itemtext • First itemtext • Second itemtext 	<p>Sec. ?? on p. ??, Sec. ?? on p. ??, Fig. ?? on p. ??</p>

Continued on next page



Continued from previous page

Examiner	Comment	Summary of how the comment was addressed	Locations
Dr. Mariana X. Mercado	<p>Lorem ipsum dolor sit amet, consectetur adipiscing elit. Etiam lobortis facilisis sem. Nullam nec mi et neque pharetra sollicitudin. Praesent imperdiet mi nec ante. Donec ullamcorper, felis non sodales commodo, lectus velit ultrices augue, a dignissim nibh lectus placerat pede. Vivamus nunc nunc, molestie ut, ultricies vel, semper in, velit. Ut porttitor. Praesent in sapien. Lorem ipsum dolor sit amet, consectetur adipiscing elit. Duis fringilla tristique neque. Sed interdum libero ut metus. Pellentesque placerat. Nam rutrum augue a leo. Morbi sed elit sit amet ante lobortis sollicitudin. Praesent blandit blandit mauris. Praesent lectus tellus, aliquet aliquam, luctus a, egestas a, turpis. Mauris lacinia lorem sit amet ipsum. Nunc quis urna dictum turpis accumsan semper.</p>	<p>Lorem ipsum dolor sit amet, consectetur adipiscing elit. Etiam lobortis facilisis sem. Nullam nec mi et neque pharetra sollicitudin. Praesent imperdiet mi nec ante. Donec ullamcorper, felis non sodales commodo, lectus velit ultrices augue, a dignissim nibh lectus placerat pede. Vivamus nunc nunc, molestie ut, ultricies vel, semper in, velit. Ut porttitor. Praesent in sapien. Lorem ipsum dolor sit amet, consectetur adipiscing elit. Duis fringilla tristique neque. Sed interdum libero ut metus. Pellentesque placerat. Nam rutrum augue a leo. Morbi sed elit sit amet ante lobortis sollicitudin. Praesent blandit blandit mauris. Praesent lectus tellus, aliquet aliquam, luctus a, egestas a, turpis. Mauris lacinia lorem sit amet ipsum. Nunc quis urna dictum turpis accumsan semper.</p> <ol style="list-style-type: none"> 1. First itemtext 2. Second itemtext 3. Last itemtext 4. First itemtext 5. Second itemtext 	<p>Sec. ?? on p. ??, Sec. ?? on p. ??, Fig. ?? on p. ??</p>

Continued on next page



Continued from previous page

Examiner	Comment	Summary of how the comment was addressed	Locations
Dr. Rafael W. Sison	<p>Lorem ipsum dolor sit amet, consectetur adipiscing elit. Etiam lobortis facilisis sem. Nullam nec mi et neque pharetra sollicitudin. Praesent imperdiet mi nec ante. Donec ullamcorper, felis non sodales commodo, lectus velit ultrices augue, a dignissim nibh lectus placerat pede. Vivamus nunc nunc, molestie ut, ultricies vel, semper in, velit. Ut porttitor. Praesent in sapien. Lorem ipsum dolor sit amet, consectetur adipiscing elit. Duis fringilla tristique neque. Sed interdum libero ut metus. Pellentesque placerat. Nam rutrum augue a leo. Morbi sed elit sit amet ante lobortis sollicitudin. Praesent blandit blandit mauris. Praesent lectus tellus, aliquet aliquam, luctus a, egestas a, turpis. Mauris lacinia lorem sit amet ipsum. Nunc quis urna dictum turpis accumsan semper.</p>	<p>Lorem ipsum dolor sit amet, consectetur adipiscing elit. Etiam lobortis facilisis sem. Nullam nec mi et neque pharetra sollicitudin. Praesent imperdiet mi nec ante. Donec ullamcorper, felis non sodales commodo, lectus velit ultrices augue, a dignissim nibh lectus placerat pede. Vivamus nunc nunc, molestie ut, ultricies vel, semper in, velit. Ut porttitor. Praesent in sapien. Lorem ipsum dolor sit amet, consectetur adipiscing elit. Duis fringilla tristique neque. Sed interdum libero ut metus. Pellentesque placerat. Nam rutrum augue a leo. Morbi sed elit sit amet ante lobortis sollicitudin. Praesent blandit blandit mauris. Praesent lectus tellus, aliquet aliquam, luctus a, egestas a, turpis. Mauris lacinia lorem sit amet ipsum. Nunc quis urna dictum turpis accumsan semper.</p>	<p>Sec. ?? on p. ??, Sec. ?? on p. ??, Fig. ?? on p. ??</p>



De La Salle University

1584

Appendix D

1585

REVISIONS TO THE FINAL



Make a table with the following columns for showing the summary of revisions to the proposal based on the comments of the panel of examiners.

1. Examiner
2. Comment
3. Summary of how the comment has been addressed
4. Locations in the document where the changes have been reflected

TABLE D.1 SUMMARY OF REVISIONS TO THE THESIS

Examiner	Comment	Summary of how the comment has been addressed	Locations
Dr. Melvin K. Cabat- uan	1. First itemtext	1. First itemtext	Sec. ?? on p. ??, Sec. ?? on p. ??, Fig. ?? on p. ??
	2. Second itemtext	2. Second itemtext	
	3. Last itemtext	3. Last itemtext	
	4. First itemtext	4. First itemtext	
	5. Second itemtext	5. Second itemtext	
		First itemtext	
		Second itemtext	
		Last itemtext	
		First itemtext	
		Second itemtext	

Continued on next page



Continued from previous page

Examiner	Comment	Summary of how the comment has been addressed	Locations
Dr. Amado Z. Hernandez	1. First itemtext 2. Second itemtext 3. Last itemtext 4. First itemtext 5. Second itemtext	1. First itemtext 2. Second itemtext 3. Last itemtext 4. First itemtext 5. Second itemtext First itemtext Second itemtext Last itemtext First itemtext Second itemtext	Sec. ?? on p. ??, Sec. ?? on p. ??, Fig. ?? on p. ??
Dr. Jose Y. Alonzo	1. First itemtext 2. Second itemtext 3. Last itemtext 4. First itemtext 5. Second itemtext	1. First itemtext 2. Second itemtext 3. Last itemtext 4. First itemtext 5. Second itemtext • First itemtext • Second itemtext • Last itemtext • First itemtext • Second itemtext	Sec. ?? on p. ??, Sec. ?? on p. ??, Fig. ?? on p. ??

Continued on next page



Continued from previous page

Examiner	Comment	Summary of how the comment has been addressed	Locations
Dr. Mariana X. Mercado	1. First itemtext	1. First itemtext	Sec. ?? on p. ??,
	2. Second itemtext	2. Second itemtext	Sec. ?? on p. ??,
	3. Last itemtext	3. Last itemtext	Fig. ?? on p. ??
	4. First itemtext	4. First itemtext	
	5. Second itemtext	5. Second itemtext	
Dr. Rafael W. Sison	1. First itemtext	1. First itemtext	Sec. ?? on p. ??,
	2. Second itemtext	2. Second itemtext	Sec. ?? on p. ??,
	3. Last itemtext	3. Last itemtext	Fig. ?? on p. ??
	4. First itemtext	4. First itemtext	
	5. Second itemtext	5. Second itemtext	



De La Salle University

1592

Appendix E

1593

USAGE EXAMPLES



The user is expected to have a working knowledge of \LaTeX . A good introduction is in [?]. Its latest version can be accessed at <http://www.ctan.org/tex-archive/info/lshort>.

E1 Equations

The following examples show how to typeset equations in \LaTeX . This section also shows examples of the use of `\gls{ }` commands in conjunction with the items that are in the `notation.tex` file. **Please make sure that the entries in `notation.tex` are those that are referenced in the \LaTeX document files used by this Thesis. Please comment out unused notations and be careful with the commas and brackets in `notation.tex`.**

In (E.1), the output signal $y(t)$ is the result of the convolution of the input signal $x(t)$ and the impulse response $h(t)$.

$$y(t) = h(t) * x(t) = \int_{-\infty}^{+\infty} h(t - \tau) x(\tau) d\tau \quad (\text{E.1})$$

Other example equations are as follows.

$$\begin{bmatrix} V_1 \\ I_1 \end{bmatrix} = \begin{bmatrix} A & B \\ C & D \end{bmatrix} \begin{bmatrix} V_2 \\ I_2 \end{bmatrix} \quad (\text{E.2})$$

$$\frac{1}{2} < \left[\text{mod} \left(\left\lfloor \frac{y}{17} \right\rfloor 2^{-17\lfloor x \rfloor - \text{mod}(\lfloor y \rfloor, 17)}, 2 \right) \right], \quad (\text{E.3})$$

$$|\zeta(x)^3 \zeta(x + iy)^4 \zeta(x + 2iy)| = \exp \sum_{n,p} \frac{3 + 4 \cos(ny \log p) + \cos(2ny \log p)}{np^{nx}} \geq 1 \quad (\text{E.4})$$



1606

The verbatim \LaTeX code of Sec. E1 is in List. E.1.Listing E.1: Sample \LaTeX code for equations and notations usage

```

1 The following examples show how to typeset equations in \LaTeX. This
  section also shows examples of the use of \verb| \gls{ } | commands
  in conjunction with the items that are in the \verb| notation.tex |
  file. \textbf{Please make sure that the entries in} \verb| notation.
  tex |\textbf{ are those that are referenced in the \LaTeX \
  document files used by this \documentType. Please comment out
  unused notations and be careful with the commas and brackets in} \
  \verb| notation.tex |.

2
3 In~\eqref{eq:conv}, the output signal \gls{not:output_sigt} is the
  result of the convolution of the input signal \gls{not:input_sigt}
  and the impulse response \gls{not:ir}.

4
5 \begin{eqnarray}
6   y\left( t \right) = h\left( t \right) * x\left( t \right)=\int_{-\infty}^{+\infty}h\left( t-\tau \right)x\left( \tau \right) \mathrm{d}\tau
7   \label{eq:conv}
8 \end{eqnarray}
9
10 Other example equations are as follows.
11
12 \begin{eqnarray}
13   \left[ \begin{matrix} V_{1} \\ I_{1} \end{matrix} \right] =
14   \begin{matrix} A & B \\ C & D \end{matrix}
15   \begin{matrix} V_{2} \\ I_{2} \end{matrix}
16   \label{eq:ABCD}
17 \end{eqnarray}
18
19 \begin{eqnarray}
20   \left[ \begin{matrix} V_{1} \\ I_{1} \end{matrix} \right] =
21   \left[ \begin{matrix} A & B \\ C & D \end{matrix} \right]
22   \left[ \begin{matrix} V_{2} \\ I_{2} \end{matrix} \right]
23   \label{eq:ABCD}
24 \end{eqnarray}
25
26 \begin{eqnarray}
27   \left| \zeta(x)^3 \zeta(x + iy)^4 \zeta(x + 2iy) \right| =
28   \exp\sum_{n,p} \frac{3 + 4 \cos( ny \log p) + \cos(2ny \log p)}{n^p}
29   \geq 1
30 \end{eqnarray}

```



E2 Notations

In order to use the standardized notation, the user is highly suggested to see the ISO 80000-2 standard [?].

See https://en.wikipedia.org/wiki/Help:Displaying_a_formula and https://en.wikipedia.org/wiki/List_of_mathematical_symbols for L^AT_EX maths and other notations, respectively.

The following were taken from `isomath-test.tex`.

E2.1 Math alphabets

If there are other symbols in place of Greek letters in a math alphabet, it uses T1 or OT1 font encoding instead of OML.

<code>mathnormal</code>	$A, B, \Gamma, \Delta, \Theta, \Lambda, \Xi, \Pi, \Sigma, \Phi, \Psi, \Omega, \alpha, \beta, \pi, \nu, \omega, v, w, 0, 1, 9$
<code>mathit</code>	$A, B, \Gamma, \Delta, \Theta, \Lambda, \Xi, \Pi, \Sigma, \Phi, \Psi, \Omega, \mathfrak{f}, \mathfrak{f}, \beta, \circ, !, v, w, 0, 1, 9$
<code>mathrm</code>	$A, B, \Gamma, \Delta, \Theta, \Lambda, \Xi, \Pi, \Sigma, \Phi, \Psi, \Omega, \mathfrak{f}, \mathfrak{f}, \beta, \circ, !, v, w, 0, 1, 9$
<code>mathbf</code>	$\mathbf{A}, \mathbf{B}, \mathbf{\Gamma}, \mathbf{\Delta}, \mathbf{\Theta}, \mathbf{\Lambda}, \mathbf{\Xi}, \mathbf{\Pi}, \mathbf{\Sigma}, \mathbf{\Phi}, \mathbf{\Psi}, \mathbf{\Omega}, \mathbf{f}, \mathbf{f}, \mathbf{\beta}, \circ, !, v, w, 0, 1, 9$
<code>mathsf</code>	$A, B, \Gamma, \Delta, \Theta, \Lambda, \Xi, \Pi, \Sigma, \Phi, \Psi, \Omega, \mathfrak{f}, \mathfrak{f}, \beta, \circ, !, v, w, 0, 1, 9$
<code>mathtt</code>	$A, B, \Gamma, \Delta, \Theta, \Lambda, \Xi, \Pi, \Sigma, \Phi, \Psi, \Omega, \uparrow, \downarrow, \beta, \circ, !, v, w, 0, 1, 9$

New alphabets bold-italic, sans-serif-italic, and sans-serif-bold-italic.

<code>mathbfit</code>	$\mathbf{A}, \mathbf{B}, \mathbf{\Gamma}, \mathbf{\Delta}, \mathbf{\Theta}, \mathbf{\Lambda}, \mathbf{\Xi}, \mathbf{\Pi}, \mathbf{\Sigma}, \mathbf{\Phi}, \mathbf{\Psi}, \mathbf{\Omega}, \alpha, \beta, \pi, \nu, \omega, v, w, 0, 1, 9$
<code>mathsf</code>	$A, B, \Gamma, \Delta, \Theta, \Lambda, \Xi, \Pi, \Sigma, \Phi, \Psi, \Omega, \alpha, \beta, \pi, \nu, \omega, v, w, 0, 1, 9$
<code>mathsfbit</code>	$\mathbf{A}, \mathbf{B}, \mathbf{\Gamma}, \mathbf{\Delta}, \mathbf{\Theta}, \mathbf{\Lambda}, \mathbf{\Xi}, \mathbf{\Pi}, \mathbf{\Sigma}, \mathbf{\Phi}, \mathbf{\Psi}, \mathbf{\Omega}, \alpha, \beta, \pi, \nu, \omega, v, w, 0, 1, 9$

Do the math alphabets match?

$\alpha x \alpha \omega \alpha x \alpha \omega \alpha x \alpha \omega \quad TC\Theta\Gamma TC\Theta\Gamma TC\Theta\Gamma$

E2.2 Vector symbols

Alphabetic symbols for vectors are boldface italic, $\lambda = e_1 \cdot a$, while numeric ones (e.g. the zero vector) are bold upright, $a + 0 = a$.

E2.3 Matrix symbols

Symbols for matrices are boldface italic, too:¹ $\mathbf{A} = \mathbf{E} \cdot \mathbf{A}$.

¹However, matrix symbols are usually capital letters whereas vectors are small ones. Exceptions are physical quantities like the force vector \mathbf{F} or the electrical field \mathbf{E} .

1624 **E2.4 Tensor symbols**

1625 Symbols for tensors are sans-serif bold italic,

$$\boldsymbol{\alpha} = \boldsymbol{e} \cdot \boldsymbol{a} \quad \Longleftrightarrow \quad \alpha_{ijl} = e_{ijk} \cdot a_{kl}.$$

1626 The permittivity tensor describes the coupling of electric field and displacement:

$$\boldsymbol{D} = \epsilon_0 \boldsymbol{\epsilon}_r \boldsymbol{E}$$



E2.5 Bold math version

The “bold” math version is selected with the commands `\boldmath` or `\mathversion{bold}`

<code>mathnormal</code>	$A, B, \Gamma, \Delta, \Theta, \Lambda, \Xi, \Pi, \Sigma, \Phi, \Psi, \Omega, \alpha, \beta, \pi, \nu, \omega, v, w, 0, 1, 9$
<code>mathit</code>	$A, B, \Gamma, \Delta, \Theta, \Lambda, \Xi, \Pi, \Sigma, \Phi, \Psi, \Omega, \mathfrak{f}, \mathfrak{fi}, \mathfrak{B}, \mathfrak{C}, \mathfrak{D}, \mathfrak{E}, \mathfrak{F}, \mathfrak{G}, \mathfrak{H}, \mathfrak{I}, \mathfrak{J}, \mathfrak{K}, \mathfrak{L}, \mathfrak{M}, \mathfrak{N}, \mathfrak{O}, \mathfrak{P}, \mathfrak{Q}, \mathfrak{R}, \mathfrak{S}, \mathfrak{T}, \mathfrak{U}, \mathfrak{V}, \mathfrak{W}, \mathfrak{X}, \mathfrak{Y}, \mathfrak{Z}, \mathfrak{a}, \mathfrak{b}, \mathfrak{c}, \mathfrak{d}, \mathfrak{e}, \mathfrak{f}, \mathfrak{g}, \mathfrak{h}, \mathfrak{i}, \mathfrak{j}, \mathfrak{k}, \mathfrak{l}, \mathfrak{m}, \mathfrak{n}, \mathfrak{o}, \mathfrak{p}, \mathfrak{q}, \mathfrak{r}, \mathfrak{s}, \mathfrak{t}, \mathfrak{u}, \mathfrak{v}, \mathfrak{w}, \mathfrak{x}, \mathfrak{y}, \mathfrak{z}, \mathfrak{0}, \mathfrak{1}, \mathfrak{2}, \mathfrak{3}, \mathfrak{4}, \mathfrak{5}, \mathfrak{6}, \mathfrak{7}, \mathfrak{8}, \mathfrak{9}}$
<code>mathrm</code>	$A, B, \Gamma, \Delta, \Theta, \Lambda, \Xi, \Pi, \Sigma, \Phi, \Psi, \Omega, \mathfrak{f}, \mathfrak{fi}, \mathfrak{B}, \mathfrak{C}, \mathfrak{D}, \mathfrak{E}, \mathfrak{F}, \mathfrak{G}, \mathfrak{H}, \mathfrak{I}, \mathfrak{J}, \mathfrak{K}, \mathfrak{L}, \mathfrak{M}, \mathfrak{N}, \mathfrak{O}, \mathfrak{P}, \mathfrak{Q}, \mathfrak{R}, \mathfrak{S}, \mathfrak{T}, \mathfrak{U}, \mathfrak{V}, \mathfrak{W}, \mathfrak{X}, \mathfrak{Y}, \mathfrak{Z}, \mathfrak{a}, \mathfrak{b}, \mathfrak{c}, \mathfrak{d}, \mathfrak{e}, \mathfrak{f}, \mathfrak{g}, \mathfrak{h}, \mathfrak{i}, \mathfrak{j}, \mathfrak{k}, \mathfrak{l}, \mathfrak{m}, \mathfrak{n}, \mathfrak{o}, \mathfrak{p}, \mathfrak{q}, \mathfrak{r}, \mathfrak{s}, \mathfrak{t}, \mathfrak{u}, \mathfrak{v}, \mathfrak{w}, \mathfrak{x}, \mathfrak{y}, \mathfrak{z}, \mathfrak{0}, \mathfrak{1}, \mathfrak{2}, \mathfrak{3}, \mathfrak{4}, \mathfrak{5}, \mathfrak{6}, \mathfrak{7}, \mathfrak{8}, \mathfrak{9}}$
<code>mathbf</code>	$A, B, \Gamma, \Delta, \Theta, \Lambda, \Xi, \Pi, \Sigma, \Phi, \Psi, \Omega, \mathfrak{f}, \mathfrak{fi}, \mathfrak{B}, \mathfrak{C}, \mathfrak{D}, \mathfrak{E}, \mathfrak{F}, \mathfrak{G}, \mathfrak{H}, \mathfrak{I}, \mathfrak{J}, \mathfrak{K}, \mathfrak{L}, \mathfrak{M}, \mathfrak{N}, \mathfrak{O}, \mathfrak{P}, \mathfrak{Q}, \mathfrak{R}, \mathfrak{S}, \mathfrak{T}, \mathfrak{U}, \mathfrak{V}, \mathfrak{W}, \mathfrak{X}, \mathfrak{Y}, \mathfrak{Z}, \mathfrak{a}, \mathfrak{b}, \mathfrak{c}, \mathfrak{d}, \mathfrak{e}, \mathfrak{f}, \mathfrak{g}, \mathfrak{h}, \mathfrak{i}, \mathfrak{j}, \mathfrak{k}, \mathfrak{l}, \mathfrak{m}, \mathfrak{n}, \mathfrak{o}, \mathfrak{p}, \mathfrak{q}, \mathfrak{r}, \mathfrak{s}, \mathfrak{t}, \mathfrak{u}, \mathfrak{v}, \mathfrak{w}, \mathfrak{x}, \mathfrak{y}, \mathfrak{z}, \mathfrak{0}, \mathfrak{1}, \mathfrak{2}, \mathfrak{3}, \mathfrak{4}, \mathfrak{5}, \mathfrak{6}, \mathfrak{7}, \mathfrak{8}, \mathfrak{9}}$
<code>mathsf</code>	$A, B, \Gamma, \Delta, \Theta, \Lambda, \Xi, \Pi, \Sigma, \Phi, \Psi, \Omega, \mathfrak{f}, \mathfrak{fi}, \mathfrak{B}, \mathfrak{C}, \mathfrak{D}, \mathfrak{E}, \mathfrak{F}, \mathfrak{G}, \mathfrak{H}, \mathfrak{I}, \mathfrak{J}, \mathfrak{K}, \mathfrak{L}, \mathfrak{M}, \mathfrak{N}, \mathfrak{O}, \mathfrak{P}, \mathfrak{Q}, \mathfrak{R}, \mathfrak{S}, \mathfrak{T}, \mathfrak{U}, \mathfrak{V}, \mathfrak{W}, \mathfrak{X}, \mathfrak{Y}, \mathfrak{Z}, \mathfrak{a}, \mathfrak{b}, \mathfrak{c}, \mathfrak{d}, \mathfrak{e}, \mathfrak{f}, \mathfrak{g}, \mathfrak{h}, \mathfrak{i}, \mathfrak{j}, \mathfrak{k}, \mathfrak{l}, \mathfrak{m}, \mathfrak{n}, \mathfrak{o}, \mathfrak{p}, \mathfrak{q}, \mathfrak{r}, \mathfrak{s}, \mathfrak{t}, \mathfrak{u}, \mathfrak{v}, \mathfrak{w}, \mathfrak{x}, \mathfrak{y}, \mathfrak{z}, \mathfrak{0}, \mathfrak{1}, \mathfrak{2}, \mathfrak{3}, \mathfrak{4}, \mathfrak{5}, \mathfrak{6}, \mathfrak{7}, \mathfrak{8}, \mathfrak{9}}$
<code>mathtt</code>	$A, B, \Gamma, \Delta, \Theta, \Lambda, \Xi, \Pi, \Sigma, \Phi, \Psi, \Omega, \mathfrak{f}, \mathfrak{fi}, \mathfrak{B}, \mathfrak{C}, \mathfrak{D}, \mathfrak{E}, \mathfrak{F}, \mathfrak{G}, \mathfrak{H}, \mathfrak{I}, \mathfrak{J}, \mathfrak{K}, \mathfrak{L}, \mathfrak{M}, \mathfrak{N}, \mathfrak{O}, \mathfrak{P}, \mathfrak{Q}, \mathfrak{R}, \mathfrak{S}, \mathfrak{T}, \mathfrak{U}, \mathfrak{V}, \mathfrak{W}, \mathfrak{X}, \mathfrak{Y}, \mathfrak{Z}, \mathfrak{a}, \mathfrak{b}, \mathfrak{c}, \mathfrak{d}, \mathfrak{e}, \mathfrak{f}, \mathfrak{g}, \mathfrak{h}, \mathfrak{i}, \mathfrak{j}, \mathfrak{k}, \mathfrak{l}, \mathfrak{m}, \mathfrak{n}, \mathfrak{o}, \mathfrak{p}, \mathfrak{q}, \mathfrak{r}, \mathfrak{s}, \mathfrak{t}, \mathfrak{u}, \mathfrak{v}, \mathfrak{w}, \mathfrak{x}, \mathfrak{y}, \mathfrak{z}, \mathfrak{0}, \mathfrak{1}, \mathfrak{2}, \mathfrak{3}, \mathfrak{4}, \mathfrak{5}, \mathfrak{6}, \mathfrak{7}, \mathfrak{8}, \mathfrak{9}}$

New alphabets bold-italic, sans-serif-italic, and sans-serif-bold-italic.

<code>mathbf</code>	$A, B, \Gamma, \Delta, \Theta, \Lambda, \Xi, \Pi, \Sigma, \Phi, \Psi, \Omega, \alpha, \beta, \pi, \nu, \omega, v, w, 0, 1, 9$
<code>mathsf</code>	$A, B, \Gamma, \Delta, \Theta, \Lambda, \Xi, \Pi, \Sigma, \Phi, \Psi, \Omega, \alpha, \beta, \pi, \nu, \omega, v, w, 0, 1, 9$
<code>mathsfbf</code>	$A, B, \Gamma, \Delta, \Theta, \Lambda, \Xi, \Pi, \Sigma, \Phi, \Psi, \Omega, \alpha, \beta, \pi, \nu, \omega, v, w, 0, 1, 9$

Do the math alphabets match?

$\alpha x \alpha \omega a x \alpha \omega a x \alpha \omega \quad TC\Theta\Gamma TC\Theta\Gamma TC\Theta\Gamma$

E2.5.1 Vector symbols

Alphabetic symbols for vectors are boldface italic, $\lambda = e_1 \cdot a$, while numeric ones (e.g. the zero vector) are bold upright, $a + 0 = a$.

E2.5.2 Matrix symbols

Symbols for matrices are boldface italic, too:² $\Lambda = E \cdot A$.

E2.5.3 Tensor symbols

Symbols for tensors are sans-serif bold italic,

$$\alpha = e \cdot a \quad \Longleftrightarrow \quad \alpha_{ijl} = e_{ijk} \cdot a_{kl}.$$

The permittivity tensor describes the coupling of electric field and displacement:

$$D = \epsilon_0 \epsilon_r E$$

²However, matrix symbols are usually capital letters whereas vectors are small ones. Exceptions are physical quantities like the force vector F or the electrical field E .



1640

The verbatim L^AT_EX code of Sec. E2 is in List. E.2.Listing E.2: Sample L^AT_EX code for notations usage

```

1641 1 % A teststring with Latin and Greek letters::
1642 2 \newcommand{\teststring}{%
1643 3 % capital Latin letters
1644 4 % A,B,C,
1645 5 A,B,
1646 6 % capital Greek letters
1647 7 %\Gamma,\Delta,\Theta,\Lambda,\Xi,\Pi,\Sigma,\Upsilon,\Phi,\Psi,
1648 8 \Gamma,\Delta,\Theta,\Lambda,\Xi,\Pi,\Sigma,\Phi,\Psi,\Omega,
1649 9 % small Greek letters
1650 10 \alpha,\beta,\pi,\nu,\omega,
1651 11 % small Latin letters:
1652 12 % compare \nu, \omega, v, and w
1653 13 v,w,
1654 14 % digits
1655 15 0,1,9
1656 16 }
1657 17
1658 18
1659 19 \subsection{Math alphabets}
1660 20
1661 21 If there are other symbols in place of Greek letters in a math
1662 22 alphabet, it uses T1 or OT1 font encoding instead of OML.
1663 23
1664 24 \begin{eqnarray*}
1665 25 \mbox{mathnormal} & & \& \& \teststring \\
1666 26 \mbox{mathit} & & \& \& \mathit{\teststring} \\
1667 27 \mbox{mathrm} & & \& \& \mathrm{\teststring} \\
1668 28 \mbox{mathbf} & & \& \& \mathbf{\teststring} \\
1669 29 \mbox{mathsf} & & \& \& \mathsf{\teststring} \\
1670 30 \mbox{mathtt} & & \& \& \mathtt{\teststring} \\
1671 31 \end{eqnarray*}
1672 32 New alphabets bold-italic, sans-serif-italic, and sans-serif-bold-
1673 33 italic.
1674 34 \begin{eqnarray*}
1675 35 \mbox{mathbfit} & & \& \& \mathbfit{\teststring} \\
1676 36 \mbox{mathsf} & & \& \& \mathsf{\teststring} \\
1677 37 \mbox{mathsf} & & \& \& \mathsf{\teststring} \\
1678 38 \mbox{mathsf} & & \& \& \mathsf{\teststring} \\
1679 39 \end{eqnarray*}
1680 40 %
1681 41 Do the math alphabets match?
1682 42 $
1683 43 \mathnormal {a x \alpha \omega}
1684 44 \mathbfit {a x \alpha \omega}
1685 45 \mathsf {a x \alpha \omega}
1686 46 \quad
1687 47 \mathsf {T C \Theta \Gamma}
1688 48 \mathbfit {T C \Theta \Gamma}
1689 49 \mathnormal {T C \Theta \Gamma}
1690 50 $
1691 51 \subsection{Vector symbols}
1692 52

```



```

1695 53 Alphabetic symbols for vectors are boldface italic,
1696 54  $\vec{\lambda} = \vec{e}_1 \cdot \vec{a}$ ,
1697 55 while numeric ones (e.g. the zero vector) are bold upright,
1698 56  $\vec{a} + \vec{0} = \vec{a}$ .
1699 57
1700 58 \subsection{Matrix symbols}
1701 59
1702 60 Symbols for matrices are boldface italic, too:%
1703 61 \footnote{However, matrix symbols are usually capital letters whereas
1704 62 vectors
1705 62 are small ones. Exceptions are physical quantities like the force
1706 63 vector  $\vec{F}$  or the electrical field  $\vec{E}$ .%
1707 64 }
1708 65  $\Lambda = E \cdot A$ .
1709 66
1710 67
1711 68 \subsection{Tensor symbols}
1712 69
1713 70 Symbols for tensors are sans-serif bold italic,
1714 71
1715 72 [
1716 73   \tensorsym{\alpha} = \tensorsym{e} \cdot \tensorsym{a}
1717 74   \quad \Longleftrightarrow \quad
1718 75   \alpha_{ijl} = e_{ijk} \cdot a_{kl}.
1719 76 ]
1720 77
1721 78
1722 79 The permittivity tensor describes the coupling of electric field and
1723 80 displacement: [
1724 81  $D = \epsilon_0 \text{\tensorsym{\epsilon}}_{\text{\mathrm{r}}} \vec{E}$ ]
1725 82
1726 83
1727 84
1728 85 \newpage
1729 86 \subsection{Bold math version}
1730 87
1731 88 The ‘‘bold’’ math version is selected with the commands
1732 89 \verb+\boldmath+ or \verb+\mathversion{bold}+
1733 90
1734 91 {\boldmath
1735 92   \begin{eqnarray*}
1736 93     \mbox{\mathnormal} & & \teststring \\
1737 94     \mbox{\mathit} & & \mathit{\teststring} \\
1738 95     \mbox{\mathrm} & & \mathrm{\teststring} \\
1739 96     \mbox{\mathbf} & & \mathbf{\teststring} \\
1740 97     \mbox{\mathsf} & & \mathsf{\teststring} \\
1741 98     \mbox{\mathtt} & & \mathtt{\teststring}
1742 99   \end{eqnarray*}
1743 100   New alphabets bold-italic, sans-serif-italic, and sans-serif-bold-
1744 101   italic.
1745 102   \begin{eqnarray*}
1746 103     \mbox{\mathbfit} & & \mathbfit{\teststring} \\
1747 104     \mbox{\mathsfit} & & \mathsfit{\teststring} \\
1748 105     \mbox{\mathsfbfit} & & \mathsfbfit{\teststring}
1749 106   \end{eqnarray*}
1750 107   %
1751 108   Do the math alphabets match?

```



```

1752 108
1753 109 $
1754 110 \mathnormal {a x \alpha \omega}
1755 111 \mathbfit {a x \alpha \omega}
1756 112 \mathsfbfit{a x \alpha \omega}
1757 113 \quad
1758 114 \mathsfbfit{T C \Theta \Gamma}
1759 115 \mathbfit {T C \Theta \Gamma}
1760 116 \mathnormal {T C \Theta \Gamma}
1761 117 $
1762 118
1763 119 \subsection{Vector symbols}
1764 120
1765 121 Alphabetic symbols for vectors are boldface italic,
1766 122 $\vec{\lambda}=\vec{e}_{1}\cdot\vec{a}$,
1767 123 while numeric ones (e.g. the zero vector) are bold upright,
1768 124 $\vec{a} + \vec{0} = \vec{a}$.
1769 125
1770 126
1771 127
1772 128
1773 129 \subsection{Matrix symbols}
1774 130
1775 131 Symbols for matrices are boldface italic, too:%
1776 132 \footnote{However, matrix symbols are usually capital letters whereas
1777 133 vectors
1778 133 are small ones. Exceptions are physical quantities like the force
1779 134 vector $\vec{F}$ or the electrical field $\vec{E}$.%
1780 135 }
1781 136 $\matrixsym{\Lambda}=\matrixsym{E}\cdot\matrixsym{A}$.
1782 137
1783 138
1784 139 \subsection{Tensor symbols}
1785 140
1786 141 Symbols for tensors are sans-serif bold italic,
1787 142
1788 143 \[
1789 144 \tensorsym{\alpha} = \tensorsym{e}\cdot\tensorsym{a}
1790 145 \quad \Longleftarrow \quad
1791 146 \alpha_{ijl} = e_{ijk}\cdot a_{kl}.
1792 147 \]
1793 148
1794 149 The permittivity tensor describes the coupling of electric field and
1795 150 displacement: \[
1796 151 \vec{D}=\epsilon_{0}\tensorsym{\epsilon}_{\mathrm{r}}\vec{E}\]
1797 152 }

```



E3 Abbreviation

This section shows examples of the use of \LaTeX commands in conjunction with the items that are in the `abbreviation.tex` and in the `glossary.tex` files. Please see List. E.3. **To lessen the \LaTeX parsing time, it is suggested that you use `\acr{ }` only for the first occurrence of the word to be abbreviated.**

Again please see List. E.3. Here is an example of first use: alternating current (ac). Next use: ac. Full: alternating current (ac). Here's an acronym referenced using `\acr` : hyper-text markup language (html). And here it is again: html. If you are used to the glossaries package, note the difference in using `\gls` : hyper-text markup language (html). And again (no difference): hyper-text markup language (html). For plural use `\glspl` . Here are some more entries:

- extensible markup language (xml) and cascading style sheet (css).
- Next use: xml and css.
- Full form: extensible markup language (xml) and cascading style sheet (css).
- Reset again.
- Start with a capital. Hyper-text markup language (html).
- Next: Html. Full: Hyper-text markup language (html).
- Prefer capitals? Extensible markup language (XML). Next: XML. Full: extensible markup language (XML).
- Prefer small-caps? Cascading style sheet (CSS). Next: CSS. Full: cascading style sheet (CSS).
- Resetting all acronyms.
- Here are the acronyms again:
- Hyper-text markup language (HTML), extensible markup language (XML) and cascading style sheet (CSS).
- Next use: HTML, XML and CSS.
- Full form: Hyper-text markup language (HTML), extensible markup language (XML) and cascading style sheet (CSS).



- 1828 • Provide your own link text: style sheet.

1829 The verbatim \LaTeX code of Sec. E3 is in List. E.3.

Listing E.3: Sample \LaTeX code for abbreviations usage

```

1 Again please see List.~\ref{lst:abbrv}. Here is an example of first use:
   \acr{ac}. Next use: \acr{ac}. Full: \gls{ac}. Here's an acronym
   referenced using \verb| \acr |: \acr{html}. And here it is again: \
   acr{html}. If you are used to the \texttt{glossaries} package, note
   the difference in using \verb| \gls |: \gls{html}. And again (no
   difference): \gls{html}. Here are some more entries:
2
3 \begin{itemize}
4
5   \item \acr{xml} and \acr{css}.
6
7   \item Next use: \acr{xml} and \acr{css}.
8
9   \item Full form: \gls{xml} and \gls{css}.
10
11  \item Reset again. \glsresetall{abbreviation}
12
13  \item Start with a capital. \Acr{html}.
14
15  \item Next: \Acr{html}. Full: \Gls{html}.
16
17  \item Prefer capitals? \renewcommand{\acronymfont}[1]{\
   MakeTextUppercase{#1}} \Acr{xml}. Next: \acr{xml}. Full: \gls{xml}
   }.
18
19  \item Prefer small-caps? \renewcommand{\acronymfont}[1]{\textsc{#1}}
   \Acr{css}. Next: \acr{css}. Full: \gls{css}.
20
21  \item Resetting all acronyms.\glsresetall{abbreviation}
22
23  \item Here are the acronyms again:
24
25  \item \Acr{html}, \acr{xml} and \acr{css}.
26
27  \item Next use: \Acr{html}, \acr{xml} and \acr{css}.
28
29  \item Full form: \Gls{html}, \gls{xml} and \gls{css}.
30
31  \item Provide your own link text: \glslink{[textbf]css}{style}
32
33 \end{itemize}

```



E4 Glossary

This section shows examples of the use of `\gls{ }` commands in conjunction with the items that are in the `glossary.tex` and `notation.tex` files. Note that entries in `notation.tex` are prefixed with “not:” label (see List. E.4).

Please make sure that the entries in `notation.tex` are those that are referenced in the \LaTeX document files used by this Thesis. Please comment out unused notations and be careful with the commas and brackets in `notation.tex` .

- Matrices are usually denoted by a bold capital letter, such as \mathbf{A} . The matrix’s (i, j) th element is usually denoted a_{ij} . Matrix \mathbf{I} is the identity matrix.
- A set, denoted as \mathcal{S} , is a collection of objects.
- The universal set, denoted as \mathcal{U} , is the set of everything.
- The empty set, denoted as \emptyset , contains no elements.
- Functional Analysis is seen as the study of complete normed vector spaces, i.e., Banach spaces.
- The cardinality of a set, denoted as $|\mathcal{S}|$, is the number of elements in the set.

The verbatim \LaTeX code for the part of Sec. E4 is in List. E.4.

Listing E.4: Sample \LaTeX code for glossary and notations usage

```

1 \begin{itemize}
2
3   \item \Glspl{matrix} are usually denoted by a bold capital letter,
      such as  $\mathbf{A}$ . The  $\text{\Gls{matrix}}$ 's  $(i,j)$ th element is
      usually denoted  $a_{ij}$ .  $\text{\Gls{matrix}}$   $\mathbf{I}$  is the
      identity  $\text{\Gls{matrix}}$ .
4
5   \item A set, denoted as  $\text{\Gls{not:set}}$ , is a collection of objects.
6
7   \item The universal set, denoted as  $\text{\Gls{not:universalSet}}$ , is the
      set of everything.
8
9   \item The empty set, denoted as  $\text{\Gls{not:emptySet}}$ , contains no
      elements.
10
11   \item  $\text{\Gls{Functional Analysis}}$  is seen as the study of complete
      normed vector spaces, i.e., Banach spaces.
12
13   \item The cardinality of a set, denoted as  $\text{\Gls{not:cardinality}}$ , is
      the number of elements in the set.
14
15 \end{itemize}

```



E5 Figure

This section shows several ways of placing figures. PDFL^AT_EX compatible files are PDF, PNG, and JPG. Please see the `figure` subdirectory.



Fig. E.1 A quadrilateral image example.



1849 Fig. E.1 is a gray box enclosed by a dark border. List. E.5 shows the corresponding
1850 \LaTeX code.

Listing E.5: Sample \LaTeX code for a single figure

```
1 \begin{figure}[!htbp]
2   \centering
3   \includegraphics[width=0.5\textwidth]{example}
4   \caption{A quadrilateral image example.}
5   \label{fig:example}
6 \end{figure}
7 \cleardoublepage
8
9 Fig.~\ref{fig:example} is a gray box enclosed by a dark border. List.~\ref{lst:onefig} shows the corresponding  $\text{\LaTeX}$  \ code.
10 \end{figure}
```



(a) A sub-figure in the top row.



(b) A sub-figure in the middle row.



(c) A sub-figure in the bottom row.

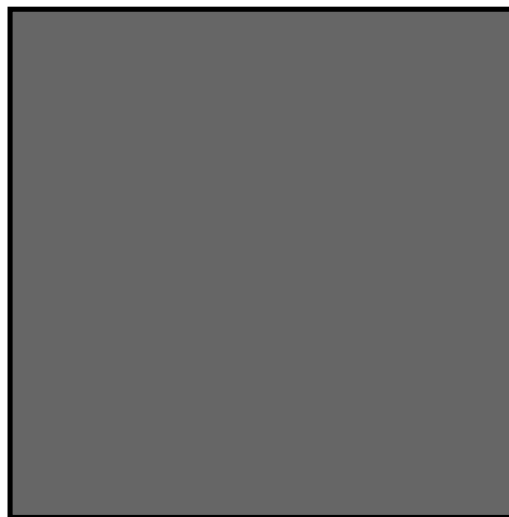
Fig. E.2 Figures on top of each other. See List. E.6 for the corresponding \LaTeX code.

Listing E.6: Sample L^AT_EX code for three figures on top of each other

```
1 \begin{figure}[!htbp]
2 \centering
3 \subbottom[A sub-figure in the top row.]{
4 \includegraphics[width=0.35\textwidth]{example_gray_box}
5 \label{fig:top}
6 }
7 \vfill
8 \subbottom[A sub-figure in the middle row.]{
9 \includegraphics[width=0.35\textwidth]{example_gray_box}
10 \label{fig:mid}
11 }
12 \vfill
13 \subbottom[A sub-figure in the bottom row.]{
14 \includegraphics[width=0.35\textwidth]{example_gray_box}
15 \label{fig:botm}
16 }
17 \caption{Figures on top of each other}
18 \label{fig:tmb}
19 \end{figure}
```



(a) A sub-figure in the upper-left corner.



(b) A sub-figure in the upper-right corner.



(c) A sub-figure in the lower-left corner.



(d) A sub-figure in the lower-right corner.

Fig. E.3 Four figures in each corner. See List. E.7 for the corresponding \LaTeX code.

Listing E.7: Sample \LaTeX code for the four figures

```

1 \begin{figure}[!htbp]
2 \centering
3 \subbottom[A sub-figure in the upper-left corner.]{
4 \includegraphics[width=0.45\textwidth]{example_gray_box}
5 \label{fig:upprleft}
6 }
7 \hfill
8 \subbottom[A sub-figure in the upper-right corner.]{
9 \includegraphics[width=0.45\textwidth]{example_gray_box}
10 \label{fig:uppright}
11 }
12 \vfill
13 \subbottom[A sub-figure in the lower-left corner.]{
14 \includegraphics[width=0.45\textwidth]{example_gray_box}
15 \label{fig:lowerleft}
16 }
17 \hfill
18 \subbottom[A sub-figure in the lower-right corner]{
19 \includegraphics[width=0.45\textwidth]{example_gray_box}
20 \label{fig:lowright}
21 }
22 \caption{Four figures in each corner. See List.\ref{lst:fourfigs} for
23 the corresponding \LaTeX \ code.}
24 \label{fig:fourfig}
25 \end{figure}

```



E6 Table

This section shows an example of placing a table (a long one). Table E.1 are the triples.

TABLE E.1 FEASIBLE TRIPLES FOR HIGHLY VARIABLE GRID

Time (s)	Triple chosen	Other feasible triples
0	(1, 11, 13725)	(1, 12, 10980), (1, 13, 8235), (2, 2, 0), (3, 1, 0)
2745	(1, 12, 10980)	(1, 13, 8235), (2, 2, 0), (2, 3, 0), (3, 1, 0)
5490	(1, 12, 13725)	(2, 2, 2745), (2, 3, 0), (3, 1, 0)
8235	(1, 12, 16470)	(1, 13, 13725), (2, 2, 2745), (2, 3, 0), (3, 1, 0)
10980	(1, 12, 16470)	(1, 13, 13725), (2, 2, 2745), (2, 3, 0), (3, 1, 0)
13725	(1, 12, 16470)	(1, 13, 13725), (2, 2, 2745), (2, 3, 0), (3, 1, 0)
16470	(1, 13, 16470)	(2, 2, 2745), (2, 3, 0), (3, 1, 0)
19215	(1, 12, 16470)	(1, 13, 13725), (2, 2, 2745), (2, 3, 0), (3, 1, 0)
21960	(1, 12, 16470)	(1, 13, 13725), (2, 2, 2745), (2, 3, 0), (3, 1, 0)
24705	(1, 12, 16470)	(1, 13, 13725), (2, 2, 2745), (2, 3, 0), (3, 1, 0)
27450	(1, 12, 16470)	(1, 13, 13725), (2, 2, 2745), (2, 3, 0), (3, 1, 0)
30195	(2, 2, 2745)	(2, 3, 0), (3, 1, 0)
32940	(1, 13, 16470)	(2, 2, 2745), (2, 3, 0), (3, 1, 0)
35685	(1, 13, 13725)	(2, 2, 2745), (2, 3, 0), (3, 1, 0)
38430	(1, 13, 10980)	(2, 2, 2745), (2, 3, 0), (3, 1, 0)
41175	(1, 12, 13725)	(1, 13, 10980), (2, 2, 2745), (2, 3, 0), (3, 1, 0)
43920	(1, 13, 10980)	(2, 2, 2745), (2, 3, 0), (3, 1, 0)
46665	(2, 2, 2745)	(2, 3, 0), (3, 1, 0)
49410	(2, 2, 2745)	(2, 3, 0), (3, 1, 0)
52155	(1, 12, 16470)	(1, 13, 13725), (2, 2, 2745), (2, 3, 0), (3, 1, 0)
54900	(1, 13, 13725)	(2, 2, 2745), (2, 3, 0), (3, 1, 0)
57645	(1, 13, 13725)	(2, 2, 2745), (2, 3, 0), (3, 1, 0)
60390	(1, 12, 13725)	(2, 2, 2745), (2, 3, 0), (3, 1, 0)
63135	(1, 13, 16470)	(2, 2, 2745), (2, 3, 0), (3, 1, 0)
65880	(1, 13, 16470)	(2, 2, 2745), (2, 3, 0), (3, 1, 0)
68625	(2, 2, 2745)	(2, 3, 0), (3, 1, 0)
71370	(1, 13, 13725)	(2, 2, 2745), (2, 3, 0), (3, 1, 0)
74115	(1, 12, 13725)	(2, 2, 2745), (2, 3, 0), (3, 1, 0)
76860	(1, 13, 13725)	(2, 2, 2745), (2, 3, 0), (3, 1, 0)
79605	(1, 13, 13725)	(2, 2, 2745), (2, 3, 0), (3, 1, 0)
82350	(1, 12, 13725)	(2, 2, 2745), (2, 3, 0), (3, 1, 0)
85095	(1, 12, 13725)	(1, 13, 10980), (2, 2, 2745), (2, 3, 0), (3, 1, 0)
87840	(1, 13, 16470)	(2, 2, 2745), (2, 3, 0), (3, 1, 0)
90585	(1, 13, 16470)	(2, 2, 2745), (2, 3, 0), (3, 1, 0)
93330	(1, 13, 13725)	(2, 2, 2745), (2, 3, 0), (3, 1, 0)
96075	(1, 13, 16470)	(2, 2, 2745), (2, 3, 0), (3, 1, 0)
98820	(1, 13, 16470)	(2, 2, 2745), (2, 3, 0), (3, 1, 0)
101565	(1, 13, 13725)	(2, 2, 2745), (2, 3, 0), (3, 1, 0)
104310	(1, 13, 16470)	(2, 2, 2745), (2, 3, 0), (3, 1, 0)
107055	(1, 13, 13725)	(2, 2, 2745), (2, 3, 0), (3, 1, 0)
109800	(1, 13, 13725)	(2, 2, 2745), (2, 3, 0), (3, 1, 0)
112545	(1, 12, 16470)	(1, 13, 13725), (2, 2, 2745), (2, 3, 0), (3, 1, 0)
115290	(1, 13, 16470)	(2, 2, 2745), (2, 3, 0), (3, 1, 0)
118035	(1, 13, 13725)	(2, 2, 2745), (2, 3, 0), (3, 1, 0)
120780	(1, 13, 16470)	(2, 2, 2745), (2, 3, 0), (3, 1, 0)
123525	(1, 13, 13725)	(2, 2, 2745), (2, 3, 0), (3, 1, 0)

Continued on next page



Continued from previous page

Time (s)	Triple chosen	Other feasible triples
126270	(1, 12, 16470)	(1, 13, 13725), (2, 2, 2745), (2, 3, 0), (3, 1, 0)
129015	(2, 2, 2745)	(2, 3, 0), (3, 1, 0)
131760	(2, 2, 2745)	(2, 3, 0), (3, 1, 0)
134505	(1, 13, 16470)	(2, 2, 2745), (2, 3, 0), (3, 1, 0)
137250	(1, 13, 13725)	(2, 2, 2745), (2, 3, 0), (3, 1, 0)
139995	(2, 2, 2745)	(2, 3, 0), (3, 1, 0)
142740	(2, 2, 2745)	(2, 3, 0), (3, 1, 0)
145485	(1, 12, 16470)	(1, 13, 13725), (2, 2, 2745), (2, 3, 0), (3, 1, 0)
148230	(2, 2, 2745)	(2, 3, 0), (3, 1, 0)
150975	(1, 13, 16470)	(2, 2, 2745), (2, 3, 0), (3, 1, 0)
153720	(1, 12, 13725)	(2, 2, 2745), (2, 3, 0), (3, 1, 0)
156465	(1, 13, 13725)	(2, 2, 2745), (2, 3, 0), (3, 1, 0)
159210	(1, 13, 13725)	(2, 2, 2745), (2, 3, 0), (3, 1, 0)
161955	(1, 13, 16470)	(2, 2, 2745), (2, 3, 0), (3, 1, 0)
164700	(1, 13, 13725)	(2, 2, 2745), (2, 3, 0), (3, 1, 0)



1854 List. E.8 shows the corresponding \LaTeX code.

Listing E.8: Sample \LaTeX code for making typical table environment

```

1855 1 \begin{center}
1856 2 {\scriptsize
1857 3 \begin{tabularx}{\textwidth}{p{0.1\textwidth}|p{0.2\textwidth}|p{0.5\textwidth}}
1858 4 \caption{Feasible triples for highly variable grid} \label{tab:triple_
1859 5 grid} \\
1860 6 \hline
1861 7 \textbf{Time (s)} &
1862 8 \textbf{Triple chosen} &
1863 9 \textbf{Other feasible triples} \\
1864 10 \hline
1865 11 \endfirsthead
1866 12 \multicolumn{3}{c}{\textit{Continued from previous page}} \\
1867 13 \hline
1868 14 \hline
1869 15 \textbf{Time (s)} &
1870 16 \textbf{Triple chosen} &
1871 17 \textbf{Other feasible triples} \\
1872 18 \hline
1873 19 \endhead
1874 20 \hline
1875 21 \multicolumn{3}{r}{\textit{Continued on next page}} \\
1876 22 \hline
1877 23 \endfoot
1878 24 \hline
1879 25 \endlastfoot
1880 26 \hline
1881 27
1882 28 0 & (1, 11, 13725) & (1, 12, 10980), (1, 13, 8235), (2, 2, 0), (3, 1, 0) \\
1883 29 & 2745 & (1, 12, 10980) & (1, 13, 8235), (2, 2, 0), (2, 3, 0), (3, 1, 0) \\
1884 30 & 5490 & (1, 12, 13725) & (2, 2, 2745), (2, 3, 0), (3, 1, 0) \\
1885 31 & 8235 & (1, 12, 16470) & (1, 13, 13725), (2, 2, 2745), (2, 3, 0), (3, 1, 0) \\
1886 32 & 10980 & (1, 12, 16470) & (1, 13, 13725), (2, 2, 2745), (2, 3, 0), (3, 1, 0) \\
1887 33 & 13725 & (1, 12, 16470) & (1, 13, 13725), (2, 2, 2745), (2, 3, 0), (3, 1, 0) \\
1888 34 & 16470 & (1, 13, 16470) & (2, 2, 2745), (2, 3, 0), (3, 1, 0) \\
1889 35 & 19215 & (1, 12, 16470) & (1, 13, 13725), (2, 2, 2745), (2, 3, 0), (3, 1, 0) \\
1890 36 & 21960 & (1, 12, 16470) & (1, 13, 13725), (2, 2, 2745), (2, 3, 0), (3, 1, 0) \\
1891 37 & 24705 & (1, 12, 16470) & (1, 13, 13725), (2, 2, 2745), (2, 3, 0), (3, 1, 0) \\
1892 38 & 27450 & (1, 12, 16470) & (1, 13, 13725), (2, 2, 2745), (2, 3, 0), (3, 1, 0) \\
1893 39 & 30195 & (2, 2, 2745) & (2, 3, 0), (3, 1, 0) \\
1894 40 & 32940 & (1, 13, 16470) & (2, 2, 2745), (2, 3, 0), (3, 1, 0) \\
1895 41 & 35685 & (1, 13, 13725) & (2, 2, 2745), (2, 3, 0), (3, 1, 0) \\
1896 42 & 38430 & (1, 13, 10980) & (2, 2, 2745), (2, 3, 0), (3, 1, 0)

```



```

1909 43 41175 & (1, 12, 13725) & (1, 13, 10980), (2, 2, 2745), (2, 3, 0), (3, 1,
1910      0) \\
1911 44 43920 & (1, 13, 10980) & (2, 2, 2745), (2, 3, 0), (3, 1, 0) \\
1912 45 46665 & (2, 2, 2745) & (2, 3, 0), (3, 1, 0) \\
1913 46 49410 & (2, 2, 2745) & (2, 3, 0), (3, 1, 0) \\
1914 47 52155 & (1, 12, 16470) & (1, 13, 13725), (2, 2, 2745), (2, 3, 0), (3, 1,
1915      0) \\
1916 48 54900 & (1, 13, 13725) & (2, 2, 2745), (2, 3, 0), (3, 1, 0) \\
1917 49 57645 & (1, 13, 13725) & (2, 2, 2745), (2, 3, 0), (3, 1, 0) \\
1918 50 60390 & (1, 12, 13725) & (2, 2, 2745), (2, 3, 0), (3, 1, 0) \\
1919 51 63135 & (1, 13, 16470) & (2, 2, 2745), (2, 3, 0), (3, 1, 0) \\
1920 52 65880 & (1, 13, 16470) & (2, 2, 2745), (2, 3, 0), (3, 1, 0) \\
1921 53 68625 & (2, 2, 2745) & (2, 3, 0), (3, 1, 0) \\
1922 54 71370 & (1, 13, 13725) & (2, 2, 2745), (2, 3, 0), (3, 1, 0) \\
1923 55 74115 & (1, 12, 13725) & (2, 2, 2745), (2, 3, 0), (3, 1, 0) \\
1924 56 76860 & (1, 13, 13725) & (2, 2, 2745), (2, 3, 0), (3, 1, 0) \\
1925 57 79605 & (1, 13, 13725) & (2, 2, 2745), (2, 3, 0), (3, 1, 0) \\
1926 58 82350 & (1, 12, 13725) & (2, 2, 2745), (2, 3, 0), (3, 1, 0) \\
1927 59 85095 & (1, 12, 13725) & (1, 13, 10980), (2, 2, 2745), (2, 3, 0), (3, 1,
1928      0) \\
1929 60 87840 & (1, 13, 16470) & (2, 2, 2745), (2, 3, 0), (3, 1, 0) \\
1930 61 90585 & (1, 13, 16470) & (2, 2, 2745), (2, 3, 0), (3, 1, 0) \\
1931 62 93330 & (1, 13, 13725) & (2, 2, 2745), (2, 3, 0), (3, 1, 0) \\
1932 63 96075 & (1, 13, 16470) & (2, 2, 2745), (2, 3, 0), (3, 1, 0) \\
1933 64 98820 & (1, 13, 16470) & (2, 2, 2745), (2, 3, 0), (3, 1, 0) \\
1934 65 101565 & (1, 13, 13725) & (2, 2, 2745), (2, 3, 0), (3, 1, 0) \\
1935 66 104310 & (1, 13, 16470) & (2, 2, 2745), (2, 3, 0), (3, 1, 0) \\
1936 67 107055 & (1, 13, 13725) & (2, 2, 2745), (2, 3, 0), (3, 1, 0) \\
1937 68 109800 & (1, 13, 13725) & (2, 2, 2745), (2, 3, 0), (3, 1, 0) \\
1938 69 112545 & (1, 12, 16470) & (1, 13, 13725), (2, 2, 2745), (2, 3, 0), (3,
1939      1, 0) \\
1940 70 115290 & (1, 13, 16470) & (2, 2, 2745), (2, 3, 0), (3, 1, 0) \\
1941 71 118035 & (1, 13, 13725) & (2, 2, 2745), (2, 3, 0), (3, 1, 0) \\
1942 72 120780 & (1, 13, 16470) & (2, 2, 2745), (2, 3, 0), (3, 1, 0) \\
1943 73 123525 & (1, 13, 13725) & (2, 2, 2745), (2, 3, 0), (3, 1, 0) \\
1944 74 126270 & (1, 12, 16470) & (1, 13, 13725), (2, 2, 2745), (2, 3, 0), (3,
1945      1, 0) \\
1946 75 129015 & (2, 2, 2745) & (2, 3, 0), (3, 1, 0) \\
1947 76 131760 & (2, 2, 2745) & (2, 3, 0), (3, 1, 0) \\
1948 77 134505 & (1, 13, 16470) & (2, 2, 2745), (2, 3, 0), (3, 1, 0) \\
1949 78 137250 & (1, 13, 13725) & (2, 2, 2745), (2, 3, 0), (3, 1, 0) \\
1950 79 139995 & (2, 2, 2745) & (2, 3, 0), (3, 1, 0) \\
1951 80 142740 & (2, 2, 2745) & (2, 3, 0), (3, 1, 0) \\
1952 81 145485 & (1, 12, 16470) & (1, 13, 13725), (2, 2, 2745), (2, 3, 0), (3,
1953      1, 0) \\
1954 82 148230 & (2, 2, 2745) & (2, 3, 0), (3, 1, 0) \\
1955 83 150975 & (1, 13, 16470) & (2, 2, 2745), (2, 3, 0), (3, 1, 0) \\
1956 84 153720 & (1, 12, 13725) & (2, 2, 2745), (2, 3, 0), (3, 1, 0) \\
1957 85 156465 & (1, 13, 13725) & (2, 2, 2745), (2, 3, 0), (3, 1, 0) \\
1958 86 159210 & (1, 13, 13725) & (2, 2, 2745), (2, 3, 0), (3, 1, 0) \\
1959 87 161955 & (1, 13, 16470) & (2, 2, 2745), (2, 3, 0), (3, 1, 0) \\
1960 88 164700 & (1, 13, 13725) & (2, 2, 2745), (2, 3, 0), (3, 1, 0) \\
1961 89 \end{tabularx}
1962 90 }
1963 91 \end{center}

```



1965

E7 Algorithm or Pseudocode Listing

1966

Table E.2 shows an example pseudocode. Note that if the pseudocode exceeds one page, it can mean that its implementation is not modular. List. E.9 shows the corresponding L^AT_EX code.

1967

1968

TABLE E.2 CALCULATION OF $y = x^n$

Input(s):	
n	: n th power; $n \in \mathbb{Z}^+$
x	: base value; $x \in \mathbb{R}^+$
Output(s):	
y	: result; $y \in \mathbb{R}^+$

Require: $n \geq 0 \vee x \neq 0$

Ensure: $y = x^n$

```
1:  $y \leftarrow 1$ 
2: if  $n < 0$  then
3:    $X \leftarrow 1/x$ 
4:    $N \leftarrow -n$ 
5: else
6:    $X \leftarrow x$ 
7:    $N \leftarrow n$ 
8: end if
9: while  $N \neq 0$  do
10:  if  $N$  is even then
11:     $X \leftarrow X \times X$ 
12:     $N \leftarrow N/2$ 
13:  else { $N$  is odd}
14:     $y \leftarrow y \times X$ 
15:     $N \leftarrow N - 1$ 
16:  end if
17: end while
```

Listing E.9: Sample L^AT_EX code for algorithm or pseudocode listing usage

```

1 \begin{table}[!htbp]
2   \caption{Calculation of  $y = x^n$ }
3   \label{tab:calcxn}
4   {\footnotesize
5     \begin{tabular}{lll}
6       \hline
7       \hline
8       {\bfseries Input(s):} & & \\
9       $n$ & : & $n$th power; $n$ \in \mathbb{Z}^{+}$ \\
10      $x$ & : & base value; $x$ \in \mathbb{R}^{+}$ \\
11      \hline
12      {\bfseries Output(s):} & & \\
13      $y$ & : & result; $y$ \in \mathbb{R}^{+}$ \\
14      \hline
15      \hline
16      \\
17    \end{tabular}
18  }
19  \begin{algorithmic}[1]
20    {\footnotesize
21      \REQUIRE $n \geq 0$ \vee $x \neq 0$
22      \ENSURE $y = x^n$
23      \STATE $y \leftarrow 1$
24      \IF{$n < 0$}
25        \STATE $X \leftarrow 1 / x$
26        \STATE $N \leftarrow -n$
27      \ELSE
28        \STATE $X \leftarrow x$
29        \STATE $N \leftarrow n$
30      \ENDIF
31      \WHILE{$N \neq 0$}
32        \IF{$N$ is even}
33          \STATE $X \leftarrow X \times X$
34          \STATE $N \leftarrow N / 2$
35        \ELSE[$N$ is odd]
36          \STATE $y \leftarrow y \times X$
37          \STATE $N \leftarrow N - 1$
38        \ENDIF
39      \ENDWHILE
40    }
41  \end{algorithmic}
42 \end{table}

```



1969

E8 Program/Code Listing

1970

List. E.10 is a program listing of a C code for computing Fibonacci numbers by calling the actual code. Please see the `code` subdirectory.

1971

Listing E.10: Computing Fibonacci numbers in C (./code/fibo.c)

```

1  /* fibo.c -- It prints out the first N Fibonacci
2  *           numbers.
3  */
4
5  #include <stdio.h>
6
7  int main(void) {
8      int n;           /* Number of fibonacci numbers we will print */
9      int i;           /* Index of fibonacci number to be printed next */
10     int current;      /* Value of the (i)th fibonacci number */
11     int next;         /* Value of the (i+1)th fibonacci number */
12     int twoaway;      /* Value of the (i+2)th fibonacci number */
13
14     printf("How many Fibonacci numbers do you want to compute? ");
15     scanf("%d", &n);
16     if (n<=0)
17         printf("The number should be positive.\n");
18     else {
19         printf("\n\n\tI\t\tFibonacci(I)\t\n\t=====\n");
20         next = current = 1;
21         for (i=1; i<=n; i++) {
22             printf("\t%d\t\t\t%d\n", i, current);
23             twoaway = current+next;
24             current = next;
25             next = twoaway;
26         }
27     }
28 }
29
30 /* The output from a run of this program was:
31
32 How many Fibonacci numbers do you want to compute? 9
33
34 I      Fibonacci(I)
35 =====
36 1      1
37 2      1
38 3      2
39 4      3
40 5      5
41 6      8
42 7      13
43 8      21
44 9      34
45
46 */

```



1972

List. E.11 shows the corresponding \LaTeX code.

Listing E.11: Sample \LaTeX code for program listing

```
1 List.~\ref{lst:fib_c} is a program listing of a C code for computing  
Fibonacci numbers by calling the actual code. Please see the \verb|  
code | subdirectory.
```



E9 Referencing

Referencing chapters: This appendix is in Appendix E, which is about examples in using various \LaTeX commands.

Referencing sections: This section is Sec. E9, which shows how to refer to the locations of various labels that have been placed in the \LaTeX files. List. E.12 shows the corresponding \LaTeX code.

Listing E.12: Sample \LaTeX code for referencing sections

```
1 Referencing sections: This section is Sec.~\ref{sec:ref}, which shows
   how to refer to the locations of various labels that have been
   placed in the \LaTeX \ files. List.~\ref{lst:refsec} shows the
   corresponding \LaTeX \ code.
```

Lorem ipsum dolor sit amet, consectetur adipiscing elit. Etiam lobortis facilisis sem. Nullam nec mi et neque pharetra sollicitudin. Praesent imperdiet mi nec ante. Donec ullamcorper, felis non sodales commodo, lectus velit ultrices augue, a dignissim nibh lectus placerat pede. Vivamus nunc nunc, molestie ut, ultricies vel, semper in, velit. Ut porttitor. Praesent in sapien. Lorem ipsum dolor sit amet, consectetur adipiscing elit. Duis fringilla tristique neque. Sed interdum libero ut metus. Pellentesque placerat. Nam rutrum augue a leo. Morbi sed elit sit amet ante lobortis sollicitudin. Praesent blandit blandit mauris. Praesent lectus tellus, aliquet aliquam, luctus a, egestas a, turpis. Mauris lacinia lorem sit amet ipsum. Nunc quis urna dictum turpis accumsan semper.



E9.1 A subsection

Referencing subsections: This section is Sec. E9.1, which shows how to refer to a subsection. List. E.13 shows the corresponding \LaTeX code.

Listing E.13: Sample \LaTeX code for referencing subsections

```
1 Referencing subsections: This section is Sec.~\ref{sec:subsec}, which
  shows how to refer to a subsection. List.~\ref{lst:refsub} shows the
  corresponding \LaTeX \ code.
```

Lorem ipsum dolor sit amet, consectetur adipiscing elit. Etiam lobortis facilisis sem. Nullam nec mi et neque pharetra sollicitudin. Praesent imperdiet mi nec ante. Donec ullamcorper, felis non sodales commodo, lectus velit ultrices augue, a dignissim nibh lectus placerat pede. Vivamus nunc nunc, molestie ut, ultricies vel, semper in, velit. Ut porttitor. Praesent in sapien. Lorem ipsum dolor sit amet, consectetur adipiscing elit. Duis fringilla tristique neque. Sed interdum libero ut metus. Pellentesque placerat. Nam rutrum augue a leo. Morbi sed elit sit amet ante lobortis sollicitudin. Praesent blandit blandit mauris. Praesent lectus tellus, aliquet aliquam, luctus a, egestas a, turpis. Mauris lacinia lorem sit amet ipsum. Nunc quis urna dictum turpis accumsan semper.



2000 **E9.1.1 A sub-subsection**

2001 Referencing sub-subsections: This section is Sec. E9.1.1, which shows how to refer to a
2002 sub-subsection. List. E.14 shows the corresponding \LaTeX code.

Listing E.14: Sample \LaTeX code for referencing sub-subsections

```
1 Referencing sub-subsections: This section is Sec.\ref{sec:subsubsec},
   which shows how to refer to a sub-subsection. List.\ref{lst:
   refsubsub} shows the corresponding \LaTeX \ code.
```

2003 Lorem ipsum dolor sit amet, consectetur adipiscing elit. Etiam lobortis facilisis sem.
2004 Nullam nec mi et neque pharetra sollicitudin. Praesent imperdiet mi nec ante. Donec
2005 ullamcorper, felis non sodales commodo, lectus velit ultrices augue, a dignissim nibh lectus
2006 placerat pede. Vivamus nunc nunc, molestie ut, ultricies vel, semper in, velit. Ut porttitor.
2007 Praesent in sapien. Lorem ipsum dolor sit amet, consectetur adipiscing elit. Duis fringilla
2008 tristique neque. Sed interdum libero ut metus. Pellentesque placerat. Nam rutrum augue
2009 a leo. Morbi sed elit sit amet ante lobortis sollicitudin. Praesent blandit blandit mauris.
2010 Praesent lectus tellus, aliquet aliquam, luctus a, egestas a, turpis. Mauris lacinia lorem sit
2011 amet ipsum. Nunc quis urna dictum turpis accumsan semper.



E10 Citing

Citing bibliography content is done using BibTeX. It requires the creation of a BibTeX file (.bib extension name), and then added in the argument of `\bibliography{ }`. For each .bib file, separate them by a comma in the argument of `\bibliography{ }` without the extension name. Building your BibTeX file (references.bib) can be done easily with a tool called JabRef (www.jabref.org).

The following subsections are examples of citations.

E10.1 Books

- [?]

- [?]

- [?]

- [?]

- [?]

- [?]

- [?]

- [?]

- [?]

- [?]

- [?]

- [?]

- [?]

- [?]

- [?]

- [?]

- [?]

- [?]



2038 • [?]

2039 • [?]

2040 • [?]

2041 • [?]

2042 • [?]

2043 • [?]

2044 • [?]

2045 • [?]

2046 • [?]

2047 • [?]

2048 • [?]

2049 • [?]

2050 • [?]

2051 • [?]

2052 • [?]

2053 • [?]

2054 • [?]

2055 • [?]

2056 • [?]

2057 • [?]

2058 • [?]

2059 • [?]

2060 • [?]

2061 • [?]

2062 • [?]

2063 • [?]



2064

E10.2 Booklets

2065

- [?]

2066

E10.3 Proceedings

2067

- [?]

2068

E10.4 In books

2069

- [?]

2070

- [?]

2071

- [?]

2072

- [?]

2073

- [?]

2074

- [?]

2075

- [?]

2076

- [?]

2077

- [?]

2078

- [?]

2079

- [?]

2080

- [?]

2081

- [?]

2082

- [?]

2083

- [?]

2084

- [?]

2085

- [?]

2086

- [?]



2087 • [?]

2088 • [?]

2089 • [?]

2090 • [?]

2091 • [?]

2092 • [?]

2093 • [?]

2094 • [?]

2095 **E10.5 In proceedings**

2096 • [?]

2097 • [?]

2098 • [?]

2099 • [?]

2100 • [?]

2101 • [?]

2102 • [?]

2103 **E10.6 Journals**

2104 • [?]

2105 • [?]

2106 • [?]

2107 • [?]

2108 • [?]

2109 • [?]



De La Salle University

2110 • [?]

2111 • [?]

2112 • [?]

2113 • [?]

2114 • [?]

2115 • [?]

2116 • [?]

2117 • [?]

2118 • [?]

2119 • [?]

2120 • [?]

2121 • [?]

2122 • [?]

2123 • [?]

2124 • [?]

2125 • [?]

2126 • [?]

2127 • [?]

2128 • [?]

2129 • [?]

2130 • [?]

2131 • [?]

2132 • [?]

2133 • [?]



2134 • [?]

2135 • [?]

2136 • [?]

2137 • [?]

2138 • [?]

2139 **E10.7 Theses/dissertations**

2140 • [?]

2141 • [?]

2142 • [?]

2143 • [?]

2144 • [?]

2145 • [?]

2146 • [?]

2147 **E10.8 Technical Reports and Others**

2148 • [?]

2149 • [?]

2150 • [?]

2151 • [?]

2152 • [?]

2153 • [?]

2154 • [?]

2155 • [?]

2156 • [?]



2157 • [?]

2158 • [?]

2159 • [?]

2160 • [?]

2161 • [?]

2162 • [?]

2163 **E10.9 Miscellaneous**

2164 • [?]

2165 • [?]

2166 • [?]

2167 • [?]

2168 • [?]

2169 • [?]

2170 • [?]

2171 • [?]

2172 • [?]

2173 • [?]

2174 • [?]

2175 • [?]

2176 • [?]



2177

E11 Index

2178

For key words or topics that are expected (or the user would like) to appear in the Index, use `\index{key}`, where `key` is an example keyword to appear in the Index. For example, Fredholm integral and Fourier operator of the following paragraph are in the Index.

2179

2180

2181

2182

2183

2184

2185

If we make a very large matrix with complex exponentials in the rows (i.e., cosine real parts and sine imaginary parts), and increase the resolution without bound, we approach the kernel of the Fredholm integral equation of the 2nd kind, namely the Fourier operator that defines the continuous Fourier transform.

List. E.15 is a program listing of the above-mentioned paragraph.

Listing E.15: Sample \LaTeX code for Index usage

```
1 If we make a very large matrix with complex exponentials in the rows (i.
  e., cosine real parts and sine imaginary parts), and increase the
  resolution without bound, we approach the kernel of the \index{
  Fredholm integral} Fredholm integral equation of the 2nd kind,
  namely the \index{Fourier} Fourier operator that defines the
  continuous Fourier transform.
```



2186

E12 Adding Relevant PDF Pages

2187

2188

2189

Examples of such PDF pages are Standards, Datasheets, Specification Sheets, Application Notes, etc. Selected PDF pages can be added (see List. E.16), but note that the options must be tweaked. See the manual of `pdfpages` for other options.

Listing E.16: Sample \LaTeX code for including PDF pages

```
1 \includepdf[pages={8-10},%  
2 offset=3.5mm -10mm,%  
3 scale=0.73,%  
4 frame,%  
5 pagecommand={},]  
6 {./reference/Xilinx2015-UltraScale-Architecture-Overview.pdf}
```



Virtex UltraScale FPGA Feature Summary

Table 6: Virtex UltraScale FPGA Feature Summary

	VU065	VU080	VU095	VU125	VU160	VU190	VU440
Logic Cells	626,640	780,000	940,800	1,253,280	1,621,200	1,879,920	4,432,680
CLB Flip-Flops	716,160	891,424	1,075,200	1,432,320	1,852,800	2,148,480	5,065,920
CLB LUTs	358,080	445,712	537,600	716,160	926,400	1,074,240	2,532,960
Maximum Distributed RAM (Mb)	4.8	3.9	4.8	9.7	12.7	14.5	28.7
Block RAM/FIFO w/ECC (36Kb each)	1,260	1,421	1,728	2,520	3,276	3,780	2,520
Total Block RAM (Mb)	44.3	50.0	60.8	88.6	115.2	132.9	88.6
CMT (1 MMCM, 2 PLLs)	10	16	16	20	30	30	30
I/O DLLs	40	64	64	80	120	120	120
Fractional PLLs	5	8	8	10	15	15	0
Maximum HP I/Os ⁽¹⁾	468	780	780	780	650	650	1,404
Maximum HR I/Os ⁽²⁾	52	52	52	104	52	52	52
DSP Slices	600	672	768	1,200	1,560	1,800	2,880
System Monitor	1	1	1	2	3	3	3
PCIe Gen3 x8	2	4	4	4	5	6	6
150G Interlaken	3	6	6	6	8	9	0
100G Ethernet	3	4	4	6	9	9	3
GTH 16.3Gb/s Transceivers	20	32	32	40	52	60	48
GTY 30.5Gb/s Transceivers	20	32	32	40	52	60	0

Notes:

1. HP = High-performance I/O with support for I/O voltage from 1.0V to 1.8V.
2. HR = High-range I/O with support for I/O voltage from 1.2V to 3.3V.



2191



UltraScale Architecture and Product Overview

Virtex UltraScale Device-Package Combinations and Maximum I/Os

Table 7: Virtex UltraScale Device-Package Combinations and Maximum I/Os

Package ⁽¹⁾⁽²⁾⁽³⁾	Package Dimensions (mm)	VU065	VU080	VU095	VU125	VU160	VU190	VU440
		HR, HP GTH, GTY	HR, HP GTH, GTY	HR, HP GTH, GTY	HR, HP GTH, GTY	HR, HP GTH, GTY	HR, HP GTH, GTY	HR, HP GTH, GTY
FFVC1517	40x40	52, 468 20, 20	52, 468 20, 20	52, 468 20, 20				
FFVD1517	40x40		52, 286 32, 32	52, 286 32, 32				
FLVD1517	40x40				52, 286 40, 32			
FFVB1760	42.5x42.5		52, 650 32, 16	52, 650 32, 16				
FLVB1760	42.5x42.5				52, 650 36, 16			
FFVA2104	47.5x47.5		52, 780 28, 24	52, 780 28, 24				
FLVA2104	47.5x47.5				52, 780 28, 24			
FFVB2104	47.5x47.5		52, 650 32, 32	52, 650 32, 32				
FLVB2104	47.5x47.5				52, 650 40, 36			
FLGB2104	47.5x47.5					52, 650 40, 36	52, 650 40, 36	
FFVC2104	47.5x47.5			52, 364 32, 32				
FLVC2104	47.5x47.5				52, 364 40, 40			
FLGC2104	47.5x47.5					52, 364 52, 52	52, 364 52, 52	
FLGB2377	50x50							52, 1248 36, 0
FLGA2577	52.5x52.5						0, 448 60, 60	
FLGA2892	55x55							52, 1404 48, 0

Notes:

1. Go to [Ordering Information](#) for package designation details.
2. All packages have 1.0mm ball pitch.
3. Packages with the same last letter and number sequence, e.g., A2104, are footprint compatible with all other UltraScale architecture-based devices with the same sequence. The footprint compatible devices within this family are outlined. See the [UltraScale Architecture Product Selection Guide](#) for details on inter-family migration.



2192



Virtex UltraScale+ FPGA Feature Summary

Table 8: Virtex UltraScale+ FPGA Feature Summary

	VU3P	VU5P	VU7P	VU9P	VU11P	VU13P
Logic Cells	689,640	1,051,010	1,379,280	2,068,920	2,147,040	2,862,720
CLB Flip-Flops	788,160	1,201,154	1,576,320	2,364,480	2,453,760	3,271,680
CLB LUTs	394,080	600,577	788,160	1,182,240	1,226,880	1,635,840
Max. Distributed RAM (Mb)	12.0	18.3	24.1	36.1	34.8	46.4
Block RAM/FIFO w/ECC (36Kb each)	720	1,024	1,440	2,160	2,016	2,688
Block RAM (Mb)	25.3	36.0	50.6	75.9	70.9	94.5
UltraRAM Blocks	320	470	640	960	1,152	1,536
UltraRAM (Mb)	90.0	132.2	180.0	270.0	324.0	432.0
CMTs (1 MMCM and 2 PLLs)	10	20	20	30	12	16
Max. HP I/O ⁽¹⁾	520	832	832	832	624	832
DSP Slices	2,280	3,474	4,560	6,840	8,928	11,904
System Monitor	1	2	2	3	3	4
GTY Transceivers 32.75Gb/s	40	80	80	120	96	128
PCIe Gen3 x16 and Gen4 x8	2	4	4	6	3	4
150G Interlaken	3	4	6	9	9	12
100G Ethernet w/RS-FEC	3	4	6	9	6	8

Notes:

1. HP = High-performance I/O with support for I/O voltage from 1.0V to 1.8V.

Virtex UltraScale+ Device-Package Combinations and Maximum I/Os

Table 9: Virtex UltraScale+ Device-Package Combinations and Maximum I/Os

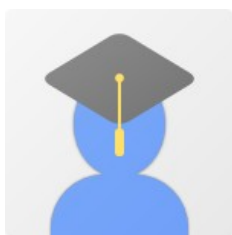
Package (1)(2)(3)	Package Dimensions (mm)	VU3P	VU5P	VU7P	VU9P	VU11P	VU13P
		HP, GTY	HP, GTY	HP, GTY	HP, GTY	HP, GTY	HP, GTY
FFVC1517	40x40	520, 40					
FLVF1924	45x45					624, 64	
FLVA2104	47.5x47.5		832, 52	832, 52	832, 52		
FHVA2104	52.5x52.5 ⁽⁴⁾						832, 52
FLVB2104	47.5x47.5		702, 76	702, 76	702, 76	624, 76	
FHVB2104	52.5x52.5 ⁽⁴⁾						702, 76
FLVC2104	47.5x47.5		416, 80	416, 80	416, 104	416, 96	
FHVC2104	52.5x52.5 ⁽⁴⁾						416, 104
FLVA2577	52.5x52.5				448, 120	448, 96	448, 128

Notes:

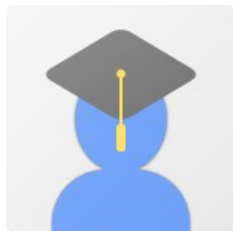
- Go to [Ordering Information](#) for package designation details.
- All packages have 1.0mm ball pitch.
- Packages with the same last letter and number sequence, e.g., A2104, are footprint compatible with all other UltraScale devices with the same sequence. The footprint compatible devices within this family are outlined.
- These 52.5x52.5mm overhang packages have the same PCB ball footprint as the corresponding 47.5x47.5mm packages (i.e., the same last letter and number sequence) and are footprint compatible.



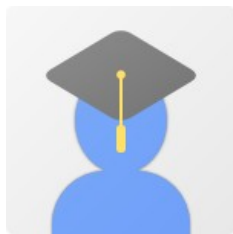
Appendix F VITA



John Carlo Theo S. Dela Cruz received the B.Sc., M.Sc., and Ph.D. degrees in chemistry all from the Pamantasan ng Pilipinas, San Juan, Metro Manila, Philippines, in 2020, 2022 and 2025 respectively. He is currently taking up his B.Sc. Computer Engineering studies. He has developed several high-speed packet-switched network systems and node modules. His research interests include high-speed packet-switched networks, high speed radio interface design, discrete simulation and statistical models for packet switches.



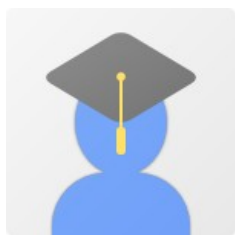
Pierre Justine P. Parel received the B.Sc., M.Sc., and Ph.D. degrees in chemistry all from the Pamantasan ng Pilipinas, San Juan, Metro Manila, Philippines, in 2020, 2022 and 2025 respectively. He is currently taking up his B.Sc. Computer Engineering studies. He has developed several high-speed packet-switched network systems and node modules. His research interests include high-speed packet-switched networks, high speed radio interface design, discrete simulation and statistical models for packet switches.



Jiro Renzo D. Tabiolo received the B.Sc., M.Sc., and Ph.D. degrees in chemistry all from the Pamantasan ng Pilipinas, San Juan, Metro Manila, Philippines, in 2020, 2022 and 2025 respectively. He is currently taking up his B.Sc. Computer Engineering studies. He has developed several high-speed packet-switched network systems



2213 and node modules. His research interests include high-speed packet-switched networks,
2214 high speed radio interface design, discrete simulation and statistical models for packet
2215 switches.



2216 Ercid Bon B. Valencerina received the B.Sc., M.Sc., and Ph.D.
2217 degrees in chemistry all from the Pamantasan ng Pilipinas, San Juan, Metro Manila,
2218 Philippines, in 2020, 2022 and 2025 respectively. He is currently taking up his B.Sc.
2219 Computer Engineering studies. He has developed several high-speed packet-switched
2220 network systems and node modules. His research interests include high-speed packet-
2221 switched networks, high speed radio interface design, discrete simulation and statistical
2222 models for packet switches.



De La Salle University

2223

Appendix G

2224

ARTICLE PAPER(S)

Article/Forum Paper Format (IEEE LaTeX format)

Michael Shell, *Member, IEEE*, John Doe, *Fellow, OSA*, and Jane Doe, *Life Fellow, IEEE*

2225

Abstract—The abstract goes here. Lorem ipsum dolor sit amet, consectetur adipiscing elit. Etiam lobortis facilisis sem. Nullam nec mi et neque pharetra sollicitudin. Praesent imperdiet mi nec ante. Donec ullamcorper, felis non sodales commodo, lectus velit ultrices augue, a dignissim nibh lectus placerat pede. Vivamus nunc nunc, molestie ut, ultricies vel, semper in, velit. Ut porttitor. Praesent in sapien. Lorem ipsum dolor sit amet, consectetur adipiscing elit. Duis fringilla tristique neque. Sed interdum libero ut metus. Pellentesque placerat. Nam rutrum augue a leo. Morbi sed elit sit amet ante lobortis sollicitudin. Praesent blandit blandit mauris. Praesent lectus tellus, aliquet aliquam, luctus a, egestas a, turpis. Mauris lacinia lorem sit amet ipsum. Nunc quis urna dictum turpis accumsan semper.

Index Terms—Computer Society, IEEE, IEEEtran, journal, LaTeX, paper, template.

I. INTRODUCTION

THIS demo file is intended to serve as a “starter file” for IEEE article papers produced under LaTeX using IEEEtran.cls version 1.8b and later. Lorem ipsum dolor sit amet, consectetur adipiscing elit. Etiam lobortis facilisis sem. Nullam nec mi et neque pharetra sollicitudin. Praesent imperdiet mi nec ante. Donec ullamcorper, felis non sodales commodo, lectus velit ultrices augue, a dignissim nibh lectus placerat pede. Vivamus nunc nunc, molestie ut, ultricies vel, semper in, velit. Ut porttitor. Praesent in sapien. Lorem ipsum dolor sit amet, consectetur adipiscing elit. Duis fringilla tristique neque. Sed interdum libero ut metus. Pellentesque placerat. Nam rutrum augue a leo. Morbi sed elit sit amet ante lobortis sollicitudin. Praesent blandit blandit mauris. Praesent lectus tellus, aliquet aliquam, luctus a, egestas a, turpis. Mauris lacinia lorem sit amet ipsum. Nunc quis urna dictum turpis accumsan semper.

A. Subsection Heading Here

Subsection text here. Lorem ipsum dolor sit amet, consectetur adipiscing elit. Etiam lobortis facilisis sem. Nullam nec mi et neque pharetra sollicitudin. Praesent imperdiet mi nec ante. Donec ullamcorper, felis non sodales commodo, lectus velit ultrices augue, a dignissim nibh lectus placerat pede. Vivamus nunc nunc, molestie ut, ultricies vel, semper in, velit. Ut porttitor. Praesent in sapien. Lorem ipsum dolor sit amet, consectetur adipiscing elit. Duis fringilla tristique neque. Sed interdum libero ut metus. Pellentesque placerat. Nam rutrum augue a leo. Morbi sed elit sit amet ante lobortis sollicitudin.

M. Shell was with the Department of Electrical and Computer Engineering, Georgia Institute of Technology, Atlanta, GA, 30332.
E-mail: see <http://www.michaelshell.org/contact.html>
J. Doe and J. Doe are with Anonymous University.



Fig. 1. Simulation results for the network.

TABLE I
AN EXAMPLE OF A TABLE

One	Two
Three	Four

Praesent blandit blandit mauris. Praesent lectus tellus, aliquet aliquam, luctus a, egestas a, turpis. Mauris lacinia lorem sit amet ipsum. Nunc quis urna dictum turpis accumsan semper.

1) Subsubsection Heading Here: Subsubsection text here.

Lorem ipsum dolor sit amet, consectetur adipiscing elit. Etiam lobortis facilisis sem. Nullam nec mi et neque pharetra sollicitudin. Praesent imperdiet mi nec ante. Donec ullamcorper, felis non sodales commodo, lectus velit ultrices augue, a dignissim nibh lectus placerat pede. Vivamus nunc nunc, molestie ut, ultricies vel, semper in, velit. Ut porttitor. Praesent in sapien. Lorem ipsum dolor sit amet, consectetur adipiscing elit. Duis fringilla tristique neque. Sed interdum libero ut metus. Pellentesque placerat. Nam rutrum augue a leo. Morbi sed elit sit amet ante lobortis sollicitudin. Praesent blandit blandit mauris. Praesent lectus tellus, aliquet aliquam, luctus a, egestas a, turpis. Mauris lacinia lorem sit amet ipsum. Nunc quis urna dictum turpis accumsan semper.

II. CONCLUSION

The conclusion goes here.

Lorem ipsum dolor sit amet, consectetur adipiscing elit. Etiam lobortis facilisis sem. Nullam nec mi et neque pharetra sollicitudin. Praesent imperdiet mi nec ante. Donec ullamcorper, felis non sodales commodo, lectus velit ultrices augue,

2226



(a) Case I



(b) Case II

Fig. 2. Simulation results for the network.

a dignissim nibh lectus placerat pede. Vivamus nunc nunc, molestie ut, ultricies vel, semper in, velit. Ut porttitor. Praesent in sapien. Lorem ipsum dolor sit amet, consectetur adipiscing elit. Duis fringilla tristique neque. Sed interdum libero ut metus. Pellentesque placerat. Nam rutrum augue a leo. Morbi sed elit sit amet ante lobortis sollicitudin. Praesent blandit blandit mauris. Praesent lectus tellus, aliquet aliquam, luctus a, egestas a, turpis. Mauris lacinia lorem sit amet ipsum. Nunc quis urna dictum turpis accumsan semper.

APPENDIX A

PROOF OF THE FIRST ZONKLAR EQUATION

Appendix one text goes here.

Lorem ipsum dolor sit amet, consectetur adipiscing elit. Etiam lobortis facilisis sem. Nullam nec mi et neque pharetra sollicitudin. Praesent imperdiet mi nec ante. Donec ullamcorper, felis non sodales commodo, lectus velit ultrices augue, a dignissim nibh lectus placerat pede. Vivamus nunc nunc, molestie ut, ultricies vel, semper in, velit. Ut porttitor. Praesent in sapien. Lorem ipsum dolor sit amet, consectetur adipiscing elit. Duis fringilla tristique neque. Sed interdum libero ut metus. Pellentesque placerat. Nam rutrum augue a leo. Morbi sed elit sit amet ante lobortis sollicitudin. Praesent blandit blandit mauris. Praesent lectus tellus, aliquet aliquam, luctus a, egestas a, turpis. Mauris lacinia lorem sit amet ipsum. Nunc quis urna dictum turpis accumsan semper.

APPENDIX B

Appendix two text goes here. [1].

Lorem ipsum dolor sit amet, consectetur adipiscing elit. Etiam lobortis facilisis sem. Nullam nec mi et neque pharetra sollicitudin. Praesent imperdiet mi nec ante. Donec ullamcorper, felis non sodales commodo, lectus velit ultrices augue, a dignissim nibh lectus placerat pede. Vivamus nunc nunc, molestie ut, ultricies vel, semper in, velit. Ut porttitor. Praesent in sapien. Lorem ipsum dolor sit amet, consectetur adipiscing elit. Duis fringilla tristique neque. Sed interdum libero ut

metus. Pellentesque placerat. Nam rutrum augue a leo. Morbi sed elit sit amet ante lobortis sollicitudin. Praesent blandit blandit mauris. Praesent lectus tellus, aliquet aliquam, luctus a, egestas a, turpis. Mauris lacinia lorem sit amet ipsum. Nunc quis urna dictum turpis accumsan semper.

ACKNOWLEDGMENT

The authors would like to thank...

REFERENCES

- [1] T. Oetiker, H. Partl, I. Hyna, and E. Schlegl, *The Not So Short Introduction to L^AT_EX 2_ε Or L^AT_EX 2_ε in 157 minutes.* n.a., 2014.